5. Systems Research and Technology Development

5.1 Fully Integrated HEV Traction Motor Drive Development Using Thermoelectrics and Film Capacitor Innovations

Principal Investigator: C. W. Ayers
Oak Ridge National Laboratory
National Transportation Research Center
2360 Cherahala Boulevard
Knoxville, TN 37932
Voice: 865-946-1342; Fax: 865-946-1400; E-mail: ayerscw@ornl.gov

DOE Technology Development Manager: Susan A. Rogers
Voice: 202-586-8997; Fax: 202-586-1600; E-mail: Susan.Rogers@ee.doe.gov

ORNL Program Manager: Mitch Olszewski
Voice: 865-946-1350; Fax: 865-946-1262; E-mail: olszewskim@ornl.gov

Objectives

The intent of this project is to produce an integrated motor and inverter with special heat transfer paths that promote and improve operation at high power density in a high-temperature environment. It is intended to apply thermoelectric (TE) device innovations to form temperature-controlled islands within the system. These temperature islands will allow high- and low-temperature devices to function side by side, for example, high-temperature silicon carbide (SiC) power electronics in close proximity with silicon electronics and film capacitors.

Silicon-based electronics need their core temperature to be controlled at or below 125ºC, and polypropylene capacitors operate best at or below 85ºC. SiC components are being tested at temperatures above 300ºC, so there is a strong application of the temperature-controlled island concept with this combination of components.

Approach

The first task was to perform literature research on TEs, evaluate what devices were commercially available, and compare different devices to see which devices would be most applicable to our intended applications. It would be important as well to evaluate what new devices are emerging on the market or under development in order to augment or redirect design ideas for an integrated motor and inverter.

Oak Ridge National Laboratory (ORNL) would then procure TE devices that best fit the design ideas, as well as film capacitors, to aid in conceptualizing an integrated motor/inverter traction drive for building and testing the following year.

Major Accomplishments

The TE research that was performed was used to produce a comparison chart of commercially available TE devices. Many manufacturers' products were evaluated, and the data have been pulled together for comparison of costs and capabilities. Informative results were obtained that provide good insight into how the available TEs perform and how some emerging TE technologies are improving performance in some helpful areas.

A motor type was chosen to provide a tangible basis for design concepts and packaging innovations. The design chosen was a commercially available General Electric 5-kW induction motor.

Physical packaging design ideas were introduced and developed. These ideas resulted in the concept of the layered SiC/TE packaging that allows silicon electronics and film capacitors to be packaged closely with the SiC. This idea utilizes TEs to keep the silicon and film capacitors cool while allowing the SiC to operate at much higher ambient temperatures.

The higher operational temperature environment enabled by this technology provides a pathway for the possibility of air cooling the entire traction drive system. The primary problems involved with air cooling a high-power system are the volume required for the system-to-ambient heat sink and the typical high air flow rate. The simplicity of air cooling is an attractive option for traction drives if the volume can be kept to a minimum, and the higher operating temperatures that can be used with SiC power devices promotes reduced volume with reasonable air flow quantities.

Technical Discussion

Thermoelectric Comparison Chart

TEs were researched extensively, looking at ongoing development, commercially available components, and emerging products or near-market technologies. The results of this research are tabulated in a spreadsheet to provide a quick means of comparing sizes, costs, heat flux, etc., for the devices. It was interesting to find that essentially all of the commercially available TE products are produced using bismuth-telluride junctions; the only differences between the products seem to be packaging shapes, thickness, bonding methods, etc. The packaging and bonding methods seem to be where the near-term innovations will be found. These parameters are the controlling factors in TE temperature limitation. Packaging and thickness seem to be the parameters that are being studied and improved to provide better efficiencies for the devices. Heat losses in TE packaging are major contributors to their low coefficient of performance (COP).

See Table 1 for an abbreviated list of manufacturers and key parameters of the TE devices. A more exhaustive list of TE devices presently available on the market is presented in Appendix A.

Emerging TE Devices

Thin film devices are an emerging technology, with products such as the MicroPelt® Peltier Coolers coming onto the market this year. The manufacturing technology for thin film TE devices, based on methods used in the semiconductor industry, produces very small and thin discrete devices. MicroPelt® device thickness is on the order of 0.4 mm. The conventional devices are thicker (such as the Advanced Thermoelectrics devices) and are built up using subcomponents with solder joints connecting the layers together, producing devices that are 2–3 mm thick. The thin film devices ORNL has evaluated are very expensive at first glance, but as a result of a much higher heat flux capability than the conventional bismuth-telluride devices, thicker, the relative price to handle a certain heat load looks much better. When cost is normalized to their ability to remove heat (i.e., dollars per unit of heat flux), the new thin-film devices are actually the cheapest devices on the market. This cost comparison is highlighted in Table 2. If the physical configuration of these can be adapted to match the application, then the thin film devices are a good cost-effective candidate for near-term development of temperature- controlled islands that can be used in our motor and inverter integration concept. With another year or two of maturity, and assuming reasonable manufacturing quantities, the cost of these devices is expected to drop much lower than the present prices.

Motor and Inverter Integration Concepts

The motor chosen earlier this fiscal year was a 5-kW induction motor (General Electric model # 5KE184AC105) that provided an easy platform for procurement, laboratory handling, and measuring/modeling. The motor model developed from this physical motor served as a productive tool for developing the SiC/TE/silicon/film capacitor layering design. It is not necessarily suggested that an induction motor is the motor of choice; this motor was simply chosen for expediency at this stage of the

Table 1. TE device manufacturer comparison data

Advanced Thermoelectrics	ST-127-1.4-6.0	25.00	40.00	40.00	4.20	3.56	71.00	8.48	150.00	$7.86
	ST-127-1.4-8.5	25.00	40.00	40.00	3.95	5.00	72.00	12.66	150.00	$5.60
ADV Engineering	A-TM-8.5-127-1.4	25.00	40.00	40.00	3.70	4.50	72.00	12.16	150.00	
ALTEC	Altec-CM-1-S-IE -127-2.0x2.0-1.15	27.00	40.00	40.00	4.70	9.38	70.00	19.95	150.00	
BHCE	TEC1-16115T125	27.00	40.00	40.00	3.00	11.78	60.00	39.25	150.00	
Custom Thermoelectric	12711-4L31-09RI	50.00	40.00	40.00	3.80	4.69	68.00	12.35	150.00	
Fandis	TM1-1274085	25.00	40.00	40.00	3.40	4.50	71.00	13.24	150.00	
Ferrotec (Thin Film)	9502/065/018MP		11.20	12.10	1.79	5.31	66.00	29.68	135.00	
INB Products	inbDT-1.2	27.00	40.00	40.00	3.60	7.19	69.00	19.97	150.00	$3.90
	inbDT-1.15	27.00	40.00	40.00	3.40	7.50	69.00	22.06	150.00	$3.73
	inbDT-1.05	27.00	40.00	40.00	3.30	8.19	69.00	24.81	150.00	$3.42
	inbDT-0.8	27.00	40.00	40.00	3.20	10.75	69.00	33.59	150.00	$2.60
INTERM	TECB-32-110-(24.7-25-400)-62-69	25.00	62.00	62.00	4.80	10.41	69.00	21.68		
Marlow	DT12-6	27.00	40.00	40.00	4.01	3.38	66.00	8.42	150.00	UA
	DT12-8	27.00	40.00	40.00	3.53	4.44	66.00	12.57	150.00	UA
Melcor	HT8-12-40	25.00	44.00	40.00	3.30	4.09	63.00	12.40	225.00	$5.68
	CP 2-127-10L	25.00	62.00	62.00	5.60	2.01	68.00	3.58	80.00	$20.79
	CP 2-127-06L	25.00	62.00	62.00	4.60	3.12	67.00	6.79	80.00	$12.65
	CP 5-31-06L	25.00	55.00	55.00	4.90	4.13	67.00	8.43	80.00	UA
Micropelt (Thin Film)	MPC-D301-M44	25.00	0.72	0.72	0.43	42.05	22.80	982.53	85.00	$0.88
	MPC-D901-M44	25.00	4.80	4.80	0.43	62.93	21.90	1463.58		
TE Technologies	HT-199-1.4-0.8	27.00	40.00	40.00	3.20	10.75	67.00	33.59	150.00	$2.95
	HT-199-1.4-1.15	27.00	40.00	40.00	3.40	7.50	69.00	22.06	150.00	$3.63
	HT-199-1.4-1.5	27.00	40.00	40.00	3.90	5.88	70.00	15.06	150.00	$4.26
	HP-199-1.4-1.15	25.00	40.00	40.00	3.60	7.50	69.00	20.83	80.00	$2.85
	HP-199-1.4-1.05	25.00	40.00	40.00	3.50	8.19	69.00	23.39	80.00	$3.00

Table 2. TE comparisons showing normalized cost per unit of heat flux

Manufacturer	Qmax W/cm^2	Delta Tmax C	Price/cm^2	Price/(W/cm^2)
Advanced Thermoelectrics	5.00	72.00	$1.24	$5.60
INB Products	10.75	69.00	$1.75	$2.60
Marlow	4.44	66.00	UA	UA
Melcor - (high temperature series)	4.09	63.00	$1.32	$5.68
Micropelt (Thin Film)	60.00	31.90	$3,495.84	$0.62
TE Technologies (high temperature series)	10.75	67.00	$1.98	$2.95
Tellurex	4.09	79.00	$1.22	$5.26

conceptual development (better availability, easier handling and testing, etc.). Permanent magnet motors are an equally acceptable candidate for this concept and are typically the preferred traction motor in most HEV developments. Scalability of the concept is not expected to be an issue when designing for larger motors (50- to 100-kW capacity).

The primary concept was developed based on the motor platform, film capacitor shaping, and TE in an attempt to provide very tight integration of the inverter into the motor. Figure 1 shows a cutaway isometric view of the motor concept. This motor concept is based on SiC power electronics and an air-

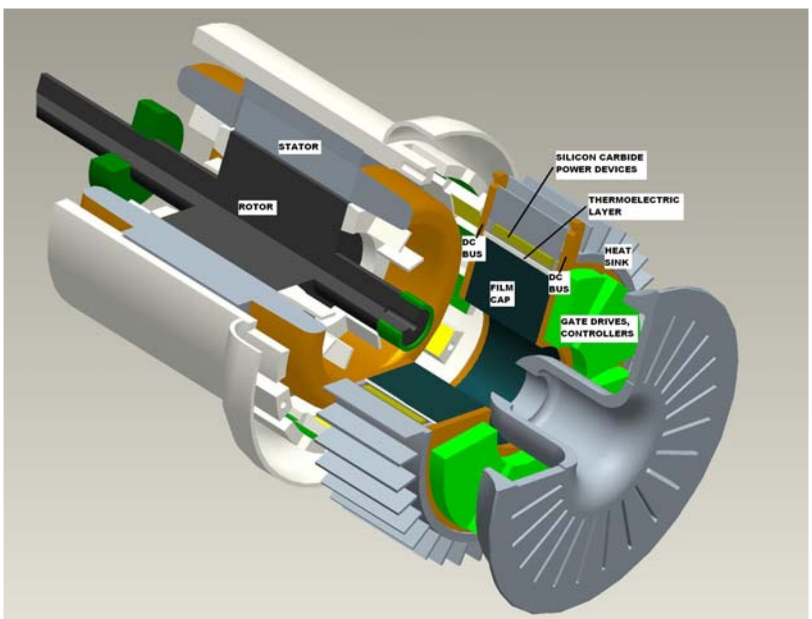

Figure 1. Cutaway view of integrated motor and inverter utilizing silicon carbide power electronics, thermoelectric temperature boundaries, silicon electronics and film capacitors.

cooled motor and inverter housing. The inverter is attached to the end of the motor casing. Although packaging the inverter into the end of the motor is not necessarily a new idea, the TE application enables much tighter packaging than before and promotes air cooling through the use of high-temperature SiC.

Figure 2 shows a view of the power electronics section of the motor concept design. This proposed arrangement shows heat flow paths from the various components in the system, in which the components that need to remain cooler are embedded in and surrounded by the warmer motor environment. The white band wrapped around the lower side of the SiC power electronics (yellow) represents the TE temperature control boundary that protects the silicon and film capacitor from the very hot SiC. The lower perimeter of these components is protected from the warmer motor environment using passive insulation techniques. The reason that passive insulation is not used on the top perimeter of these components is the need to promote heat flow up and out of their core (i.e., the "cool zone"); in other words, the capacitor and control electronics produce some minimal heat. The heat removal for the capacitor and controls can only be accomplished with a heat pumping action (TEs) to draw the heat from this area and remove it through the hotter zone.

There can be several arrangements of electronics in this situation, and this is one embodiment of the concept. The main point to be made is that as integration increases, there is an increased likelihood that components with incompatible heat capacities will be adjacent to each other. This method of integration requires a small amount of power, but it can potentially greatly increase the power density of the traction drive while simultaneously enabling air cooling for the whole system.

The simplicity of air cooling is a desirable characteristic for vehicle traction drive cooling because it offers a continuously available low-temperature source, no problem with leaks, and no need for pumps or piping (probably only a fan and some ducting would be required). Although heat sink volume will continue to be the critical issue, an air-cooling method would allow simplification of the system and reduction of active components and weight.

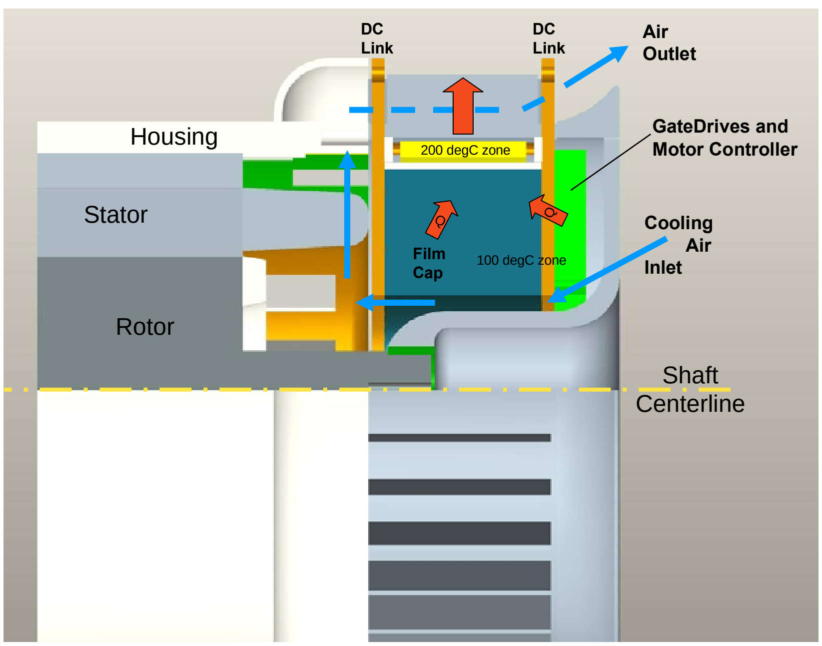

Figure 2. Motor concept section view showing detail of component arrangement and proposed heat flow path.

Thermal Mechanical Modeling of the Concept

ORNL has performed some basic thermal modeling to validate several ideas:

- show air-cooling viability for the integrated package
- show feasibility of use of TEs in relation to system COP
- evaluate temperature profiles throughout the layers to indicate if the packaging/layering concept allows reasonable temperatures in the cold zone and at the TE interfaces

Mechanical models developed with ProEngineer Wildfire software have been thermally analyzed using ProEngineer Mechanica finite element software. Figure 3 shows the mechanical model produced in Wildfire, exploded and labeled to show the subcomponents of the assembly. The primary subcomponents, starting at the bottom of the assembly, are (1) the cold-zone components (silicon-based gate drivers, digital signal processor controller, and film capacitor), (2) the thermoelectric device layer, and (3) the SiC power electronics devices. This design was modeled using the specific material properties for each layer or component, and the heat generated in each section was calculated and input into the software. Using data acquired from research on the TE devices, power consumption for the TE boundary layer was calculated and used as input into the thermal model (i.e., the losses that are incurred in the TE devices as a result of their inefficiencies). Also, based on TE research, it was established that the TE boundary layer can maintain certain temperature differences at corresponding heat flux values. Based on these findings, temperature boundary constraints were established for the upper and lower surfaces of the TE boundary. The TE device itself was not modeled in detail but is basically assumed to control upper and lower surface temperature, generate a certain amount of internal heat, and provide a conduit for the heat flux coming from the lower components.

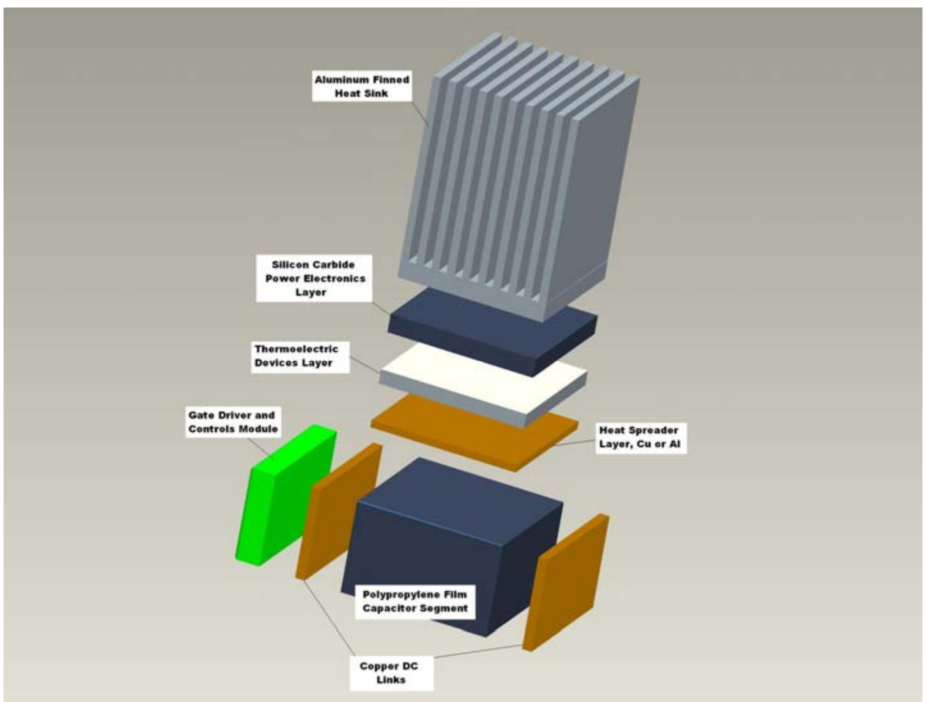

Figure 3. Exploded view of ProEngineer mechanical model used to analyze the thermal performance of the ORNL SiC-TE motor/inverter integration concept.

The model constraints and assumptions are listed in Table 3. Volumetric heat generation values were calculated for potted-module style components such as gate drivers, digital signal processors, and SiC power sections, based on estimated heat losses and their approximate sizes and shapes. The modeling was performed in three stages with two simplified models of upper and lower sections and a third model as an entire cross-section of the concept. This was done to provide a validation of how the TE device interacts with the system without having to actually model the internal conditions of the TE itself—in other words, to treat the TE as a black box.

Table 3. Thermal model calculations and assumptions

Subcomponent description	Constraint	Material
Gate drive and controller module	280,000 W/m^3	Thermal potting mixture
Film capacitor	5,000 W/m^3	Polypropylene
Silicon carbide power electronics	750,000 W/m^3	Thermal potting mixture
TE boundary layer	5.2 W	Ceramic (approximation)
TE cold surface	100°C	—
TE hot surface	200°C	—
Ambient temperature	120°C	—
Heat transfer coefficient	100 W/m^{2}K	—
DC links	—	Copper

The first thermal model (shown in Figure 4) is made up of the cold zone components, configured in the way the laboratory model was designed, and is used to evaluate heat flows and temperature distribution in the lower section. The copper dc links for the inverter design make up two sides of the model, sandwiching the film capacitor block in between. This design places the electronics, that is, digital

First Model - Lower Section: Assumes TE keeps top surface at 100 C

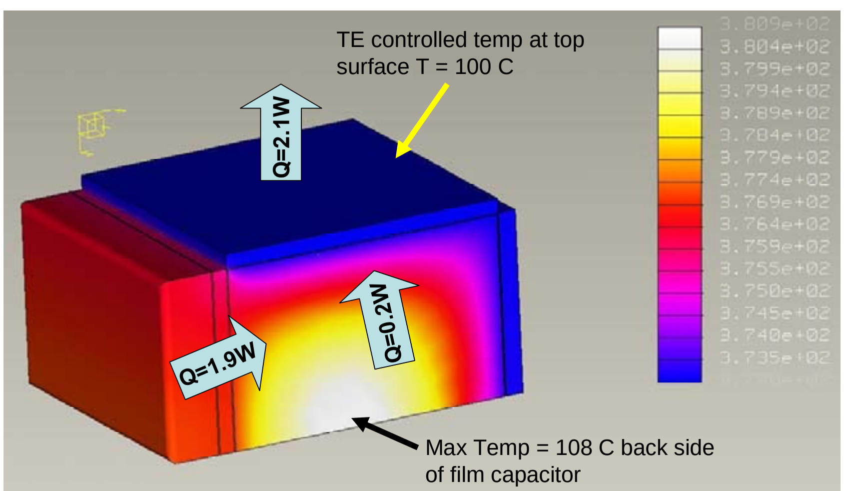

Figure 4. First model analyzed showing the "cold zone" heat flows—the top layer (just a copper heat spreader) interfaces with the rest of the system through the TE layer (not in this model). The silicon electronics are shown on the lower left and the film capacitor cross-section is the major component in the lower middle portion. This model shows temperature distribution for these estimated heat flows.

signal processor controller and gate drivers, on the outside of one of the dc links (left side). Heat in this zone is generated in the silicon electronics section (about 1.9 W) and in the film capacitor (lower middle, about 0.2 W). The constraints in this model consist of insulation all around the unit, except on the top surface, which removes a total heat flux of 2.1 W (up through the TE "black box" device, next layer). The specifications for these subcomponents can be found in Table 3. The TE device is not needed in this model and is omitted to keep the analysis simple.

The second model seen in Figure 5 was developed to look at heat flow and temperature for the upper or "hot zone" components. This unit includes the SiC power device module and a finned heat sink to transfer heat to the ambient air. The constraints for this model consist of (1) heat flux entering the bottom surface (lower section's heat plus TE device losses) of 7.3 W, (2) SiC module losses of 7.1 W, and (3) insulation all around except for the finned heat sink surfaces. The heat sink surfaces are given a heat transfer coefficient of 100 W/m^2K; for a fourth condition, the ambient air temperature is set at 120°C for these analyses. The TE device is not included in this model segment for simplicity.

The third model (Figure 6) represents the entire cross-section of the SiC/silicon/film cap layering concept. The TE device is included in this model, but is represented by a "black box" with boundary constraints. Except for the addition of the TE device, this model is basically made up of Model 1 and Model 2. The boundary constraints for these two models are included as required with the addition of the TE device. The results from this thermal model closely match the results from the first two models, in temperature distribution and maximum temperatures seen at critical parts of the system, and these results provide good validation for the total system model. In future work, this model can be used to perform "what-if" cases for different designs or other concepts.

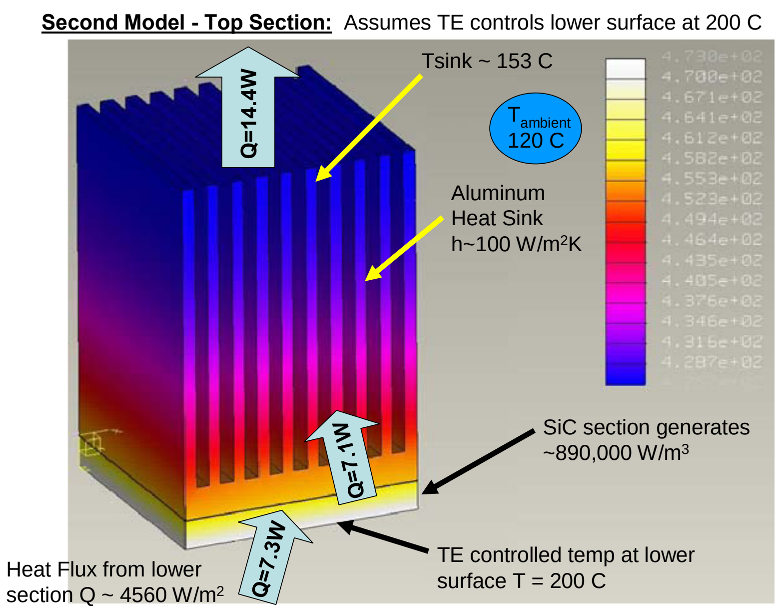

Figure 5. Second model showing the "hot zone" heat flows. The lower surface (SiC section) rests on top of the TE device. The heat from the SiC and the lower section moves upward to the heat sink and then to ambient. This model shows the temperature distribution for the upper section using the heat generated in the SiC and the heat flux from the lower section (Model 1).

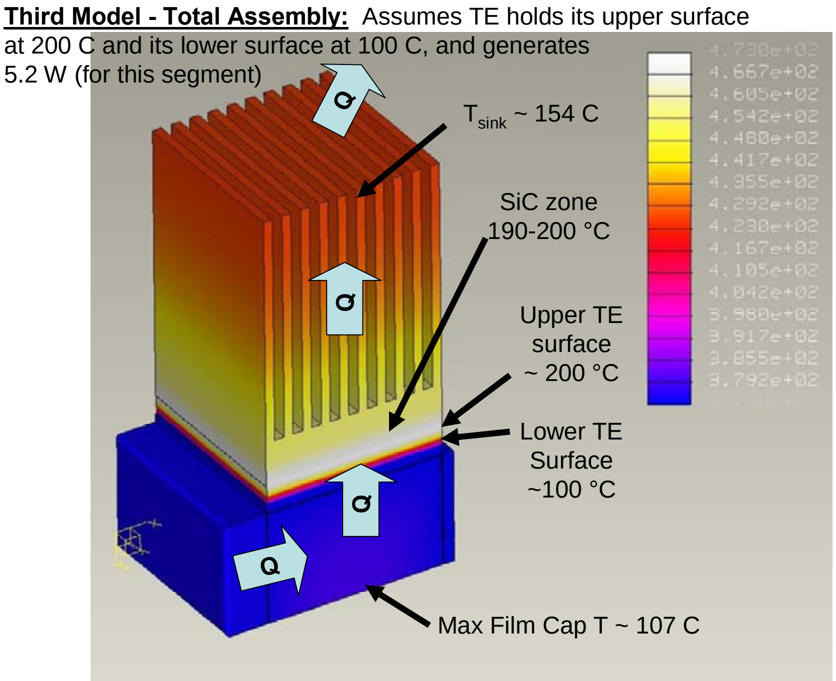

Figure 6. This third model shows the whole assembly where Model 1 and Model 2 structures are basically joined together using the TE boundary layer. This more complex model (with assumptions about the TE boundary layer) is validated by observing the temperature profile and seeing a close match with the system temperatures in Models 1 and 2.

TEs in general are found to have a relatively low heat flux carrying capability and in single layers have a limited temperature rise/drop capability across their boundaries. The low heat flux (i.e., ~5–10 W/cm^2) capability makes them unsuitable for use directly to remove heat from conventional power electronics, which require on the order of 50–100 W/cm^2 in conventional inverter designs. It was originally desired to produce a concept where power electronics were cooled directly as needed in a high-integration design, but the heat flux numbers proved to be too small for this idea. Thin film TE devices are rapidly approaching the required heat flux numbers, however, and in the near future may be suitable to be incorporated into various applications of direct power electronics high flux cooling with reasonable efficiencies.

This understanding of TE heat flux limitations influenced the design ideas that were evaluated during this project The main result of that has been the development of the concept of temperature-controlled islands that allow silicon electronics and film capacitors to be used in close proximity with SiC power electronics. In this design scenario, the SiC power electronics can be allowed to operate at much higher than conventional temperatures (>200ºC), which makes the use of air cooling much more viable (reasonable heat sink size would then be possible). What limits the use of high-temperature SiC in a tightly integrated motor drive is the relatively low-temperature environment required for the silicon control electronics and dc filtering capacitors. These devices need an environment much closer to 80–90ºC. Figure 7 depicts a basic layout of the integration concept and shows how the TE layers provide a lower-temperature island to protect the silicon and film capacitor. This lower-temperature island allows

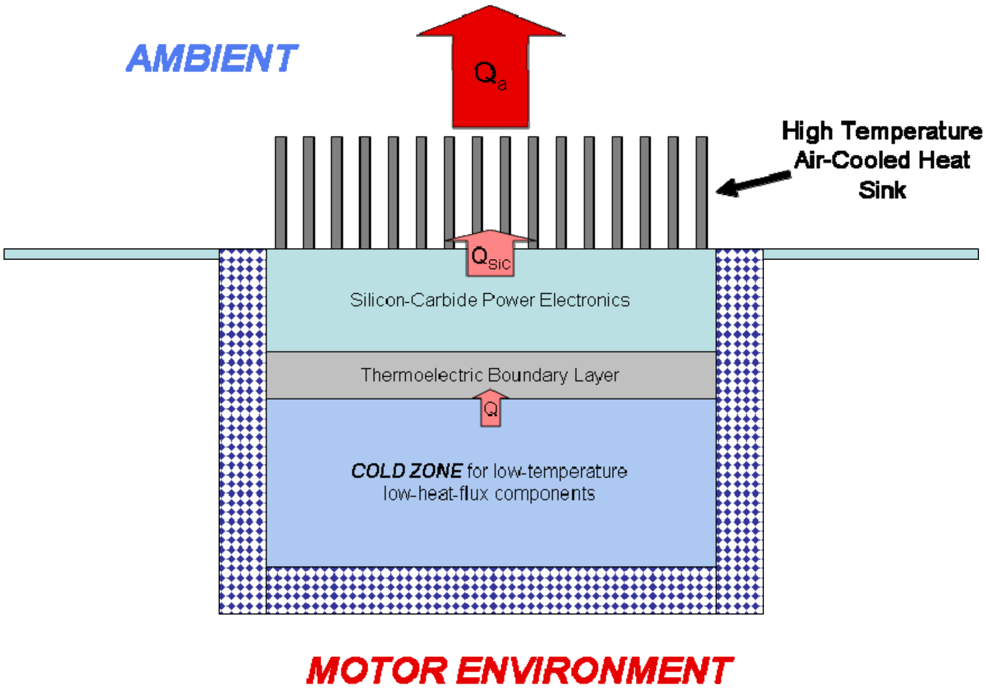

Figure 7. Cold zone produced by TE layer. Cold zone components are protected from high-temperature SiC and motor zones by the heat pumping action of the TEs.

for improved reliability, better utilization of the silicon and much reduced volume/weight for the film capacitor.

Although the heat flux is low, the internal heat must be removed from the silicon electronics and film capacitor(s). Otherwise, the internal temperature of these components will rise to excessive levels and result in failure. This packaging concept requires that this heat energy be transferred out to the ambient zone by traveling through a higher-temperature zone. Because this is against the natural flow of heat, the TEs are used to provide a heat pumping action to remove the energy from the cold zone (80–90°C) out through the hot zone (>200°C).

Thermoelectric Performance and Multilayer Benefits Modeling:

Because of the high heat flux capabilities of the Micropelt TE devices and the project initiative to perform analysis on the most advanced thermoelectric technology, a model of this device was constructed using Matlab. The model is based on data provided by the manufacturer specifications and consists of analysis of the cooling capability of the device in relation to temperature and input current. This provides a COP relationship to temperature and cooling capability per TE device.

The requirements to maintain the silicon control devices and dc filtering capacitors at or below 100ºC and to allow the SiC to reach temperatures exceeding 150ºC produce temperature gradients in excess of 50ºC. This condition necessitated the use of a multilayer strategy as seen in Figure 8. Using the model developed in Matlab and combining the concept of layering, the maximum obtainable COP was determined for each load based on a particular temperature difference and a number of layers.

The analysis conducted with the Matlab model revealed that an increase in the maximum temperature difference and COP could be obtained with increased layers as seen in Figure 9. There seems to be a

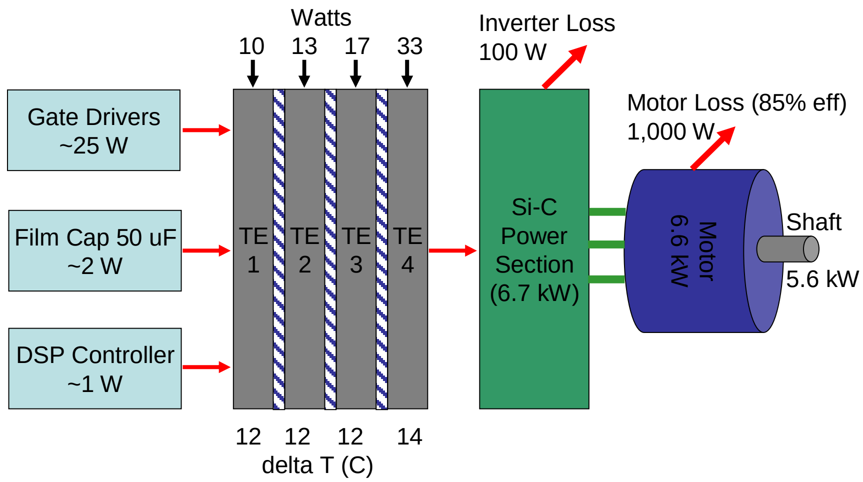

Figure 8. Power flow schematic in the SiC/TE/silicon/film capacitor integration concept.

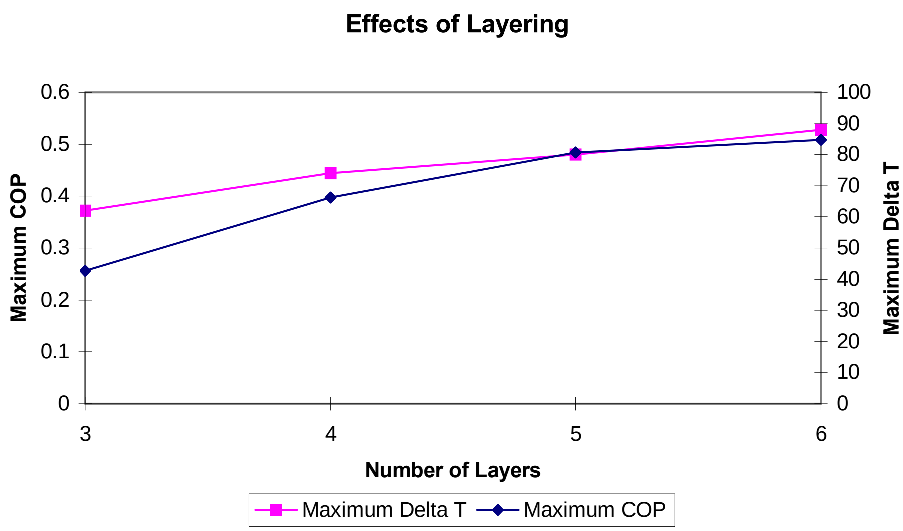

Figure 9. The effect of layering on maximum temperature difference.

diminishing return on increasing the number of layers, as seen in Figure 9, but we have limited data at this point. Continued research must be done to fully understand this phenomenon. If this is a real phenomenon, it would be of great interest to determine what part of the system causes this drop in COP/layer as the number of layers increases. Understanding this effect could direct future research and development for TE devices.

To make use of this data, a value for the heat load was necessary. For the motor assembly developed, the heat load stems from the gate drivers, dc filter capacitor, and digital signal processor controller. The gate drivers were estimated to produce a maximum of 4 W each or a total of 24 W. The DSP controller from manufacturer specifications produces a maximum of approximately 1W. The capacitor heat load is a more difficult estimate and was determined through a voltage-power factor matrix provided in Table 4. For this matrix, a 6.6-kW motor is assumed, and the inverter is expected to be operating in full-over modulation. The capacitor expected to be used in the motor assembly has a capacitance of 500 µF and an ESR of 0.0031 at 10 kHz. From this table, the maximum heat load is approximately 2 W.

From these calculations, the final heat flux is expected to be extremely low with less than 1-W/cm^2 cooling requirements. Using this heat flux number and varying the temperature gradient, Table 5 was created. This table demonstrates the COP in terms of the number of layers and temperature difference.

Table 4. Capacitor power dissipation (W) due to voltage and power factor effects

	PF								
Voltage	**0.6**	**0.65**	**0.7**	**0.75**	**0.8**	**0.85**	**0.9**	**0.95**	**1**
130	0.193	0.296	0.685	0.998	1.254	1.466	1.644	1.795	1.923
150	0.145	0.223	0.514	0.749	0.942	1.101	1.235	1.348	1.445
170	0.113	0.173	0.400	0.583	0.733	0.857	0.961	1.050	1.125
190	0.090	0.139	0.320	0.467	0.587	0.686	0.770	0.840	0.900
210	0.074	0.114	0.262	0.382	0.481	0.562	0.630	0.688	0.737
230	0.062	0.095	0.219	0.319	0.401	0.468	0.525	0.573	0.614
250	0.052	0.080	0.185	0.270	0.339	0.396	0.445	0.485	0.520
270	0.045	0.069	0.159	0.231	0.291	0.340	0.381	0.416	0.446
290	0.039	0.060	0.138	0.200	0.252	0.295	0.330	0.361	0.387
310	0.034	0.052	0.120	0.175	0.221	0.258	0.289	0.316	0.338
330	0.030	0.046	0.106	0.155	0.195	0.228	0.255	0.279	0.298
350	0.027	0.041	0.094	0.138	0.173	0.202	0.227	0.248	0.265
370	0.024	0.037	0.085	0.123	0.155	0.181	0.203	0.222	0.237
390	0.021	0.033	0.076	0.111	0.139	0.163	0.183	0.199	0.214
410	0.019	0.030	0.069	0.100	0.126	0.147	0.165	0.180	0.193
430	0.018	0.027	0.063	0.091	0.115	0.134	0.150	0.164	0.176
450	0.016	0.025	0.057	0.083	0.105	0.122	0.137	0.150	0.161
470	0.015	0.023	0.052	0.076	0.096	0.112	0.126	0.137	0.147
490	0.014	0.021	0.048	0.070	0.088	0.103	0.116	0.126	0.135
510	0.013	0.019	0.044	0.065	0.081	0.095	0.107	0.117	0.125
530	0.012	0.018	0.041	0.060	0.075	0.088	0.099	0.108	0.116
550	0.011	0.017	0.038	0.056	0.070	0.082	0.092	0.100	0.107
570	0.010	0.015	0.036	0.052	0.065	0.076	0.086	0.093	0.100
590	0.009	0.014	0.033	0.048	0.061	0.071	0.080	0.087	0.093
610	0.009	0.013	0.031	0.045	0.057	0.067	0.075	0.082	0.087

Table 5. COP in terms of number of layers and temperature gradient

		Layers		
Temperature	**3 layers**	**4 layers**	**5 layers**	**6 layers**
50	0.049	0.075		0.111
60	0.023	0.043		0.07
70	X	0.022		0.044
80	X	X		
88	X	X	X	0.0154

Conclusions

Tighter integration of conventional electronics into a SiC based motor/traction drive, which creates thermal compatibility problems, can be aided by embedding TE layers strategically into the package. Combining SiC power electronics with conventional silicon controls and polypropylene film dc link capacitors, utilizing TE thermal control "islands," enables air cooling of the entire traction drive. The viability of air cooling is further enhanced when this concept is used in combination with higher temperature motor windings and advanced magnets.

Research indicates presently available TE maximum temperature rating/gradient and maximum heat flux are a little low. Emerging devices show great promise to make this concept highly attractive, so the project has been put on hold for the following year to evaluate these devices as they become available. Thin film Te cost on the surface appears very high, but their ability to produce high heat flux at a reasonable delta T brings the relative cost down lower than conventional TEs that do not perform as well.

Future Direction

When the project resumes, prototype models need to be built to validate the information that is being seen in the models. Further modeling needs to be performed to evaluate the entire traction drive heat removal system. Data from these models will indicate viability of air cooling of the whole system including motor/gears, SiC power electronics, silicon controls, and the dc link film capacitor.

When the technology of thin film TEs matures to a greater degree, ORNL will pursue further development of this or similar system concepts, possibly in partnership with a company such as MicroPelt®. Their work in the area of thin film devices looks very promising for the next year.

The need is to produce a geometry suitable for integration into the SiC/TE/silicon/film capacitor, using an array of devices in a flexible/conformable substrate. Multiple layering of the devices can be achieved by a coiled TE layer wrapped around the capacitor and electronics core, which can be made with a flexible circuit board containing thin film TE devices.

Three Areas of Particular Interest as TEs Mature

1. Maximum temperature limitations presently are approximately 80–150ºC. This temperature needs to approach 200ºC and higher to make this concept most feasible.
2. Heat flux numbers with good delta T need to improve above the present ~10 W/cm^2 at a few degrees C delta T. The multiple layering concept helps mitigate the problem with limited delta T, but higher numbers are still needed such that a maximum of 2–3 layers can produce a total delta T of ~150–200ºC.
3. Efficiency of the devices needs to improve. Thin film technology appears to be improving the COP of the TE device. This is definitely of interest and will benefit this concept, but it is not a critical path for this type of motor/inverter integration.

Publications

M. Starke, "Thermoelectrics for Cooling Power Electronics," Masters Thesis, University of Tennessee, August 2006

Patents

"Motor and Inverter Drive Design Concept Integrating Silicon Carbide Power Devices with Silicon Controls and Capacitors Utilizing Thermoelectrics," provisional patent filed July 8, 2006, with the U.S. Patent and Trademark Office.

References

1. J. Vandersande and J. Fleurial, "Thermal Management of Power Electronics using Thermoelectric Coolers," pp. 253–255 in *15th International Thermoelectrics Conference, March 1996*.
2. D. M. Rowe, *CRC Handbook of Thermoelectrics*, G. S. Nolas, J. Sharp, H. J. Goldsmid, *Thermoelectrics: Basic Principles and New Materials Developments*, Springer-Verlag Berlin Heidelberg, 2001.
3. G. W. Sutton, *Direct Energy Conversion*, McGraw-Hill, 1966.
4. D. T. Morelli, "Potential Applications of Advanced Thermoelectrics in the Automobile Industry," pp. 383–386 in *15th International Conference on Thermoelectrics, March 1996*.
5. G. Min, D. M. Rowe, and F. Volklein, "Integrated Thin Film Thermoelectric Cooler," *Electronics Letters*, **34**, p. 222–223 (January 1998).
6. H. Bottner, "Micropelt Miniaturized Thermoelectric Devices: Small Size, High Cooling Power Densities, Short Response Time," pp. 1–8 in *24th International Conference on Thermoelectrics, June 2005*.
7. H. Bottner, J. Nurnus, M. Braun, J. Wollenstein, F. Volkert, and A. Schubert, "Micropelt: State of the Art, Road Map and Applications," Infineon Technologies AG, München, Germany, 2004.
8. http://www.illinoiscapacitor.com/techcenter/lifecalculators.asp, Illinois Capacitor, Inc., 2006.
9. A. M. Hava, R. J. Kerkman, and T. A. Lipo, "Simple Analytical and Graphical Methods for Carrier-Based PWM-VSI Drives," *IEEE Transactions on Power Electronics*, **14**(1), 49–61 (January 1999).

Appendix A. Thermoelectric Device Manufacturer Comparison Data

MANUFACTURERS

Manufacturer	Product	Operating Th	Dimensions L	W	H	Qmax	Delta Tmax	Power Density	Max Operating Th	Price/W/cm^2
		C	mm	mm	mm	W/cm^2	C	kW/L		
3 Stone Company	TES1-0401A	25.00	3.40	1.80	2.40	3.59	67.00	14.98		$2.23
(Hong Kong)	TES1-0801A	25.00	3.40	3.40	2.40	3.72	67.00	15.50		$2.29
	TES1-1201A	25.00	5.00	3.40	2.40	3.82	67.00	15.93		$2.35
	TES1-1801A	25.00	5.00	5.00	2.40	3.88	67.00	16.17		$2.84
	TES1-3201A	25.00	6.60	6.60	2.40	3.95	67.00	16.45		$3.04
	TES1-0401B	25.00	4.20	2.20	2.70	3.46	67.00	12.83		$2.31
	TES1-0801B	25.00	4.20	4.20	2.70	3.68	67.00	13.65		$2.31
	TES1-1201B	25.00	6.20	4.20	2.70	3.73	67.00	13.80		$2.42
	TES1-1801B	25.00	6.20	6.20	2.70	3.80	67.00	14.07		$2.90
	TES1-3201B	25.00	8.30	8.30	2.70	3.76	67.00	13.92		$3.19
	TES1-0401C	25.00	2.20	4.20	2.40	4.33	67.00	18.04		$1.85
	TES1-0801C	25.00	4.20	4.20	2.40	4.59	67.00	19.13		$1.85
	TES1-1201C	25.00	4.20	6.20	2.40	4.65	67.00	19.36		$1.94
	TES1-1801C	25.00	6.20	6.20	2.40	4.73	67.00	19.73		$2.32
	TES1-3201C	25.00	8.30	8.30	2.40	4.69	67.00	19.54		$2.56
	TES1-0402D	25.00	2.20	4.20	2.20	5.84	67.00	26.56		$1.37
	TES1-0802D	25.00	4.23	4.20	2.20	6.08	67.00	27.63		$1.40
	TES1-1202D	25.00	4.20	6.20	2.20	6.18	67.00	28.10		$1.46
	TES1-1802D	25.00	6.20	6.20	2.20	6.32	67.00	28.73		$1.74
	TES1-3202D	25.00	8.30	8.30	2.20	6.27	67.00	28.50		$1.91
	TES1-0401E	25.00	1.80	3.40	2.40	3.59	67.00	14.98		$2.23
	TES1-0801E	25.00	3.40	3.40	2.40	3.72	67.00	15.50		$2.29
	TES1-1201E	25.00	3.40	5.00	2.40	3.82	67.00	15.93		$2.35
	TES1-1801E	25.00	5.00	5.00	2.40	3.88	67.00	16.17		$2.84
	TES1-3201E	25.00	6.60	6.60	2.40	3.95	67.00	16.45		$3.04
	TES1-0401F	25.00	2.20	4.20	2.70	3.46	67.00	12.83		$2.31
	TES1-0801F	25.00	4.20	4.20	2.70	3.68	67.00	13.65		$2.31
	TES1-1201F	25.00	4.20	6.20	2.70	3.73	67.00	13.80		$2.42
	TES1-1801F	25.00	6.20	6.20	2.70	3.80	67.00	14.07		$2.90
	TES1-3201F	25.00	8.30	8.30	2.70	3.76	67.00	13.92		$3.19
	TES1-0401G	25.00	2.20	4.20	2.40	4.33	67.00	18.04		$1.85
	TES1-0801G	25.00	4.20	4.20	2.40	4.59	67.00	19.13		$1.85
	TES1-1201G	25.00	4.20	6.20	2.40	4.65	67.00	19.36		$1.94
	TES1-1801G	25.00	6.20	6.20	2.40	4.73	67.00	19.73		$2.32
	TES1-3201G	25.00	8.30	8.30	2.40	4.69	67.00	19.54		$2.56
	TES1-0402H	25.00	2.20	4.20	2.20	5.84	67.00	26.56		$1.37
	TES1-0802H	25.00	4.20	4.20	2.20	6.12	67.00	27.83		$1.39
	TES1-1202H	25.00	4.20	6.20	2.20	6.18	67.00	28.10		$1.46
	TES1-1802H	25.00	6.20	6.20	2.20	6.32	67.00	28.73		$1.74
	TES1-3202H	25.00	8.30	8.30	2.20	6.27	67.00	28.50		$1.91
	TES1-3602H	25.00	6.60	13.20	2.20	4.13	67.00	18.78		
	TES1-0701I	25.00	1.80	3.40	2.40	6.21	67.00	25.87		$1.37
	TES1-1101I	25.00	3.40	5.00	2.40	3.53	67.00	14.71		$2.55
	TES1-1701I	25.00	3.40	5.00	2.40	5.41	67.00	22.55		$2.03
	TES1-3101I	25.00	5.00	6.60	2.40	5.06	67.00	21.09		$2.37
	TES1-0701J	25.00	4.20	4.20	2.40	3.23	67.00	13.46		$2.63
	TES1-1101J	25.00	4.20	6.20	2.70	3.42	67.00	12.66		$2.63
	TES1-1701J	25.00	6.20	6.20	2.70	3.56	67.00	13.20		$3.09
	TES1-3101J	25.00	8.30	8.30	2.70	3.64	67.00	13.49		$3.29
	TES1-0701K	25.00	4.20	4.20	2.70	4.02	67.00	14.91		$2.11
	TES1-1101K	25.00	4.20	6.20	2.70	4.26	67.00	15.79		$2.11
	TES1-1701K	25.00	6.20	6.20	2.40	4.47	67.00	18.64		$2.46
	TES1-3101K	25.00	8.30	8.30	2.40	4.54	67.00	18.93		$2.64
	TES1-0702L	25.00	4.20	4.20	2.20	5.39	67.00	24.48		$1.58
	TES1-1102L	25.00	6.20	6.20	2.20	3.88	67.00	17.62		$2.32
	TES1-1702L	25.00	6.20	6.20	2.20	5.98	67.00	27.20		$1.84
	TES1-1702L	25.00	6.60	6.60	2.20	5.99	67.00	27.24		$1.84
	TES1-3102L	25.00	8.30	8.30	2.20	6.07	67.00	27.58		$1.98
	TES1-0702M	25.00	6.00	6.00	3.40	2.78	67.00	8.17		$2.34
	TES1-1702M	25.00	12.00	9.00	3.40	2.22	67.00	6.54		$3.60
	TES1-3102M	25.00	12.00	12.00	3.40	3.06	67.00	8.99		$2.78
	TES1-6302M	25.00	18.00	25.00	3.40	2.00	67.00	5.88		$5.00
	TES1-7102M	25.00	8.00	18.00	3.40	7.01	67.00	20.63		$1.43

	TES1-0702N	25.00	12.00	8.00	4.00	1.25	67.00	3.13		$4.80
	TES1-1702N	25.00	15.00	12.00	4.00	1.61	67.00	4.03		$4.03
	TES1-3102N	25.00	20.00	15.00	4.00	1.77	67.00	4.42		$3.68
	TES1-4902N	25.00	20.00	20.00	4.00	1.98	67.00	4.94		$4.05
Advanced Thermoelectric	ST-71-1.0-3.0	25.00	22.40	22.40	3.20	3.14	71.00	9.81	150.00	$5.22
	ST-127-1.0-3.0	25.00	30.00	30.00	3.95	3.11	71.00	7.88	150.00	$5.32
	ST-71-1.0-4.0	25.00	22.40	22.40	4.20	3.85	71.00	9.16	150.00	$4.32
	ST-127-1.0-4.0	25.00	30.00	30.00	3.95	4.22	72.00	10.69	150.00	$3.97
	ST-127-1.4-4.0	25.00	40.00	40.00	4.20	2.38	72.00	5.65	150.00	$7.63
	ST-71-1.4-6.0	25.00	30.00	30.00	4.20	3.56	72.00	8.47	150.00	$4.73
	ST-127-1.4-6.0	25.00	40.00	40.00	4.20	3.56	71.00	8.48	150.00	$5.26
	ST-71-1.4-8.5	25.00	30.00	30.00	3.95	5.00	72.00	12.66	150.00	$3.52
	ST-127-1.4-8.5	25.00	40.00	40.00	3.95	5.00	72.00	12.66	150.00	$3.96
ADV Engineering	A-TM 8.5-127-1.4		40.00	40.00	3.70	4.50	72.00	12.16	150.00	
(Russia)	A-TM 6.0-127-1.4		40.00	40.00	4.20	3.31	72.00	7.89	150.00	
	A-TM 3.9-127-1.4		40.00	40.00	5.10	3.31	73.00	6.50	150.00	
	A-TM 3.9-127-1.0		30.00	30.00	3.90	3.78	71.00	9.69	150.00	
	A-TM 37.5-49-3.0		40.00	40.00	4.30	8.13	71.00	18.90	150.00	
	A-TM 6.0-31-1.4		20.00	20.00	4.20	3.13	72.00	7.44	150.00	
Altec	Altec-CM-1-S-SQ-7-0.8x0.8-2.5		6.00	6.00	4.40	1.67	72.00	3.79	200.00	
(Ukraine)	Altec-CM-1-S-SQ-17-0.8x0.8-2.5		9.00	9.00	44.00	1.85	72.00	0.42	200.00	
	Altec-CM-1-S-SQ-31-0.8x0.8-2.5		12.00	12.00	4.40	1.88	72.00	4.26	200.00	
	Altec-CM-1-S-SQ-63-0.8x0.8-2.5		12.00	24.00	4.40	1.88	72.00	4.26	200.00	
	Altec-CM-1-S-SQ-71-0.8x0.8-2.5		18.00	18.00	4.40	1.88	72.00	4.28	200.00	
	Altec-CM-1-S-SQ-127-0.8x0.8-2.5		24.00	24.00	4.40	1.91	72.00	4.34	200.00	
	Altec-CM-1-S-SQ-7-0.8x0.8-2.0		6.00	6.00	3.90	1.94	71.00	4.99	200.00	
	Altec-CM-1-S-SQ-17-0.8x0.8-2.0		9.00	9.00	3.90	2.22	71.00	5.70	200.00	
	Altec-CM-1-S-SQ-31-0.8x0.8-2.0		12.00	12.00	3.90	2.29	71.00	5.88	200.00	
	Altec-CM-1-S-SQ-63-0.8x0.8-2.0		12.00	24.00	3.90	2.33	71.00	5.97	200.00	
	Altec-CM-1-S-SQ-71-0.8x0.8-2.0		18.00	18.00	3.90	2.35	71.00	6.01	200.00	
	Altec-CM-1-S-SQ-127-0.8x0.8-2.0		24.00	24.00	3.90	2.34	71.00	6.01	200.00	
	Altec-CM-1-S-SQ-7-0.8x0.8-1.5		6.00	6.00	3.40	2.78	70.00	8.17	200.00	
	Altec-CM-1-S-SQ-17-0.8x0.8-1.5		9.00	9.00	3.40	2.96	70.00	8.71	200.00	
	Altec-CM-1-S-SQ-31-0.8x0.8-1.5		12.00	12.00	3.40	2.99	70.00	8.78	200.00	
	Altec-CM-1-S-SQ-63-0.8x0.8-1.5		12.00	24.00	3.40	3.06	70.00	8.99	200.00	
	Altec-CM-1-S-SQ-71-0.8x0.8-1.5		18.00	48.00	3.40	1.16	70.00	3.40	200.00	
	Altec-CM-1-S-SQ-127-0.8x0.8-1.5		24.00	24.00	3.40	3.09	70.00	9.09	200.00	
	Altec-CM-1-S-SQ-7-0.8x0.8-1.3		6.00	6.00	3.20	3.06	69.00	9.55	200.00	
	Altec-CM-1-S-SQ-17-0.8x0.8-1.3		9.00	9.00	3.20	3.33	69.00	10.42	200.00	
	Altec-CM-1-S-SQ-31-0.8x0.8-1.3		12.00	12.00	3.20	3.40	69.00	10.63	200.00	
	Altec-CM-1-S-SQ-63-0.8x0.8-1.3		12.00	24.00	3.20	3.47	69.00	10.85	200.00	
	Altec-CM-1-S-SQ-71-0.8x0.8-1.3		18.00	18.00	3.20	3.49	69.00	10.90	200.00	
	Altec-CM-1-S-SQ-127-0.8x0.8-1.3		24.00	24.00	3.20	3.51	69.00	10.96	200.00	
	Altec-CM-1-S-SQ-7-0.8x0.8-1.15		6.00	6.00	3.10	3.61	68.00	11.65	200.00	
	Altec-CM-1-S-SQ-17-0.8x0.8-1.15		9.00	9.00	3.10	3.70	68.00	11.95	200.00	
	Altec-CM-1-S-SQ-31-0.8x0.8-1.15		12.00	12.00	3.10	3.82	68.00	12.32	200.00	
	Altec-CM-1-S-SQ-63-0.8x0.8-1.15		12.00	24.00	3.10	3.89	68.00	12.54	200.00	
	Altec-CM-1-S-SQ-71-0.8x0.8-1.15		18.00	18.00	3.10	3.89	68.00	12.54	200.00	
	Altec-CM-1-S-SQ-127-0.8x0.8-1.15		24.00	24.00	3.10	3.91	68.00	12.60	200.00	
	Altec-CM-1-S-SQ-7-1.0x1.0-2.5		8.00	8.00	4.50	1.41	72.00	3.13	200.00	
	Altec-CM-1-S-SQ-17-1.0x1.0-2.5		12.00	12.00	4.50	1.53	72.00	3.40	200.00	
	Altec-CM-1-S-SQ-31-1.0x1.0-2.5		15.00	15.00	4.50	1.78	72.00	3.95	200.00	
	Altec-CM-1-S-SQ-63-1.0x1.0-2.5		15.00	30.00	4.50	1.82	72.00	4.05	200.00	
	Altec-CM-1-S-SQ-71-1.0x1.0-2.5		23.00	23.00	4.50	1.74	72.00	3.86	200.00	
	Altec-CM-1-S-SQ-127-1.0x1.0-2.5		30.00	30.00	4.50	1.83	72.00	4.07	200.00	
	Altec-CM-1-S-SQ-7-1.0x1.0-2.0		8.00	8.00	4.00	1.72	71.00	4.30	200.00	
	Altec-CM-1-S-SQ-17-1.0x1.0-2.0		12.00	12.00	4.00	1.88	71.00	4.69	200.00	
	Altec-CM-1-S-SQ-31-1.0x1.0-2.0		15.00	15.00	4.00	2.22	71.00	5.56	200.00	
	Altec-CM-1-S-SQ-63-1.0x1.0-2.0		15.00	30.00	4.00	2.24	71.00	5.61	200.00	
	Altec-CM-1-S-SQ-71-1.0x1.0-2.0		23.00	23.00	4.00	2.16	71.00	5.39	200.00	
	Altec-CM-1-S-SQ-127-1.0x1.0-2.0		30.00	30.00	4.00	2.27	71.00	5.67	200.00	
	Altec-CM-1-S-SQ-7-1.0x1.0-1.5		8.00	8.00	3.50	2.34	70.00	6.70	200.00	
	Altec-CM-1-S-SQ-17-1.0x1.0-1.5		12.00	12.00	3.50	2.50	70.00	7.14	200.00	
	Altec-CM-1-S-SQ-31-1.0x1.0-1.5		15.00	15.00	3.50	2.89	70.00	8.25	200.00	
	Altec-CM-1-S-SQ-63-1.0x1.0-1.5		15.00	30.00	3.50	2.96	70.00	8.44	200.00	

Altec-CM-1-S-SQ-71-1.0x1.0-1.5	23.00	23.00	3.50	2.84	70.00	8.10	200.00
Altec-CM-1-S-SQ-127-1.0x1.0-1.5	30.00	30.00	3.50	2.98	70.00	8.51	200.00
Altec-CM-1-S-SQ-7-1.0x1.0-1.3	8.00	8.00	3.30	2.66	69.00	8.05	200.00
Altec-CM-1-S-SQ-17-1.0x1.0-1.3	12.00	12.00	3.30	2.85	69.00	8.63	200.00
Altec-CM-1-S-SQ-31-1.0x1.0-1.3	15.00	15.00	3.30	3.33	69.00	10.10	200.00
Altec-CM-1-S-SQ-63-1.0x1.0-1.3	15.00	30.00	3.30	3.40	69.00	10.30	200.00
Altec-CM-1-S-SQ-71-1.0x1.0-1.3	23.00	23.00	3.30	3.25	69.00	9.85	200.00
Altec-CM-1-S-SQ-127-1.0x1.0-1.3	30.00	30.00	3.30	3.42	69.00	10.37	200.00
Altec-CM-1-S-SQ-7-1.0x1.0-1.15	8.00	8.00	3.20	2.97	68.00	9.28	200.00
Altec-CM-1-S-SQ-17-1.0x1.0-1.15	12.00	12.00	3.20	3.13	68.00	9.77	200.00
Altec-CM-1-S-SQ-31-1.0x1.0-1.15	15.00	15.00	3.20	3.64	68.00	11.39	200.00
Altec-CM-1-S-SQ-63-1.0x1.0-1.15	15.00	30.00	3.20	3.73	68.00	11.67	200.00
Altec-CM-1-S-SQ-71-1.0x1.0-1.15	23.00	23.00	3.20	3.57	68.00	11.16	200.00
Altec-CM-1-S-SQ-127-1.0x1.0-1.15	30.00	30.00	3.20	3.76	68.00	11.74	200.00
Altec-CM-1-S-SQ-7-1.0x1.0-2.5	8.00	8.00	4.50	1.41	72.00	3.13	200.00
Altec-CM-1-S-SQ-17-1.0x1.0-2.5	12.00	12.00	4.50	1.53	72.00	3.40	200.00
Altec-CM-1-S-SQ-31-1.0x1.0-2.5	15.00	15.00	4.50	1.78	72.00	3.95	200.00
Altec-CM-1-S-SQ-63-1.0x1.0-2.5	15.00	30.00	4.50	1.82	72.00	4.05	200.00
Altec-CM-1-S-SQ-71-1.0x1.0-2.5	23.00	23.00	4.50	1.74	72.00	3.86	200.00
Altec-CM-1-S-SQ-127-1.0x1.0-2.5	30.00	30.00	4.50	1.83	72.00	4.07	200.00
Altec-CM-1-S-SQ-7-1.0x1.0-2.0	8.00	8.00	4.00	1.72	71.00	4.30	200.00
Altec-CM-1-S-SQ-17-1.0x1.0-2.0	12.00	12.00	4.00	1.88	71.00	4.69	200.00
Altec-CM-1-S-SQ-31-1.0x1.0-2.0	15.00	15.00	4.00	2.22	71.00	5.56	200.00
Altec-CM-1-S-SQ-63-1.0x1.0-2.0	15.00	30.00	4.00	2.24	71.00	5.61	200.00
Altec-CM-1-S-SQ-71-1.0x1.0-2.0	23.00	23.00	4.00	2.16	71.00	5.39	200.00
Altec-CM-1-S-SQ-127-1.0x1.0-2.0	30.00	30.00	4.00	2.27	71.00	5.67	200.00
Altec-CM-1-S-SQ-7-1.0x1.0-1.5	8.00	8.00	3.50	2.34	70.00	6.70	200.00
Altec-CM-1-S-SQ-17-1.0x1.0-1.5	12.00	12.00	3.50	2.50	70.00	7.14	200.00
Altec-CM-1-S-SQ-31-1.0x1.0-1.5	15.00	15.00	3.50	2.89	70.00	8.25	200.00
Altec-CM-1-S-SQ-63-1.0x1.0-1.5	15.00	30.00	3.50	2.96	70.00	8.44	200.00
Altec-CM-1-S-SQ-71-1.0x1.0-1.5	23.00	23.00	3.50	2.84	70.00	8.10	200.00
Altec-CM-1-S-SQ-127-1.0x1.0-1.5	30.00	30.00	3.50	2.98	70.00	8.51	200.00
Altec-CM-1-S-SQ-7-1.0x1.0-1.3	8.00	8.00	3.30	2.66	69.00	8.05	200.00
Altec-CM-1-S-SQ-17-1.0x1.0-1.3	12.00	12.00	3.30	2.85	69.00	8.63	200.00
Altec-CM-1-S-SQ-31-1.0x1.0-1.3	15.00	15.00	3.30	3.33	69.00	10.10	200.00
Altec-CM-1-S-SQ-63-1.0x1.0-1.3	15.00	30.00	3.30	3.40	69.00	10.30	200.00
Altec-CM-1-S-SQ-71-1.0x1.0-1.3	23.00	23.00	3.30	3.25	69.00	9.85	200.00
Altec-CM-1-S-SQ-127-1.0x1.0-1.3	30.00	30.00	3.30	3.42	69.00	10.37	200.00
Altec-CM-1-S-SQ-7-1.0x1.0-1.15	8.00	8.00	3.20	2.97	68.00	9.28	200.00
Altec-CM-1-S-SQ-17-1.0x1.0-1.15	12.00	12.00	3.20	3.13	68.00	9.77	200.00
Altec-CM-1-S-SQ-31-1.0x1.0-1.15	15.00	15.00	3.20	3.64	68.00	11.39	200.00
Altec-CM-1-S-SQ-63-1.0x1.0-1.15	15.00	30.00	3.20	3.73	68.00	11.67	200.00
Altec-CM-1-S-SQ-71-1.0x1.0-1.15	23.00	23.00	3.20	3.57	68.00	11.16	200.00
Altec-CM-1-S-SQ-127-1.0x1.0-1.15	30.00	30.00	3.20	3.76	68.00	11.74	200.00
Altec-CM-1-S-SQ-7-1.2x1.2-2.5	8.00	8.00	4.90	2.03	72.00	4.15	200.00
Altec-CM-1-S-SQ-17-1.2x1.2-2.5	12.00	12.00	4.90	2.22	72.00	4.54	200.00
Altec-CM-1-S-SQ-31-1.2x1.2-2.5	15.00	15.00	4.90	2.58	72.00	5.26	200.00
Altec-CM-1-S-SQ-63-1.2x1.2-2.5	15.00	30.00	4.90	2.62	72.00	5.35	200.00
Altec-CM-1-S-SQ-71-1.2x1.2-2.5	23.00	23.00	4.90	2.51	72.00	5.13	200.00
Altec-CM-1-S-SQ-127-1.2x1.2-2.5	30.00	30.00	4.90	2.64	72.00	5.40	200.00
Altec-CM-1-S-SQ-7-1.2x1.2-2.0	8.00	8.00	4.40	2.50	71.00	5.68	200.00
Altec-CM-1-S-SQ-17-1.2x1.2-2.0	12.00	12.00	4.40	2.78	71.00	6.31	200.00
Altec-CM-1-S-SQ-31-1.2x1.2-2.0	15.00	15.00	4.40	3.16	71.00	7.17	200.00
Altec-CM-1-S-SQ-63-1.2x1.2-2.0	15.00	30.00	4.40	3.29	71.00	7.47	200.00
Altec-CM-1-S-SQ-71-1.2x1.2-2.0	23.00	23.00	4.40	3.16	71.00	7.17	200.00
Altec-CM-1-S-SQ-127-1.2x1.2-2.0	30.00	30.00	4.40	3.31	71.00	7.53	200.00
Altec-CM-1-S-SQ-7-1.2x1.2-1.5	8.00	8.00	3.90	3.44	70.00	8.81	200.00
Altec-CM-1-S-SQ-17-1.2x1.2-1.5	12.00	12.00	3.90	3.61	70.00	9.26	200.00
Altec-CM-1-S-SQ-31-1.2x1.2-1.5	15.00	15.00	3.90	4.27	70.00	10.94	200.00
Altec-CM-1-S-SQ-63-1.2x1.2-1.5	15.00	30.00	3.90	4.31	70.00	11.05	200.00
Altec-CM-1-S-SQ-71-1.2x1.2-1.5	23.00	23.00	3.90	4.14	70.00	10.62	200.00
Altec-CM-1-S-SQ-127-1.2x1.2-1.5	30.00	30.00	3.90	4.36	70.00	11.17	200.00
Altec-CM-1-S-SQ-7-1.2x1.2-1.3	8.00	8.00	3.70	3.91	69.00	10.56	200.00
Altec-CM-1-S-SQ-17-1.2x1.2-1.3	12.00	12.00	3.70	4.17	69.00	11.26	200.00
Altec-CM-1-S-SQ-31-1.2x1.2-1.3	15.00	15.00	3.70	4.84	69.00	13.09	200.00
Altec-CM-1-S-SQ-63-1.2x1.2-1.3	15.00	30.00	3.70	4.93	69.00	13.33	200.00
Altec-CM-1-S-SQ-71-1.2x1.2-1.3	23.00	23.00	3.70	4.74	69.00	12.82	200.00
Altec-CM-1-S-SQ-127-1.2x1.2-1.3	30.00	30.00	3.70	4.98	69.00	13.45	200.00

	Altec-CM-1-S-SQ-7-1.2x1.2-1.15	8.00	8.00	3.50	4.22	68.00	12.05	200.00
	Altec-CM-1-S-SQ-17-1.2x1.2-1.15	12.00	12.00	3.50	4.58	68.00	13.10	200.00
	Altec-CM-1-S-SQ-31-1.2x1.2-1.15	15.00	15.00	3.50	5.33	68.00	15.24	200.00
	Altec-CM-1-S-SQ-63-1.2x1.2-1.15	15.00	30.00	3.50	5.44	68.00	15.56	200.00
	Altec-CM-1-S-SQ-71-1.2x1.2-1.15	23.00	23.00	3.50	5.22	68.00	14.91	200.00
	Altec-CM-1-S-SQ-127-1.2x1.2-1.15	30.00	30.00	3.50	5.48	68.00	15.65	200.00
	Altec-CM-1-S-SQ-7-1.4x1.4-2.5	10.00	10.00	4.90	1.80	72.00	3.67	200.00
	Altec-CM-1-S-SQ-17-1.4x1.4-2.5	15.00	15.00	4.90	1.96	72.00	3.99	200.00
	Altec-CM-1-S-SQ-31-1.4x1.4-2.5	20.00	20.00	4.90	2.03	72.00	4.13	200.00
	Altec-CM-1-S-SQ-63-1.4x1.4-2.5	20.00	40.00	4.90	2.05	72.00	4.18	200.00
	Altec-CM-1-S-SQ-71-1.4x1.4-2.5	30.00	30.00	4.90	2.06	72.00	4.20	200.00
	Altec-CM-1-S-SQ-127-1.4x1.4-2.5	40.00	40.00	4.90	2.06	72.00	4.21	200.00
	Altec-CM-1-S-SQ-7-1.4x1.4-2.0	10.00	10.00	4.40	2.30	71.00	5.23	200.00
	Altec-CM-1-S-SQ-17-1.4x1.4-2.0	15.00	15.00	4.40	2.40	71.00	5.45	200.00
	Altec-CM-1-S-SQ-31-1.4x1.4-2.0	20.00	20.00	4.40	2.48	71.00	5.63	200.00
	Altec-CM-1-S-SQ-63-1.4x1.4-2.0	20.00	40.00	4.40	2.53	71.00	5.74	200.00
	Altec-CM-1-S-SQ-71-1.4x1.4-2.0	30.00	30.00	4.40	2.53	71.00	5.76	200.00
	Altec-CM-1-S-SQ-127-1.4x1.4-2.0	40.00	40.00	4.40	2.54	71.00	5.78	200.00
	Altec-CM-1-S-SQ-7-1.4x1.4-1.5	10.00	10.00	3.90	3.00	70.00	7.69	200.00
	Altec-CM-1-S-SQ-17-1.4x1.4-1.5	15.00	15.00	3.90	3.16	70.00	8.09	200.00
	Altec-CM-1-S-SQ-63-1.4x1.4-1.5	20.00	40.00	3.90	3.31	70.00	8.49	200.00
	Altec-CM-1-S-SQ-71-1.4x1.4-1.5	30.00	30.00	3.90	3.32	70.00	8.52	200.00
	Altec-CM-1-S-SQ-127-1.4x1.4-1.5	40.00	40.00	3.90	3.34	70.00	8.57	200.00
	Altec-CM-1-S-SQ-7-1.4x1.4-1.3	10.00	10.00	3.70	3.40	69.00	9.19	200.00
	Altec-CM-1-S-SQ-31-2.0x2.0-2.5	20.00	20.00	4.90	4.08	72.00	8.32	200.00
	Altec-CM-1-S-SQ-63-2.0x2.0-2.5	20.00	40.00	4.90	4.15	72.00	8.47	200.00
	Altec-CM-1-S-SQ-71-2.0x2.0-2.5	30.00	30.00	4.90	4.17	72.00	8.50	200.00
	Altec-CM-1-S-SQ-127-2.0x2.0-2.5	40.00	40.00	4.90	4.19	72.00	8.55	200.00
	Altec-CM-1-S-SQ-7-2.0x2.0-2.0	10.00	10.00	4.80	4.60	71.00	9.58	200.00
	Altec-CM-1-S-SQ-17-2.0x2.0-2.0	15.00	15.00	4.80	4.89	71.00	10.19	200.00
	Altec-CM-1-S-SQ-31-2.0x2.0-2.0	20.00	20.00	4.80	5.03	71.00	10.47	200.00
	Altec-CM-1-S-SQ-63-2.0x2.0-2.0	20.00	40.00	4.80	5.10	71.00	10.63	200.00
	Altec-CM-1-S-SQ-71-2.0x2.0-2.0	30.00	30.00	4.80	5.11	71.00	10.65	200.00
	Altec-CM-1-S-SQ-127-2.0x2.0-2.0	40.00	40.00	4.80	5.14	71.00	10.72	200.00
	Altec-CM-1-S-SQ-7-2.0x2.0-1.5	10.00	10.00	4.60	6.00	70.00	13.04	200.00
	Altec-CM-1-S-SQ-17-2.0x2.0-1.5	15.00	15.00	4.60	6.44	70.00	14.01	200.00
	Altec-CM-1-S-SQ-31-2.0x2.0-1.5	20.00	20.00	4.60	6.63	70.00	14.40	200.00
	Altec-CM-1-S-SQ-63-2.0x2.0-1.5	20.00	40.00	4.60	6.74	70.00	14.65	200.00
	Altec-CM-1-S-SQ-71-2.0x2.0-1.5	30.00	30.00	4.60	6.77	70.00	14.71	200.00
	Altec-CM-1-S-SQ-127-2.0x2.0-1.5	40.00	40.00	4.60	6.80	70.00	14.78	200.00
	Altec-CM-1-S-SQ-7-2.0x2.0-1.3	10.00	10.00	4.70	6.90	69.00	14.68	200.00
	Altec-CM-1-S-SQ-17-2.0x2.0-1.3	15.00	15.00	4.70	7.33	69.00	15.60	200.00
	Altec-CM-1-S-SQ-31-2.0x2.0-1.3	20.00	20.00	4.70	7.55	69.00	16.06	200.00
	Altec-CM-1-S-SQ-63-2.0x2.0-1.3	20.00	40.00	4.70	7.68	69.00	16.33	200.00
	Altec-CM-1-S-SQ-71-2.0x2.0-1.3	30.00	30.00	4.70	7.70	69.00	16.38	200.00
	Altec-CM-1-S-SQ-127-2.0x2.0-1.3	40.00	40.00	4.70	7.74	69.00	16.48	200.00
	Altec-CM-1-S-SQ-7-2.0x2.0-1.15	10.00	10.00	4.70	8.10	68.00	17.23	200.00
	Altec-CM-1-S-SQ-17-2.0x2.0-1.15	15.00	15.00	4.70	8.62	68.00	18.35	200.00
	Altec-CM-1-S-SQ-31-2.0x2.0-1.15	20.00	20.00	4.70	8.90	68.00	18.94	200.00
	Altec-CM-1-S-SQ-63-2.0x2.0-1.15	20.00	40.00	4.70	9.03	68.00	19.20	200.00
	Altec-CM-1-S-SQ-71-2.0x2.0-1.15	30.00	30.00	4.70	9.07	68.00	19.29	200.00
	Altec-CM-1-S-SQ-127-2.0x2.0-1.15	40.00	40.00	4.70	9.11	68.00	19.39	200.00
Custom Thermoelectric	00901-9G30-11D	5.99	4.00	2.92	2.71	68.00	9.29	225.00
	01801-9G30-11B	8.13	6.10	2.92	2.62	68.00	8.98	225.00
	03601-9G30-11B	13.46	10.16	2.92	1.90	68.00	6.51	225.00
	00901-9G30-15D	5.99	4.00	2.46	3.67	68.00	14.93	225.00
	03601-9G30-15B	13.46	10.16	2.46	2.59	68.00	10.52	225.00
	00901-9G30-18D	5.99	4.00	2.24	4.17	68.00	18.63	225.00
	01801-9G30-18B	8.13	6.10	2.24	4.23	68.00	18.90	225.00
	03601-9G30-18B	13.46	10.16	2.24	3.14	68.00	14.04	225.00
	04101-9G30-20B	19.05	12.19	3.94	2.33	68.00	5.90	225.00
	04101-9G30-27B	19.05	12.19	3.43	3.14	68.00	9.16	225.00
	00901-9L31-04B	19.05	15.75	5.28	0.79	68.00	1.49	225.00
	01701-9L31-04B	23.11	23.11	5.28	0.86	68.00	1.62	225.00
	03101-9L31-04B	31.75	31.75	5.28	0.81	68.00	1.53	225.00
	04901-9L31-04B	38.10	38.10	5.28	0.89	68.00	1.68	225.00
	0711-9L31-04B	29.72	29.72	4.57	2.10	68.00	4.60	225.00

	12601-9L31-04B		49.78	49.78	5.28	1.34	68.00	2.53	225.00
	12701-9L31-04B		42.67	42.67	5.28	1.83	68.00	3.47	225.00
	12701-9L31-04C		50.80	50.80	5.28	1.29	68.00	2.45	225.00
	00901-9L31-06B		19.05	15.75	4.70	1.18	68.00	2.52	225.00
	01701-9L31-06B		23.11	23.11	4.70	1.25	68.00	2.67	225.00
	03101-9L31-06B		31.75	31.75	4.70	1.21	68.00	2.57	225.00
	04901-9L31-06B		38.10	38.10	4.70	1.33	68.00	2.83	225.00
	0711-9L31-06B		29.72	29.72	4.06	3.17	68.00	7.81	225.00
	12601-9L31-06B		49.78	49.78	4.70	2.00	68.00	4.26	225.00
	12701-9L31-06B		42.67	42.67	4.70	2.75	68.00	5.84	225.00
	12701-9L31-06C		50.80	50.80	4.70	1.94	68.00	4.12	225.00
	00901-9L31-09B		19.05	15.75	5.28	1.77	68.00	3.36	225.00
	01701-9L31-09B		23.11	23.11	5.28	1.89	68.00	3.58	225.00
	03101-9L31-09B		31.75	31.75	5.28	1.82	68.00	3.44	225.00
	04901-9L31-09B		38.10	38.10	5.28	2.00	68.00	3.78	225.00
	0711-9L31-09B		29.72	29.72	3.56	4.76	68.00	13.36	225.00
	12601-9L31-09B		49.78	49.78	5.28	3.01	68.00	5.69	225.00
	12701-9L31-09B		42.67	42.67	5.28	4.12	68.00	7.81	225.00
	12701-9L31-09C		50.80	50.80	5.28	2.91	68.00	5.51	225.00
	00901-9L31-14B		19.05	15.75	4.70	2.77	68.00	5.89	225.00
	01701-9L31-14B		23.11	23.11	4.70	2.92	68.00	6.21	225.00
	03101-9L31-14B		31.75	31.75	4.70	2.83	68.00	6.02	225.00
	04901-9L31-14B		38.10	38.10	4.70	3.11	68.00	6.61	225.00
	12601-9L31-14B		49.78	49.78	4.70	4.67	68.00	9.94	225.00
	12701-9L31-14C		50.80	50.80	4.70	4.53	68.00	9.63	225.00
Huimao	TEC1-007106T150	27.00	30.00	30.00	3.90	3.51	65.00	9.00	150.00
(Beijing)	TEC1-007110T150	27.00	30.00	30.00	3.30	5.86	62.00	17.74	150.00
	TEC1-007112T150	27.00	38.00	38.00	3.90	4.38	63.00	11.22	150.00
	TEC1-007118T150	27.00	38.00	38.00	3.40	6.57	60.00	19.31	150.00
	TEC1-007106T200	27.00	30.00	30.00	3.90	3.51	65.00	9.00	200.00
	TEC1-007110T200	27.00	30.00	30.00	3.30	5.86	62.00	17.74	200.00
	TEC1-007112T200	27.00	38.00	38.00	3.90	4.38	63.00	11.22	200.00
	TEC1-007118T200	27.00	38.00	38.00	3.40	6.57	60.00	19.31	200.00
	TEC1-007106T250	27.00	30.00	30.00	3.90	3.51	65.00	9.00	250.00
	TEC1-007110T250	27.00	30.00	30.00	3.30	5.86	62.00	17.74	250.00
	TEC1-007112T250	27.00	38.00	38.00	3.90	4.38	63.00	11.22	250.00
	TEC1-007118T250	27.00	38.00	38.00	3.40	6.57	60.00	19.31	250.00
	TEC1-12706T150	27.00	40.00	40.00	3.90	3.53	65.00	9.05	150.00
	TEC1-12710T150	27.00	40.00	40.00	3.30	5.89	62.00	17.84	150.00
	TEC1-12712T150	27.00	50.00	50.00	3.90	4.52	63.00	11.59	150.00
	TEC1-12718T150	27.00	50.00	50.00	3.40	6.78	60.00	19.95	150.00
	TEC1-12706T200	27.00	40.00	40.00	3.90	3.53	65.00	9.05	200.00
	TEC1-12710T200	27.00	40.00	40.00	3.30	5.89	62.00	17.84	200.00
	TEC1-12712T200	27.00	50.00	50.00	3.90	4.52	63.00	11.59	200.00
	TEC1-12718T200	27.00	50.00	50.00	3.40	6.78	60.00	19.95	200.00
	TEC1-12706T250	27.00	40.00	40.00	3.90	3.53	65.00	9.05	250.00
	TEC1-12710T250	27.00	40.00	40.00	3.30	5.89	62.00	17.84	250.00
	TEC1-12712T250	27.00	50.00	50.00	3.90	4.52	63.00	11.59	250.00
	TEC1-12718T250	27.00	50.00	50.00	3.40	6.78	60.00	19.95	250.00
	TEC1-03140T150	27.00	40.00	40.00	5.00	5.34	63.00	10.69	150.00
	TEC1-03140T200	27.00	40.00	40.00	5.00	5.34	63.00	10.69	200.00
	TEC1-03140T250	27.00	40.00	40.00	5.00	5.34	63.00	10.69	250.00
Fandis	TM1-1273030-NX	25.00	30.00	30.00	3.80	2.94	71.00	7.75	150.00
(Italy)	TM1-1273039-NX	25.00	30.00	30.00	3.60	3.78	71.00	10.49	150.00
	TM1-1274039-NX	25.00	40.00	40.00	4.70	2.13	69.00	4.52	150.00
	TM1-1274060-NX	25.00	40.00	40.00	3.80	3.31	71.00	8.72	150.00
	TM1-1274085-NX	25.00	40.00	40.00	3.40	4.50	71.00	13.24	150.00
	TM2-1274050-N	25.00	40.00	40.00	11.70	1.06	95.00	0.91	150.00
	TM2-1274065-N	25.00	40.00	40.00	7.50	2.19	86.00	2.92	150.00
Ferrotec	9500/018/012 M P		6.05	6.05	2.09	3.55	66.00	16.99	135.00
	9502/031/012 M P		7.97	7.97	2.09	3.62	66.00	17.32	135.00
	9502/065/012 M P		12.10	11.20	2.09	3.54	66.00	16.95	135.00
	9500/018/018 M P		6.05	6.05	1.79	5.19	66.00	29.00	135.00
	9502/031/018 M P		7.97	7.97	1.79	5.35	66.00	29.90	135.00
	9502/065/018 M P		12.10	11.20	1.79	5.31	66.00	29.68	135.00

	9501/128/030 B		29.70	29.70	3.94	3.29	72.00	8.34	135.00	
	9501/127/030 B		29.70	29.70	3.94	3.29	72.00	8.34	135.00	
	9501/071/030 B		22.40	22.40	3.18	3.19	72.00	10.03	135.00	
	9501/031/030 B		15.10	15.10	3.18	3.07	72.00	9.65	135.00	
	9501/023/030 B		7.39	22.40	3.18	3.14	72.00	9.88	135.00	
	9501/017/030 B		11.50	11.50	3.18	2.87	72.00	9.04	135.00	
	9501/128/040 B		29.70	29.70	3.94	4.31	72.00	10.93	135.00	
	9500/128/040 B		39.70	39.70	4.16	2.41	72.00	5.80	135.00	
	9501/127/040 B		29.70	29.70	3.94	4.31	72.00	10.93	135.00	
	9500/127/040 B		39.70	39.70	4.16	2.41	72.00	5.80	135.00	
	9501/071/040 B		22.40	22.40	3.18	4.19	72.00	13.16	135.00	
	9500/071/040 B		29.80	29.80	4.16	2.36	72.00	5.68	135.00	
	9501/063/040 B		21.10	39.70	4.16	2.15	72.00	5.17	135.00	
	9500/035/040 B		15.10	29.80	4.16	2.22	72.00	5.34	135.00	
	9501/031/040 B		15.10	15.10	3.18	4.08	72.00	12.83	135.00	
	9500/031/040 B		20.00	20.00	4.16	2.33	72.00	5.59	135.00	
	9501/023/040 B		7.39	22.40	3.18	4.17	72.00	13.11	135.00	
	9501/017/040 B		11.50	11.50	3.18	3.86	72.00	12.13	135.00	
	9500/017/040 B		15.01	15.10	4.16	2.25	72.00	5.41	135.00	
	9500/035/060 B		15.10	29.80	4.16	3.56	72.00	8.55	135.00	
	9500/031/060 B		20.00	20.00	4.16	3.50	72.00	8.41	135.00	
	9500/017/060 B		15.10	15.10	4.16	3.33	72.00	8.01	135.00	
	9500/071/060 B		29.80	29.80	4.16	3.60	72.00	8.66	135.00	
	9500/127/060 B		39.70	39.70	4.16	3.62	72.00	8.69	135.00	
	9501/127/060 B		29.70	29.70	3.61	6.46	72.00	17.90	135.00	
	9500/128/060 B		39.70	39.70	4.16	3.62	72.00	8.69	135.00	
	9500/017/085 B		15.10	15.10	3.94	4.82	72.00	12.24	135.00	
	9500/031/085 B		20.00	20.00	3.94	5.00	72.00	12.69	135.00	
	9500/035/085 B		15.10	29.80	3.94	4.89	72.00	12.41	135.00	
	9500/063/085 B		39.70	39.70	3.94	2.54	72.00	6.44	135.00	
	9500/071/085 B		29.80	29.80	3.94	5.07	72.00	12.86	135.00	
	9500/127/085 B		39.70	39.70	3.94	5.08	72.00	12.88	135.00	
	9500/128/085 B		39.70	39.70	3.94	5.08	72.00	12.88	135.00	
	9500/031/090 B		29.80	29.80	4.60	2.48	72.00	5.39	135.00	
	9500/071/090 B		29.80	29.80	3.94	5.29	72.00	13.43	135.00	
	9500/097/090 B		29.80	29.80	3.55	7.32	72.00	20.62	135.00	
	9501/063/100 B		20.10	39.70	3.64	5.89	72.00	16.18	135.00	
	9500/127/100 B		39.70	39.70	3.64	6.03	72.00	16.56	135.00	
	9504/071/120 B		40.10	40.10	4.65	3.92	72.00	8.43	135.00	
	9504/017/150 B		22.00	22.00	4.65	3.93	72.00	8.44	135.00	
	9500/031/150 B		29.80	29.80	4.60	3.94	72.00	8.57	135.00	
	9504/071/150 B		40.10	40.10	4.65	4.91	72.00	10.57	135.00	
	9504/031/240 B		39.70	39.70	4.62	3.49	72.00	7.55	135.00	
	9504/031/400 B		55.00	55.00	4.85	3.04	72.00	6.27	135.00	
HB	TEC1-07103HTS		30.00	30.00	4.90	1.33	65.00	2.72	225.00	$3.74
	TEC1-07108HT		30.00	30.00	3.80	4.22	65.00	11.11	225.00	$1.13
	TEC1-12703HT		40.00	40.00	4.70	1.59	65.00	3.39	225.00	$3.76
	TEC1-12703HTS		40.00	40.00	4.70	1.34	65.00	2.86	225.00	$4.65
	TEC1-12705HT		40.00	40.00	4.20	2.69	65.00	6.40	225.00	$2.04
	TEC1-12706HTS		40.00	40.00	3.80	2.63	65.00	6.91	225.00	$2.19
	TEC1-12707HT		40.00	40.00	3.70	3.69	65.00	9.97	225.00	$1.62
	TEC1-12707HTS		40.00	40.00	3.70	3.16	65.00	8.53	225.00	$1.98
	TEC1-12708HTS		40.00	40.00	3.50	3.56	65.00	10.18	225.00	$1.75
	TEC1-12710HT		40.00	40.00	3.30	5.28	65.00	16.00	225.00	$1.19
	TEC1-12710HTS		40.00	40.00	3.30	4.44	65.00	13.45	225.00	$1.47
	TEC1-12715HT		50.00	50.00	4.30	5.12	65.00	11.91	225.00	$3.75
	TEC1-12715HTS		50.00	50.00	4.30	4.32	65.00	10.05	225.00	$4.61
	TEC-12730HT		62.00	62.00	4.80	6.61	65.00	13.77	225.00	$2.71
	TEC-12730HTS		62.00	62.00	4.80	5.54	65.00	11.54	225.00	$3.34
Hitech	QTEC 2-017.03	27.00	15.00	15.00	4.90	1.73	65.00	3.54	200.00	
	QTEC 2-031.03	27.00	20.00	20.00	4.90	1.80	65.00	3.67	200.00	
	QTEC 2-035.03	27.00	30.00	15.00	4.90	1.81	65.00	3.70	200.00	
	QTEC 2-049.03	27.00	25.00	25.00	4.90	1.81	65.00	3.69	200.00	
	QTEC 2-063.03	27.00	40.00	20.00	4.90	1.81	65.00	3.70	200.00	
	QTEC 2-071.03	27.00	30.00	30.00	4.90	1.82	65.00	3.72	200.00	
	QTEC 2-127.03	27.00	40.00	40.00	4.90	1.83	65.00	3.74	200.00	

	QTEC 2-017.04	27.00	15.00	15.00	4.70	2.00	65.00	4.26	200.00
	QTEC 2-031.04	27.00	20.00	20.00	4.70	2.05	65.00	4.36	200.00
	QTEC 2-035.04	27.00	30.00	15.00	4.70	2.04	65.00	4.35	200.00
	QTEC 2-049.04	27.00	25.00	25.00	4.70	2.06	65.00	4.39	200.00
	QTEC 2-063.04	27.00	40.00	20.00	4.70	2.06	65.00	4.39	200.00
	QTEC 2-071.04	27.00	30.00	30.00	4.70	2.08	65.00	4.42	200.00
	QTEC 2-127.04	27.00	40.00	40.00	4.70	2.09	65.00	4.44	200.00
	QTEC 2-017.05	27.00	15.00	15.00	4.00	2.44	65.00	6.11	200.00
	QTEC 2-031.05	27.00	20.00	20.00	4.00	2.50	65.00	6.25	200.00
	QTEC 2-035.05	27.00	30.00	15.00	4.00	2.51	65.00	6.28	200.00
	QTEC 2-049.05	27.00	25.00	25.00	4.00	2.53	65.00	6.32	200.00
	QTEC 2-063.05	27.00	40.00	20.00	4.00	2.53	65.00	6.31	200.00
	QTEC 2-071.05	27.00	30.00	30.00	4.00	2.53	65.00	6.33	200.00
	QTEC 2-127.05	27.00	40.00	40.00	4.00	2.56	65.00	6.41	200.00
	QTEC 2-017.06	27.00	15.00	15.00	3.80	3.07	65.00	8.07	200.00
	QTEC 2-031.06	27.00	20.00	20.00	3.80	3.13	65.00	8.22	200.00
	QTEC 2-035.06	27.00	30.00	15.00	3.80	3.16	65.00	8.30	200.00
	QTEC 2-049.06	27.00	25.00	25.00	3.80	3.20	65.00	8.42	200.00
	QTEC 2-063.06	27.00	40.00	20.00	3.80	3.19	65.00	8.39	200.00
	QTEC 2-071.06	27.00	30.00	30.00	3.80	3.19	65.00	8.39	200.00
	QTEC 2-127.06	27.00	40.00	40.00	3.80	3.21	65.00	8.45	200.00
	QTEC 2-017.08	27.00	15.00	15.00	3.30	4.09	65.00	12.39	200.00
	QTEC 2-031.08	27.00	20.00	20.00	3.30	4.20	65.00	12.73	200.00
	QTEC 2-035.08	27.00	30.00	15.00	3.30	4.22	65.00	12.79	200.00
	QTEC 2-049.08	27.00	25.00	25.00	3.30	4.24	65.00	12.85	200.00
	QTEC 2-063.08	27.00	40.00	20.00	3.30	4.28	65.00	12.95	200.00
	QTEC 2-071.08	27.00	30.00	30.00	3.30	4.28	65.00	12.96	200.00
	QTEC 2-127.08	27.00	40.00	40.00	3.30	4.30	65.00	13.03	200.00
	QTEC 2-031.09	27.00	30.00	30.00	5.60	1.17	65.00	2.08	200.00
	QTEC 2-049.09	27.00	36.00	36.00	5.60	2.28	65.00	4.06	200.00
	QTEC 2-071.09	27.00	44.00	44.00	5.60	2.23	65.00	3.98	200.00
	QTEC 2-127.09	27.00	62.00	62.00	5.60	2.02	65.00	3.60	200.00
	QTEC 2-031.14	27.00	30.00	30.00	4.60	3.28	65.00	7.13	200.00
	QTEC 2-049.14	27.00	36.00	36.00	4.60	3.56	65.00	7.73	200.00
	QTEC 2-071.14	27.00	44.00	44.00	4.60	3.47	65.00	7.55	200.00
	QTEC 2-127.14	27.00	62.00	62.00	4.60	3.13	65.00	6.81	200.00
INB Products	inbC2-040-065-31-17	27.00	11.50	11.50	6.60	2.34	85.00	3.55	200.00
	inbC2-055-065-31-17	27.00	15.00	15.00	7.20	2.69	85.00	3.73	200.00
	inbC2-055-065-71-31	27.00	20.00	20.00	7.20	3.16	85.00	4.39	200.00
	inbC2-040-050-127-63	27.00	30.00	30.00	7.10	1.79	85.00	2.52	200.00
	inbC2-055-045-127-63	27.00	40.00	40.00	7.50	2.16	85.00	2.88	200.00
	inbC1-017.03	27.00	15.00	15.00	4.90	1.73	65.00	3.54	150.00
	inbC1-031.03	27.00	20.00	20.00	4.90	1.80	65.00	3.67	150.00
	inbC1-035.03	27.00	30.00	15.00	4.90	1.81	65.00	3.70	150.00
	inbC1-049.03	27.00	25.00	25.00	4.90	1.81	65.00	3.69	150.00
	inbC1-063.03	27.00	40.00	20.00	4.90	1.81	65.00	3.70	150.00
	inbC1-071.03	27.00	30.00	30.00	4.90	1.82	65.00	3.72	150.00
	inbC1-127.03	27.00	40.00	40.00	4.90	1.83	65.00	3.74	150.00
	inbC1-017.04	27.00	15.00	15.00	4.70	2.00	65.00	4.26	150.00
	inbC1-031.04	27.00	20.00	20.00	4.70	2.05	65.00	4.36	150.00
	inbC1-035.04	27.00	30.00	15.00	4.70	2.04	65.00	4.35	150.00
	inbC1-049.04	27.00	25.00	25.00	4.70	2.06	65.00	4.39	150.00
	inbC1-063.04	27.00	40.00	20.00	4.70	2.06	65.00	4.39	150.00
	inbC1-071.04	27.00	30.00	30.00	4.70	2.08	65.00	4.42	150.00
	inbC1-127.04	27.00	40.00	40.00	4.70	2.09	65.00	4.44	150.00
	inbC1-017.05	27.00	15.00	15.00	4.00	2.44	65.00	6.11	150.00
	inbC1-031.05	27.00	20.00	20.00	4.00	2.50	65.00	6.25	150.00
	inbC1-035.05	27.00	30.00	15.00	4.00	2.51	65.00	6.28	150.00
	inbC1-049.05	27.00	25.00	25.00	4.00	2.53	65.00	6.32	150.00
	inbC1-063.05	27.00	40.00	20.00	4.00	2.53	65.00	6.31	150.00
	inbC1-071.05	27.00	30.00	30.00	4.00	2.53	65.00	6.33	150.00
	inbC1-127.05	27.00	40.00	40.00	4.00	2.56	65.00	6.41	150.00
	inbC1-017.06	27.00	15.00	15.00	3.80	3.07	65.00	8.07	150.00
	inbC1-035.06	27.00	30.00	15.00	3.80	3.16	65.00	8.30	150.00
	inbC1-049.06	27.00	25.00	25.00	3.80	3.20	65.00	8.42	150.00
	inbC1-063.06	27.00	40.00	20.00	3.80	3.19	65.00	8.39	150.00
	inbC1-071.06	27.00	30.00	30.00	3.80	3.19	65.00	8.39	150.00

	inbC1-127.06	27.00	40.00	40.00	3.80	3.21	65.00	8.45	150.00
	inbC1-017.08	27.00	15.00	15.00	3.30	4.09	65.00	12.39	150.00
	inbC1-031.08	27.00	20.00	20.00	3.30	4.20	65.00	12.73	150.00
	inbC1-035.08	27.00	30.00	15.00	3.30	4.22	65.00	12.79	150.00
	inbC1-049.08	27.00	25.00	25.00	3.30	4.24	65.00	12.85	150.00
	inbC1-063.08	27.00	40.00	20.00	3.30	4.28	65.00	12.95	150.00
	inbC1-071.08	27.00	30.00	30.00	3.30	4.28	65.00	12.96	150.00
	inbC1-127.08	27.00	40.00	40.00	3.30	4.30	65.00	13.03	150.00
	inbC1-031.09	27.00	30.00	30.00	5.60	2.09	65.00	3.73	150.00
	inbC1-049.09	27.00	36.00	36.00	5.60	2.28	65.00	4.06	150.00
	inbC1-071.09	27.00	44.00	44.00	5.60	2.23	65.00	3.98	150.00
	inbC1-127.09	27.00	62.00	62.00	5.60	2.02	65.00	3.60	150.00
	inbC1-031.14	27.00	30.00	30.00	4.60	3.28	65.00	7.13	150.00
	inbC1-049.14	27.00	36.00	36.00	4.60	3.56	65.00	7.73	150.00
	inbC1-071.14	27.00	44.00	44.00	4.60	3.47	65.00	7.55	150.00
	inbC1-127.14	27.00	62.00	62.00	4.60	3.13	65.00	6.81	150.00
	inbC1-127.14-50	27.00	50.00	50.00	4.70	4.82	65.00	10.26	150.00
Interm	TECB-1-1-(15.4-6.0-51.4)-40-71	25.00	40.00	40.00	3.60	3.21	71.00	8.92	250.00
	TECB-1-3-(15.4-8.5-68.8)-40-69	25.00	40.00	40.00	3.30	4.30	69.00	13.03	250.00
	TECB-1-14-(15.4-3.9-33.4)-40-72	25.00	40.00	40.00	4.70	2.09	72.00	4.44	250.00
	TECB-1-29-(15.4-10-86)-40-71	25.00	40.00	40.00	3.50	5.38	71.00	15.36	250.00
	TECB-1-33-(15.4-1.0-8.6)-40-72	25.00	40.00	40.00	4.80	0.54	72.00	1.12	250.00
	TECB-1-34-(15.4-11.4-97)-40-70	25.00	40.00	40.00	3.30	6.09	70.00	18.47	250.00
	TECB-2-2-(15.4-3.9-33.4)-30-71	25.00	30.00	30.00	3.20	3.71	71.00	11.60	250.00
	TECB-2-43-(15.4-4.8-41.0)-30-69	25.00	30.00	30.00	3.00	4.56	69.00	15.19	250.00
	TECB-2-44-(15.4-3.5-30.2)-30-70	25.00	30.00	30.00	3.40	3.36	70.00	9.87	250.00
	TECB-2-45-(15.4-2.4-20.7)-30-71	25.00	30.00	30.00	4.10	2.30	71.00	5.61	250.00
	TECB-13-13-(8.6-3.9-18.7)-30-72	25.00	30.00	30.00	4.60	2.08	72.00	4.52	250.00
	TECB-13-46-(8.6-4.2-21.0)-30-72	25.00	30.00	30.00	4.40	2.33	72.00	5.30	250.00
	TECB-13-47-(8.6-4.7-23.0)-30-71	25.00	30.00	30.00	4.20	2.56	71.00	6.08	250.00
	TECB-13-48-(8.6-5.1-25.2)-30-70	25.00	30.00	30.00	4.00	2.80	70.00	7.00	250.00
	TECB-13-49-(8.6-6.0-29.6)-30-70	25.00	30.00	30.00	3.70	3.29	70.00	8.89	250.00
	TECB-14-88-(12-6-40)-40-71	25.00	40.00	40.00	3.50	2.50	71.00	7.14	250.00
	TECB-14-91-(12-6.5-44)-40-71	25.00	40.00	40.00	3.40	2.75	71.00	8.09	250.00
	TECB-14-92-(12-7-47)-40-71	25.00	40.00	40.00	3.30	2.94	71.00	8.90	250.00
	TECB-15-15-(24.7-11.4-173)-40-69	25.00	40.00	40.00	3.00	10.81	69.00	36.04	250.00
	TECB-15-16-(24.7-7.9-120)-40-69	25.00	40.00	40.00	3.40	7.50	69.00	22.06	250.00
	TECB-15-26-(24.0-3.9-52)-40-71	25.00	40.00	40.00	4.20	3.25	71.00	7.74	250.00
	TECB-15-50-(24.7-9.5-130)-40-69	25.00	40.00	40.00	3.30	8.13	69.00	24.62	250.00
	TECB-15-101-(24.7-14.5-220)-40-69	25.00	40.00	40.00	2.90	13.75	69.00	47.41	250.00
	TECB-16-89-(24.2-7-100)-30-70	25.00	30.00	30.00	3.10	11.11	70.00	35.84	250.00
	TECB-16-93-(24.2-6.3-90)-30-70	25.00	30.00	30.00	3.20	10.00	70.00	31.25	250.00
	TECB-16-94-(24.2-5.7-81)-30-70	25.00	30.00	30.00	3.30	9.00	70.00	27.27	250.00
	TECB-17-17-(15.4-14.0-120)-62-71	25.00	62.00	62.00	5.00	3.12	71.00	6.24	250.00
	TECB-17-21-(15.4-8.3-72)-62-71	25.00	62.00	62.00	5.90	1.87	71.00	3.17	250.00
	TECB-17-51-(15.4-9.3-81)-62-71	25.00	62.00	62.00	5.70	2.11	71.00	3.70	250.00
	TECB-17-52-(15.4-11.1-94.4)-62-71	25.00	62.00	62.00	5.50	2.46	71.00	4.47	250.00
	TECB-17-53-(15.4-12.6-107)-62-70	25.00	62.00	62.00	5.30	2.78	70.00	5.25	250.00
	TECB-18-18-(8.6-2.5-12)-23-71	25.00	23.00	23.00	3.60	2.27	71.00	6.30	250.00
	TECB-18-54-(8.6-2.1-9.9)-23-72	25.00	23.00	23.00	4.00	1.87	72.00	4.68	250.00
	TECB-18-55-(8.6-2.3-10.6)-23-71	25.00	23.00	23.00	3.80	2.00	71.00	5.27	250.00
	TECB-18-56-(8.6-3.3-15.0)-23-71	25.00	23.00	23.00	3.40	2.84	71.00	8.34	250.00
	TECB-18-57-(8.6-3.9-18.1)-23-71	25.00	23.00	23.00	3.20	3.42	71.00	10.69	250.00
	TECB-18-87-(8.2-3.7-20)-23-71	25.00	28.00	23.50	3.30	3.04	71.00	9.21	250.00
	TECB-21-102-(42-12-300)-55-69	25.00	55.00	55.00	4.00	9.92	69.00	24.79	250.00
	TECB-21-103-(42-15-330)-50-69	25.00	55.00	55.00	4.00	10.91	69.00	27.27	250.00
	TECB-21-104-(42-16.7-350)-50-69	25.00	55.00	55.00	3.80	11.57	69.00	30.45	250.00
	TECB-21-105-(42-20-400)-50-68	25.00	55.00	55.00	3.50	13.22	68.00	37.78	250.00
	TECB-22-22-(17.4-6.0-57)-40-71	25.00	40.00	40.00	3.80	3.56	71.00	9.38	250.00
	TECB-22-58-(17.4-4.0-39)-40-71	25.00	40.00	40.00	4.30	2.44	71.00	5.67	250.00
	TECB-22-59-(17.4-4.8-45.5)-40-71	25.00	40.00	40.00	4.10	2.84	71.00	6.94	250.00
	TECB-22-60-(17.4-5.5-52.2)-40-70	25.00	40.00	40.00	3.90	3.26	70.00	8.37	250.00
	TECB-22-61-(17.4-7.3-70.0)-40-70	25.00	40.00	40.00	3.50	4.38	70.00	12.50	250.00
	TECB-22-62-(17.4-8.1-77.4)-40-70	25.00	40.00	40.00	3.30	4.84	70.00	14.66	250.00
	TECB-25-25-(15.4-8.5-72)-70-71	25.00	70.00	70.00	5.70	1.47	71.00	2.58	250.00
	TECB-25-30-(15.4-11.4-100)-70-70	25.00	70.00	70.00	5.50	2.04	70.00	3.71	250.00
	TECB-25-35-(15.4-14-125)-70-70	25.00	70.00	70.00	5.00	2.55	70.00	5.10	250.00

	TECB-25-63-(15.4-17-150)-70-70	25.00	70.00	70.00	4.00	3.06	70.00	7.65	250.00	
	TECB-25-64-(15.4-10.2-88)-70-71	25.00	70.00	70.00	5.70	1.80	71.00	3.15	250.00	
	TECB-26-90-(30-19-300)-70-69	25.00	70.00	70.00	5.70	6.12	71.00	10.74	250.00	
	TECB-26-95-(30-17.5-275)-70-69	25.00	70.00	70.00	5.80	5.61	71.00	9.68	250.00	
	TECB-26-96-(30-16.4-260)-70-69	25.00	70.00	70.00	5.90	5.31	71.00	8.99	250.00	
	TECB-27-27-(19-14-147)-40-70	25.00	40.00	40.00	3.10	9.19	70.00	29.64	250.00	
	TECB-27-65-(19-11.6-123)-40-70	25.00	40.00	40.00	3.30	7.50	70.00	22.73	250.00	
	TECB-27-66-(19-9.8-106)-40-70	25.00	40.00	40.00	3.50	6.63	70.00	18.93	250.00	
	TECB-27-67-(19-8.6-93.3)-40-71	25.00	40.00	40.00	3.70	5.83	71.00	15.76	250.00	
	TECB-27-68-(19-7.6-83.0)-40-71	25.00	40.00	40.00	3.90	5.19	71.00	13.30	250.00	
	TECB-28-28-(2.5-3.9-5.4)-20-72	25.00	20.00	20.00	4.70	1.35	72.00	2.87	250.00	
	TECB-28-69-(2.5-4.4-6.0)-20-71	25.00	20.00	20.00	4.50	1.50	71.00	3.33	250.00	
	TECB-28-70-(2.5-5.0-6.9)-20-71	25.00	20.00	20.00	4.30	1.73	71.00	4.01	250.00	
	TECB-28-71-(2.5-5.4-7.5)-20-71	25.00	20.00	20.00	4.10	1.88	71.00	4.57	250.00	
	TECB-29-109-(24.7-11.5-175)-50-69	25.00	50.00	50.00	4.00	7.00	69.00	17.50	250.00	
	TECB-32-32-(24.7-19.0-300)-62-69	25.00	62.00	62.00	5.10	7.80	69.00	15.30	250.00	
	TECB-32-72-(24.7-17.0-270)-62-69	25.00	62.00	62.00	5.30	7.02	69.00	13.25	250.00	
	TECB-32-73-(24.7-15.0-240)-62-69	25.00	62.00	62.00	5.50	6.24	69.00	11.35	250.00	
	TECB-32-74-(24.7-13.0-200)-62-70	25.00	62.00	62.00	5.70	5.20	70.00	9.13	250.00	
	TECB-32-110-(24.7-25.0-400)-62-69	25.00	62.00	62.00	4.80	10.41	69.00	21.68	250.00	
	TECB-39-97-(30-15.2-270)-50-69	25.00	50.00	50.00	5.50	10.80	69.00	19.64	250.00	
	TECB-39-98-(30-14.0-255)-50-69	25.00	50.00	50.00	5.60	10.20	69.00	18.21	250.00	
	TECB-39-99-(30-12.7-240)-50-69	25.00	50.00	50.00	5.70	9.60	69.00	16.84	250.00	
	TECB-39-100-(30-12.7-240)-50-69	25.00	50.00	50.00	6.10	4.40	70.00	7.21	250.00	
	TECB-40-40-(17.4-6.0-58)-50-71	25.00	50.00	50.00	4.00	2.32	71.00	5.80	250.00	
	TECB-40-75-(17.4-4.0-38)-50-71	25.00	50.00	50.00	4.60	1.52	71.00	3.30	250.00	
	TECB-40-76-(17.4-4.6-45.2)-50-71	25.00	50.00	50.00	4.40	1.81	71.00	4.11	250.00	
	TECB-40-77-(17.4-5.5-52.3)-50-71	25.00	50.00	50.00	4.20	2.09	71.00	4.98	250.00	
	TECB-40-78-(17.4-6.9-66.0)-50-70	25.00	50.00	50.00	3.80	2.64	70.00	6.95	250.00	
	TECB-41-41-(30-3.0-50)-40-71	25.00	40.00	40.00	3.20	3.13	71.00	9.77	250.00	
	TECB-41-79-(30-2.7-45)-40-71	25.00	40.00	40.00	3.40	2.81	71.00	8.27	250.00	
	TECB-41-80-(30-2.5-42.3)-40-71	25.00	40.00	40.00	3.60	2.64	71.00	7.34	250.00	
	TECB-41-81-(30-2.3-37.8)-40-72	25.00	40.00	40.00	3.80	2.36	72.00	6.22	250.00	
	TECB-41-82-(30-2.1-34.5)-40-72	25.00	40.00	40.00	4.00	2.16	72.00	5.39	250.00	
Kryotherm	TB-7-1,0-2,5		8.00	8.00	4.80	1.56	70.00	3.26	150.00	$5.82
	TB-17-1,0-2,5		11.50	11.50	4.80	1.89	70.00	3.94	150.00	$5.21
	TB-31-1,0-2,5		14.80	14.80	4.80	2.05	70.00	4.28	150.00	$5.66
	TB-63-1,0-2,5		15.00	15.00	4.80	4.04	70.00	8.43	150.00	$3.14
	TB-71-1,0-2,5		23.00	23.00	4.80	1.93	70.00	4.02	150.00	$6.72
	TB-83-1,0-2,5		22.00	19.00	4.80	2.87	70.00	5.98	150.00	$4.70
	TB-127-1,0-2,5		30.00	30.00	4.80	2.03	70.00	4.24	150.00	$6.98
	TB-7-1,0-2,0		8.00	8.00	4.30	2.03	70.00	4.72	150.00	$3.15
	TB-17-1,0-2,0		11.50	11.50	4.30	2.34	70.00	5.45	150.00	$3.58
	TB-31-1,0-2,0		14.80	14.80	4.30	2.56	70.00	5.95	150.00	$3.99
	TB-63-1,0-2,0		15.00	30.00	4.30	2.53	70.00	5.89	150.00	$4.42
	TB-71-1,0-2,0		23.00	23.00	4.30	2.42	70.00	5.63	150.00	$4.96
	TB-83-1,0-2,0		22.00	19.00	4.30	3.56	70.00	8.29	150.00	$3.65
	TB-127-1,0-2,0		30.00	30.00	4.30	2.54	70.00	5.92	150.00	$5.34
	TB-71-1,4-3,175		30.00	30.00	5.60	1.83	72.00	3.27	150.00	$9.88
	TB-7-1,0-1,5		8.00	8.00	3.80	2.66	69.00	6.99	150.00	$2.35
	TB-17-1,0-1,5		11.50	11.50	3.80	3.02	69.00	7.96	150.00	$2.71
	TB-31-1,0-1,5		14.80	14.80	3.80	3.33	69.00	8.77	150.00	$3.00
	TB-63-1,0-1,5		15.00	30.00	3.80	3.29	69.00	8.65	150.00	$3.28
	TB-71-1,0-1,5		23.00	23.00	3.80	3.16	69.00	8.31	150.00	$3.64
	TB-83-1,0-1,5		22.00	19.00	3.80	4.67	69.00	12.28	150.00	$2.63
	TB-127-1,0-1,5		30.00	30.00	3.80	3.32	69.00	8.74	150.00	$4.06
	TB-7-1,0-1,3		8.00	8.00	3.60	2.97	69.00	8.25	150.00	$2.11
	TB-17-1,0-1,3		11.50	11.50	3.60	3.48	69.00	9.66	150.00	$2.36
	TB-23-1,0-1,3		30.00	5.00	3.60	4.13	69.00	11.48	150.00	$2.36
	TB-31-1,0-1,3		14.80	14.80	3.60	3.83	69.00	10.65	150.00	$2.82
	TB-63-1,0-1,3		15.00	30.00	3.60	3.80	69.00	10.56	150.00	$3.09
	TB-71-1,0-1,3		23.00	23.00	3.60	3.65	69.00	10.13	150.00	$3.15
	TB-83-1,0-1,3		22.00	19.00	3.60	5.38	69.00	14.95	150.00	$2.23
	TB-127-1,0-1,3		30.00	30.00	3.60	3.83	69.00	10.65	150.00	$3.29
	TB-32-1,0-0,8		40.00	6.00	3.10	5.88	69.00	18.95	150.00	$1.91
	TB-127-1,0-0,8		30.00	30.00	3.10	6.22	69.00	20.07	150.00	$2.31
	TB-195-1,0-0,8		50.00	25.00	3.10	6.88	69.00	22.19	150.00	$4.62

	TB-7-1,4-2,5		10.00	10.00	4.90	2.10	72.00	4.29	150.00	$4.12
	TB-17-1,4-2,5		15.00	15.00	4.90	2.22	72.00	4.54	150.00	$4.77
	TB-31-1,4-2,5		20.00	20.00	4.90	2.28	72.00	4.64	150.00	$5.45
	TB-63-1,4-2,5		20.00	40.00	4.90	2.33	72.00	4.74	150.00	$5.85
	TB-71-1,4-2,5		30.00	30.00	4.90	2.32	72.00	4.74	150.00	$6.24
	TB-127-1,4-2,5		40.00	40.00	4.80	2.34	72.00	4.87	150.00	$6.31
	TB-71-1,4-1,8		30.00	30.00	4.20	3.10	70.00	7.38	150.00	$4.65
	TB-7-1,4-1,5		10.00	10.00	4.00	3.30	70.00	8.25	150.00	$2.48
	TB-17-1,4-1,5		15.00	15.00	4.00	3.56	70.00	8.89	150.00	$2.87
	TB-31-1,4-1,5		20.00	20.00	4.00	3.65	70.00	9.13	150.00	$3.12
	TB-63-1,4-1,5		20.00	40.00	4.00	3.71	70.00	9.28	150.00	$3.39
	TB-71-1,4-1,5		30.00	30.00	4.00	3.71	70.00	9.28	150.00	$3.72
	TB-127-1,4-1,5		40.00	40.00	3.90	3.75	70.00	9.62	150.00	$4.48
	TB-127-1,4-1,2		40.00	40.00	3.60	4.69	70.00	13.02	150.00	$3.71
	TB-7-1,4-1,15		10.00	10.00	3.60	4.20	69.00	11.67	150.00	$2.06
	TB-17-1,4-1,15		15.00	15.00	3.60	4.53	69.00	12.59	150.00	$2.54
	TB-31-1,4-1,15		20.00	20.00	3.60	4.65	69.00	12.92	150.00	$2.89
	TB-63-1,4-1,15		20.00	40.00	3.60	4.74	69.00	13.16	150.00	$2.91
	TB-71-1,4-1,15		30.00	30.00	3.60	4.78	69.00	13.27	150.00	$3.14
	TB-127-1,4-1,15		40.00	40.00	3.40	4.75	69.00	13.97	150.00	$4.06
	TB-127-1.4-1.05		40.00	40.00	3.30	5.25	69.00	15.91	150.00	$4.11
	TB-7-2,0-2,5		14.80	14.80	4.80	1.92	72.00	3.99	150.00	$4.69
	TB-17-2,0-2,5		22.00	22.00	4.80	2.11	72.00	4.39	150.00	$5.74
	TB-31-2,0-2,5		30.00	30.00	4.80	2.08	72.00	4.33	150.00	$6.59
	TB-71-2,0-2,5		40.00	40.00	4.80	2.69	72.00	5.60	150.00	$11.39
	TB-127-2,0-2,5		48.00	48.00	4.80	3.30	72.00	6.87	150.00	$14.85
	TB-127-2,0-2,5		55.00	55.00	4.80	2.51	72.00	5.23	150.00	$19.50
	TB-127-2,0-2,5		62.00	62.00	4.80	1.98	72.00	4.12	150.00	$24.78
	TB-127-2,0-1,65		48.00	48.00	4.00	4.82	70.00	12.04	150.00	$9.91
	TB-7-2,0-1,5		14.80	14.80	3.80	3.06	70.00	8.05	150.00	$4.12
	TB-17-2,0-1,5		22.00	22.00	3.80	3.37	70.00	8.86	150.00	$4.16
	TB-31-2,0-1,5		30.00	30.00	3.80	3.31	70.00	8.71	150.00	$4.32
	TB-71-2,0-1,5		40.00	40.00	3.80	4.25	70.00	11.18	150.00	$6.92
	TB-127-2,0-1,5		48.00	48.00	3.80	5.30	70.00	13.93	150.00	$9.29
	TB-127-2,0-1,5		55.00	55.00	4.80	4.03	70.00	8.40	150.00	$12.20
	TB-127-2,0-1,5		62.00	62.00	3.90	3.17	70.00	8.14	150.00	$15.50
	TB-127-2,0-1,15		48.00	48.00	3.40	6.77	69.00	19.91	150.00	$6.76
	TB-32-2,8-1,5		40.00	40.00	4.00	3.75	70.00	9.38	150.00	$5.15
	TB-31-5,0-2,5		55.00	55.00	6.00	3.70	70.00	6.17	150.00	$10.16
	TB-31-5,0-1,5		55.00	55.00	5.00	6.15	70.00	12.30	150.00	$5.81
Marlow	DT12-2.5	27.00	30.00	30.00	4.04	2.56	66.00	6.33	150.00	
	DT12-2.5-01L	27.00	30.00	30.00	4.04	2.56	66.00	6.33	150.00	
	DT12-4	27.00	30.00	30.00	3.43	4.00	66.00	11.66	150.00	
	DT12-4-01	27.00	30.00	30.00	3.43	4.00	66.00	11.66	150.00	
	DT12-4-01L	27.00	30.00	30.00	3.43	4.00	66.00	11.66	150.00	
	DT12-4-01S	27.00	30.00	30.00	3.43	4.00	66.00	11.66	150.00	
	DT12-4-06LS	27.00	30.00	30.00	3.43	4.00	66.00	11.66	150.00	
	DT12-6	27.00	40.01	40.01	4.01	3.37	66.00	8.41	150.00	
	DT12-6-01L	27.00	40.01	40.01	4.01	3.37	66.00	8.41	150.00	
	DT12-6-01LS	27.00	40.01	40.01	4.01	3.37	66.00	8.41	150.00	
	DT12-6-01S	27.00	40.01	40.01	4.01	3.37	66.00	8.41	150.00	
	DT12-6-05	27.00	40.01	40.01	4.01	3.37	66.00	8.41	150.00	
	DT12-8	27.00	40.01	40.01	3.53	4.44	66.00	12.56	150.00	
	DT12-8-01L	27.00	40.01	40.01	3.53	4.44	66.00	12.56	150.00	
	DT3-2.5	27.00	16.00	16.00	4.04	2.34	65.00	5.80	150.00	
	DT3-2.5-01	27.00	16.00	16.00	4.04	2.34	65.00	5.80	150.00	
	DT3-4	27.00	16.00	16.00	3.43	3.52	65.00	10.25	150.00	
	DT3-4-01L	27.00	16.00	16.00	3.43	3.52	65.00	10.25	150.00	
	DT3-6	27.00	19.99	19.99	4.01	3.25	65.00	8.11	150.00	
	DT3-6-01	27.00	19.99	19.99	4.01	3.25	65.00	8.11	150.00	
	DT3-6-01LS	27.00	19.99	19.99	4.01	3.25	65.00	8.11	150.00	
	DT3-6-01S	27.00	19.99	19.99	4.01	3.25	65.00	8.11	150.00	
	DT3-8	27.00	19.99	19.99	3.63	4.25	65.00	11.72	150.00	
	DT6-2.5	27.00	23.50	23.50	4.04	2.35	65.00	5.83	150.00	
	DT6-2.5-01L	27.00	23.50	23.50	4.04	2.35	65.00	5.83	150.00	
	DT6-2.5-01LS	27.00	23.50	23.50	4.04	2.35	65.00	5.83	150.00	
	DT6-4	27.00	23.50	23.50	3.43	3.62	65.00	10.56	150.00	

	DT6-4-01	27.00	23.50	23.50	3.43	3.62	65.00	10.56	150.00
	DT6-4-01L	27.00	23.50	23.50	3.43	3.62	65.00	10.56	150.00
	DT6-4-01LS	27.00	23.50	23.50	3.43	3.62	65.00	10.56	150.00
	DT6-6	27.00	30.00	30.00	4.01	3.33	65.00	8.31	150.00
	DT6-6-01L	27.00	30.00	30.00	4.01	3.33	65.00	8.31	150.00
	DT6-8	27.00	30.00	30.00	3.63	4.33	65.00	11.94	150.00
	DT6-8-01L	27.00	30.00	30.00	3.63	4.33	65.00	11.94	150.00
	MI1010T	27.00	3.96	3.96	2.41	3.00	61.00	12.44	150.00
	MI1011T	27.00	6.60	6.60	2.41	2.30	61.00	9.53	150.00
	MI1012T	27.00	8.79	8.79	2.41	2.72	61.00	11.28	150.00
	MI1012T-01AC	27.00	8.79	8.79	2.41	2.72	61.00	11.28	150.00
	MI1013T	27.00	13.16	13.16	2.41	2.77	61.00	11.50	150.00
	MI1015T	27.00	8.79	10.97	2.39	2.70	61.00	11.28	150.00
	MI1020T	27.00	3.91	3.91	2.16	5.89	64.00	27.25	150.00
	MI1020T-02AC	27.00	3.91	3.91	2.16	5.89	64.00	27.25	150.00
	MI1021T	27.00	6.60	6.60	2.16	5.05	64.00	23.38	150.00
	MI1021T-02AC	27.00	6.60	6.60	2.16	5.05	64.00	23.38	150.00
	MI1022T	27.00	8.79	8.79	2.16	5.18	64.00	23.97	150.00
	MI1023T	27.00	13.16	13.16	2.16	5.31	64.00	24.59	150.00
	MI1023T-02AC	27.00	13.16	13.16	2.16	5.31	64.00	24.59	150.00
	MI1025T	27.00	8.79	10.97	2.16	5.39	64.00	24.97	150.00
	NL1010T	27.00	3.96	3.96	2.41	3.00	61.00	12.44	150.00
	NL1011T	27.00	6.60	6.60	2.41	2.30	61.00	9.53	150.00
	NL1012T	27.00	8.79	8.79	2.41	2.72	61.00	11.28	150.00
	NL1013T	27.00	13.16	13.16	2.41	2.77	61.00	11.50	150.00
	NL1015T	27.00	8.79	10.97	2.39	2.70	61.00	11.28	150.00
	NL1020T	27.00	3.96	3.96	2.16	5.74	64.00	26.57	150.00
	NL1021T	27.00	6.60	6.60	2.16	5.05	64.00	23.38	150.00
	NL1022T	27.00	8.79	8.79	2.16	5.18	64.00	23.97	150.00
	NL1023T	27.00	13.16	13.16	2.16	5.31	64.00	24.59	150.00
	NL1025T	27.00	8.79	10.97	2.16	5.39	64.00	24.97	150.00
	RC12-2.5	27.00	30.00	30.00	4.04	2.56	66.00	6.33	150.00
	RC12-4	27.00	30.00	30.00	3.43	4.00	66.00	11.66	150.00
	RC12-6	27.00	40.13	40.13	4.01	3.35	66.00	8.36	150.00
	RC12-8	27.00	40.13	40.13	3.63	4.41	66.00	12.15	150.00
	RC3-2.5	27.00	16.00	16.00	4.04	2.34	65.00	5.80	150.00
	RC3-4	27.00	16.00	16.00	3.43	3.52	65.00	10.25	150.00
	RC3-6	27.00	19.99	19.99	4.01	3.25	65.00	8.11	150.00
	RC3-8	27.00	19.99	19.99	3.63	4.25	65.00	11.72	150.00
	RC6-2.5	27.00	23.50	23.50	4.04	2.35	65.00	5.83	150.00
	RC6-4	27.00	23.50	23.50	3.43	3.62	65.00	10.56	150.00
	RC6-6	27.00	30.00	30.00	4.01	3.33	66.00	8.31	150.00
	RC6-8	27.00	30.00	30.00	3.63	4.33	65.00	11.94	150.00
	SP1507	27.00	11.28	11.28	2.44	4.24	64.00	17.39	150.00
	SP1848	27.00	25.40	25.40	4.88	3.26	62.00	6.67	150.00
	SP1848-03AC	27.00	25.40	25.40	4.88	3.26	62.00	6.67	150.00
	SP5025	27.00	5.97	6.22	2.51	5.12	64.00	20.39	150.00
	SP5162	27.00	5.99	6.15	1.65	6.24	68.00	37.84	150.00
	SP5255	27.00	6.02	8.18	1.65	6.70	68.00	40.61	150.00
	SP5446	27.00	5.99	12.19	1.65	6.85	68.00	41.50	150.00
Melcor	H OT 1.2-18-F2A	25.00	7.20	6.00	2.70	3.38	64.00	12.52	225.00
	H OT 1.2-24-F2A	25.00	10.80	6.60	2.50	2.76	64.00	11.05	225.00
	H OT 1.2-30-F2A	25.00	12.30	6.20	2.40	3.19	64.00	13.28	225.00
	H OT 1.2-31-F2A	25.00	11.00	8.80	2.70	2.59	64.00	9.60	225.00
	H OT 1.2-65-F2A	25.00	13.20	13.20	2.70	3.06	64.00	11.35	225.00
	H OT 1.5-30-F2A	25.00	12.30	6.20	2.20	3.97	64.00	18.06	225.00
	H OT 1.5-31-F2A	25.00	11.00	8.80	2.40	3.23	64.00	13.47	225.00
	H OT 1.5-65-F2A	25.00	13.20	12.10	2.40	4.11	64.00	17.14	225.00
	H OT 2.0-30-F2A	25.00	12.30	10.30	1.80	3.19	64.00	17.72	225.00
	H OT 2.0-65-F2A	25.00	13.20	13.20	2.20	5.03	64.00	22.85	225.00
	HT2-12-30	25.00	34.00	30.00	3.60	1.96	63.00	5.45	225.00
	HT3-12-30	25.00	34.00	30.00	3.20	2.35	63.00	7.35	225.00
	HT4-12-40	25.00	34.00	30.00	3.20	3.24	63.00	10.11	225.00
	HT6-12-40	25.00	34.00	30.00	3.80	2.84	63.00	7.48	225.00
	HT8-7-30	25.00	44.00	40.00	3.60	2.90	63.00	8.05	225.00
	HT8-12-40	25.00	44.00	40.00	3.30	4.09	63.00	12.40	225.00
	HT9-3-25	25.00	29.00	25.00	4.90	2.76	66.00	5.63	225.00

Micropelt	MPC-D301-M44	25.00	0.72	0.72	0.43	42.05	22.80	982.53	85.00	$0.88
(Thin Film)	MPC-D901-M44	25.00	4.80	4.80	0.43	62.93	21.90	1463.58		
TE Technologies	VT-127-1.0-1.3-71	27.00	30.00	30.00	3.60	4.00	71.00	11.11	200.00	
	VT-127-1.4-1.15-71	27.00	40.00	40.00	3.40	5.00	71.00	14.71	200.00	
	VT-127-1.4-1.5-72	27.00	40.00	40.00	3.90	3.88	72.00	9.94	200.00	
	VT-199-1.4-0.8	27.00	40.00	40.00	3.20	10.75	67.00	33.59	200.00	
	VT-199-1.4-1.15	27.00	40.00	40.00	3.40	7.50	69.00	22.06	200.00	
	VT-199-1.4-1.5	27.00	40.00	40.00	3.90	5.88	70.00	15.06	200.00	
Tellurex	CZ-1.0-127-1.27	50.00	34.00	31.00	3.20	3.67	79.00	11.47	100.00	
	CZ-1.4-127-1.65	50.00	40.00	40.00	3.70	3.50	79.00	9.46	100.00	
	CZ1-1.4-127-1.14	50.00	44.00	40.00	3.20	4.58	79.00	14.31	100.00	
	CZ1-1.4-219-1.14	50.00	54.00	54.00	3.20	4.77	79.00	14.90	100.00	
Thermion	1MC04-004-03		1.60	3.20	1.70	14.65	70.00	86.17	175.00	
	1MC04-008-03		3.20	3.20	1.70	14.65	70.00	86.17	175.00	
	1MC04-012-03		3.20	4.80	1.70	14.97	70.00	88.08	175.00	
	1MC04-018-03		4.80	4.80	1.70	14.76	70.00	86.81	175.00	
	1MC04-032-03		6.40	6.40	1.70	14.65	70.00	86.17	175.00	
	1MC04-064-03		9.60	8.00	1.70	14.32	70.00	84.25	175.00	
	1MC04-004-02		3.20	1.60	1.60	21.48	68.00	134.28	175.00	
	1MC04-008-02		3.20	3.20	1.60	21.48	68.00	134.28	175.00	
	1MC04-012-02		4.80	3.20	1.60	21.48	68.00	134.28	175.00	
	1MC04-018-02		4.80	4.80	1.60	21.70	68.00	135.63	175.00	
	1MC04-032-02		6.40	6.40	1.60	21.48	68.00	134.28	175.00	
	1MC04-060-02		9.60	8.00	1.60	20.83	68.00	130.21	175.00	

5.2 Studies of Competitive Products

5.2.1 Benchmarking of Competitive Technologies

Principal Investigator: Robert Staunton
Oak Ridge National Laboratory
National Transportation Research Center
2360 Cherahala Boulevard
Knoxville, TN 37932
Voice: 865-946-1351; Fax: 865-946-1262; E-mail:stauntonrh@ornl.gov

DOE Technology Development Manager: Susan A. Rogers
Voice: 202-586-8997; Fax: 202-586-1600; E-mail: Susan.Rogers@ee.doe.gov

ORNL Program Manager: Mitch Olszewski
Voice: 865-946-1350; Fax: 865-946-1262; E-mail: olszewskim@ornl.gov

---

Objectives

The Benchmarking of Competitive Technologies project is intended to conduct electrical and mechanical studies of hybrid electric vehicle (HEV) and plug-in hybrid electric vehicle (PHEV) systems as new system innovations are developed and introduced into the automotive market. The testing produces valuable data on efficiency, torque, speed, and voltage-current relationships that cannot be obtained from other open-literature sources. The full inspection and characterization of the electric motors and inverters also defines their thermal system performance in terms of temperature and corresponding sustainable power levels. Testing of these systems helps to rapidly advance the domestic technology base of electric traction drive systems suitable for HEV/PHEV applications.

The Oak Ridge National Laboratory (ORNL) testing program documents how the systems are manufactured and packaged and what performance limitations exist. These data are obtained by (1) thorough design inspections/assessments, (2) instrumenting the motor/inverter system, and (3) conducting locked-rotor, back-electromotive force (back-emf), thermal, and performance tests over the entire design envelope. These data permit ORNL to determine mechanical and electrical losses and map the inverter and/or motor efficiencies over the entire torque-speed domain.

Approach

Benchmarking of HEV traction drive systems provides detailed electrical and mechanical data from known permanent magnet synchronous motors (PMSMs) and inverters and yields information concerning their thermal performance. The overall approach of this project is to thoroughly define the systems and then perform a detailed evaluation of their performance in a controlled laboratory environment. This approach has proved to be technically sound and quite successful.

During the year, the efficiency mapping tests of the Prius were completed using a test plan developed in the prior year. This same methodology was duplicated for the evaluation of Accord subsystems. Accord activities included preparing the motor with a new rotor shaft design and motor end plates; preparing the inverter through analysis of the circuit and the construction of an auxiliary circuit; and tests that included back-emf, locked rotor, and efficiency mapping.

The technical approach for performing benchmarking evaluations during the year included the following tasks:

- Complete Prius subsystem testing, share detailed test data, and fully document the benchmarking activities. (Completed: May 2006)

- Test the performance of the Accord motor, inverter, and components in the laboratory to generate baseline performance data. (Completed: July 2006)
- Provide the auto company partners with a consistent, open-literature source for complete characterization of Accord technology recently introduced in the marketplace. (Completed: September 2006)
- Query DOE and industry partners regarding emerging technology issues and which competitive technologies hold the greatest technical interest. (Completion: duration of project)
- Based on resources, complete additional limited benchmark assessments of emerging hybrid technology selected by the FCVT program and/or FCVT technical partners. (Completed: September 2006)
- Continue to apply benchmarking information to assist in program planning efforts, developing and executing specific projects, and to support the partnership with the original equipment manufacturers at U.S. Council for Automotive Research. (Completion: duration of project)
- Confirm the realism of performance goals for the technologies and components and identify technology gaps. (Completion: duration of project)
- Use benchmarking data to validate/refine multiproject R&D modeling efforts so that they may be better used in developing new prototype designs to support research. (Successfully completed by some reseachers—ongoing as new results are published)
- Use results to confirm the validity of the project technology thrust and avoid duplication of existing efforts. (Completion: duration of project)
- Provide technical insights that can be used to guide research efforts. (Completion: corresponds to presentation and report dates)

Major Accomplishments

The FY 2006 accomplishments have made it possible to combine test data with design, packaging, and fabrication assessments to enable analysts to determine how various commercial HEV traction systems, such as the Accord and the Prius, compare with system and program technology targets (peak-power-to-weight and -volume ratios). ORNL and other researchers have used data from the benchmarking project in motor models such as Motorsoft SPEEDCAD, Flux2D (FEA), and PSAT (ORNL/Sentech). Other researchers at ORNL have used the data to (1) perform fabrication and cost analyses for the Prius motor and (2) conduct thermal control studies using ORNL's HEATING 7.3, a general-purpose, finite-difference conduction heat transfer model. Ongoing work on another model, developed as part of the benchmarking project, is described in "Future Direction."

The following summarize other major accomplishments of the project during the year:

- The efficiency mapping tests of the Prius PMSM and inverter were completed in a specially prepared test cell using an ORNL controller system developed for this project.
- The benchmarking design and packaging evaluation were completed for the Accord subsystems.
- The Accord motor was prepared with a new rotor shaft design and motor end plates, and the inverter was prepared through analysis of the circuit and the construction of auxiliary circuitry.
- Tests were completed on the Accord subsystems that included back-emf, locked rotor, and efficiency mapping.
- Prius and Accord technical evaluations and test results were documented, and technical reports were issued for both during the year.
- Special by-request benchmarking evaluations were also completed and are documented in this report (see Technical Discussion).

Technical Discussion

The 2005 hybrid Accord is an example of how the automotive industry is introducing hybrid technology to preexisting vehicle models. This Accord design is considered to be a "mild hybrid" because of the small power rating of the integrated motor assist (IMA) and the fact that it is used only for acceleration assist to the engine. The PMSM/inverter system is not used for acceleration without engine power as in the case of a “strong hybrid.” After the vehicle reaches highway speeds, the IMA is used to contribute torque during moderate or strong accelerations.

In contrast, the Prius was designed from the beginning to be a hybrid vehicle and is considered to be a “strong hybrid.” Many of the significant Accord vs Prius design differences are summarized in Table 1.

The Accord PMSM casing is very narrow (68 mm) to allow it to be inserted between the engine and torque converter. Consequently, the motor was designed without a full casing (ends are missing), and the rotor was designed without a shaft and bearings. In preparation for motor operation in the ORNL laboratory, a shaft was designed and installed in the rotor, and end plates with bearings were designed and installed. The completed, stand-alone motor assembly is shown in Figure 1. The completed test stand is shown in Figure 2.

Locked Rotor Test

A series of locked rotor tests were performed to determine the torque-producing behavior of the PMSM motor. A motorized mechanical-gear mechanism was used to precisely position and lock the rotor based on readings from the absolute position sensor in the motor.

A motor-driven gear mechanism was used to rotate the motor incrementally every 5 electrical degrees, and the fixture remained rigidly locked each time a set level of dc current was applied. Torque values were obtained from an in-line shaft torque sensor when the motor windings were energized. The resulting Accord and Prius data were used to produce torque-vs-shaft-angle plots, which are shown in Figure 3 for various current levels and more than one-half an electrical cycle. The levels of torque that were produced reflect the absolute maximum torque obtainable from the motor for each current (magnetic

Table 1. Differences between the hybrid Accord and the Prius

Design feature	Hybrid Accord	Prius
Motor peak power rating, kW	12.4 @ 840 rpm	50 @ 1200–1540 rpm
Motor peak torque rating, Nm	136	400
Separate generator	No	Yes (although the motor also serves as a generator)
PMSM used for initial acceleration	Engine assist	Exclusively
Source of power to PMSM	Battery	Generator and battery
Purpose of the hybrid system	Primarily performance	Primarily improved fuel economy
PMSM rotor design	Interior permanent magnets embedded near the rotor surface	Interior permanent magnets with “V” configuration at each pole
Number of rotor poles	16	8
Boost converter used	No	Yes
Inverter bus voltage	144	200–500
PMSM cooling	Passive cooling	Water/glycol loop
Inverter cooling	Forced air convection	Water/glycol loop
Location of inverter	Behind rear seat in passenger compartment	Engine compartment
Physical integration of the PMSM	Flat (68-mm) motor-only assembly located between engine and torque converter; the rotor shaft is replaced by dual rotor hubs with bolt flanges	PMSM is included in an engine-mounted casing (“axle assembly”) that contains the generator and planetary gear/reduction gear assemblies

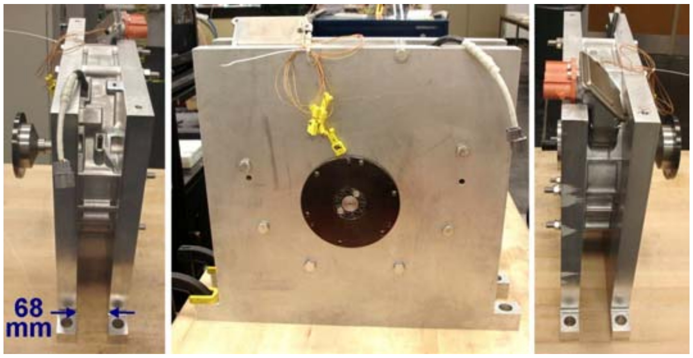

Figure 1. Accord motor with custom-designed end plates and shaft.

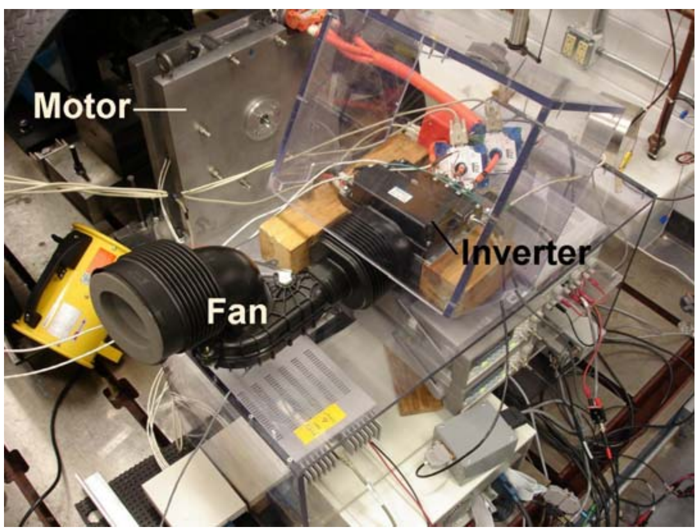

Figure 2. Preparation of test cell for Accord performance testing.

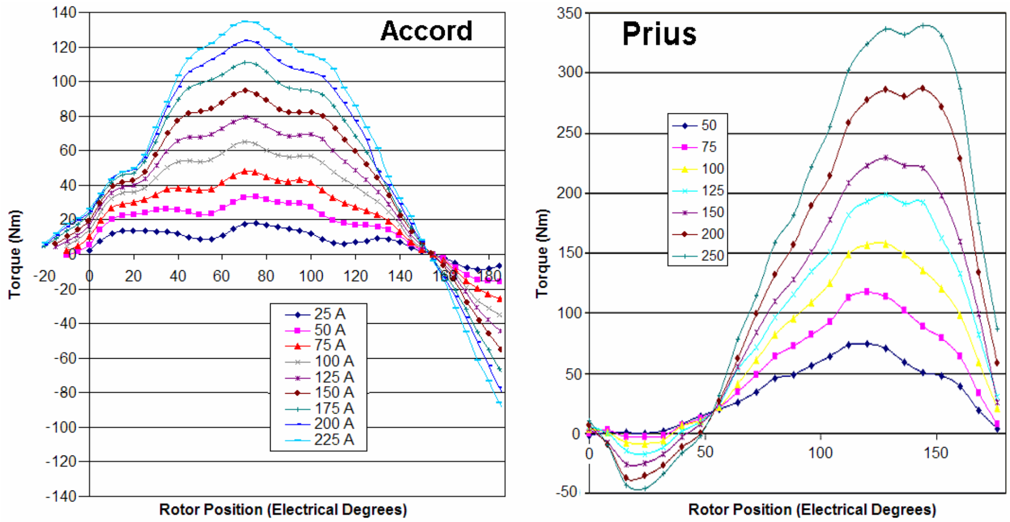

Figure 3. Accord/Prius locked-rotor torque vs electrical position at varying levels of stator current.

torque and reluctance torque). In contrast to an operating motor, there are no eddy current core losses, losses due to windage, and bearing friction.

Prius testing did not continue to the full torque specification of 400 Nm because of rapidly escalating stator winding temperatures. To collect several sets of data for averaging, it was necessary to remain at each speed-torque combination for about 20 s.

Accord/Prius Efficiency Mapping Data

Figures 4 through 6 show comparisons of the Accord and Prius Efficiency contour maps for the motor, inverter, and motor plus inverter, respectively. In each case, the bottom plot is for the Prius, and it shows comments pertaining to how the Prius efficiency compares with Accord efficiency for the designated area of the map. These comments are "broad-brush" comparisons and should not be taken in a precise, mathematical sense. For instance, very narrow contour regions of the map may be disregarded in the interest of placing emphasis on the larger, more significant areas.

The most important conclusion to be drawn from these figures is the fact that, in terms of efficiency, the Prius inverter excels, the Accord motor excels (except in the high-speed, low-torque region), and the combined HEV system efficiency is essentially the same except at the low-speed (<1000 rpm), high-torque region* where the Accord efficiency excels and the high-speed range where the Prius excels.

*Expressions such as "low-speed, high torque" for the Accord and Prius systems simply refer to corresponding areas or domains in the speed-load maps, even though the actual torque values may be quite different.

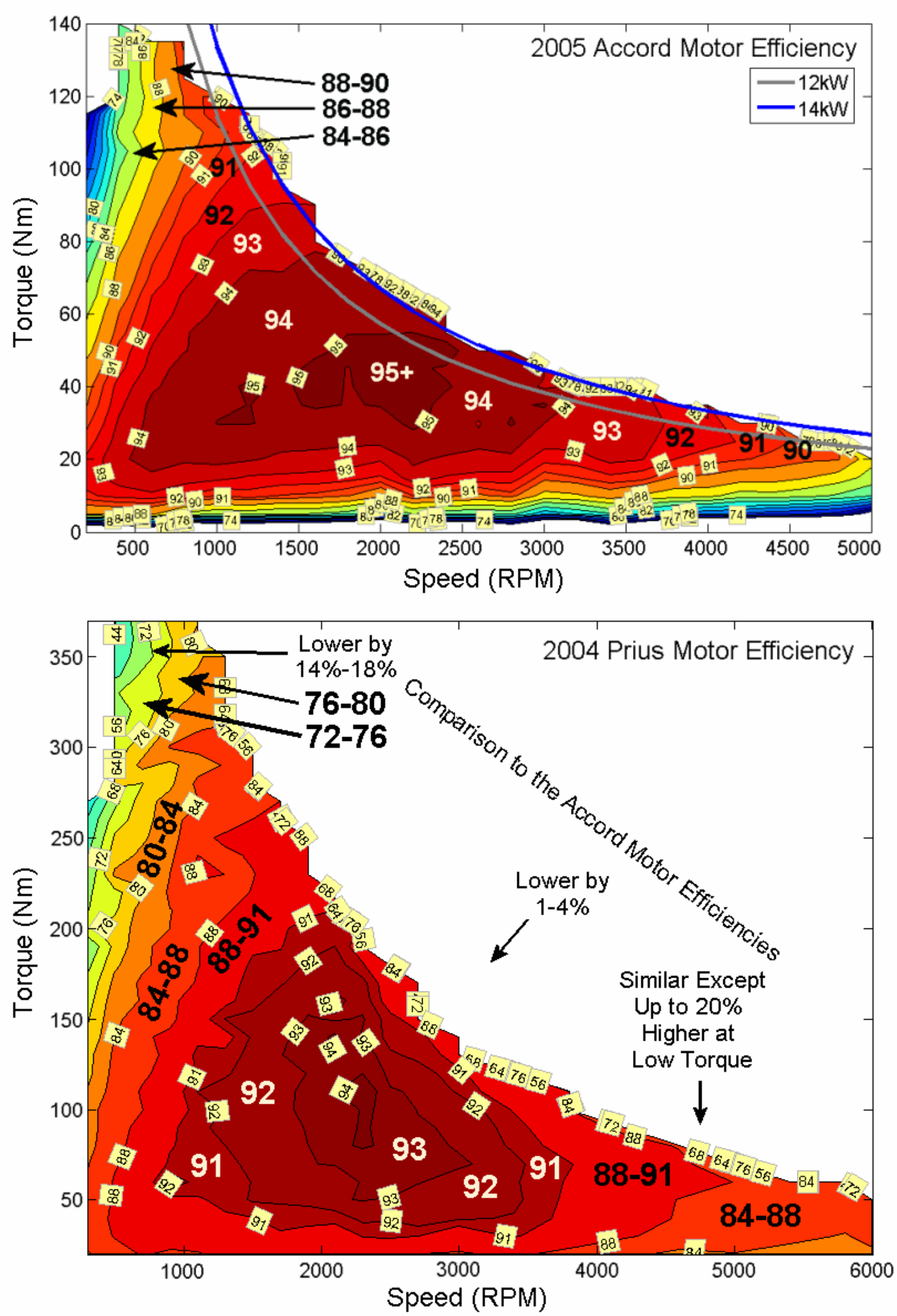

Figure 4. Comparison of Accord and Prius motor efficiency contour maps.

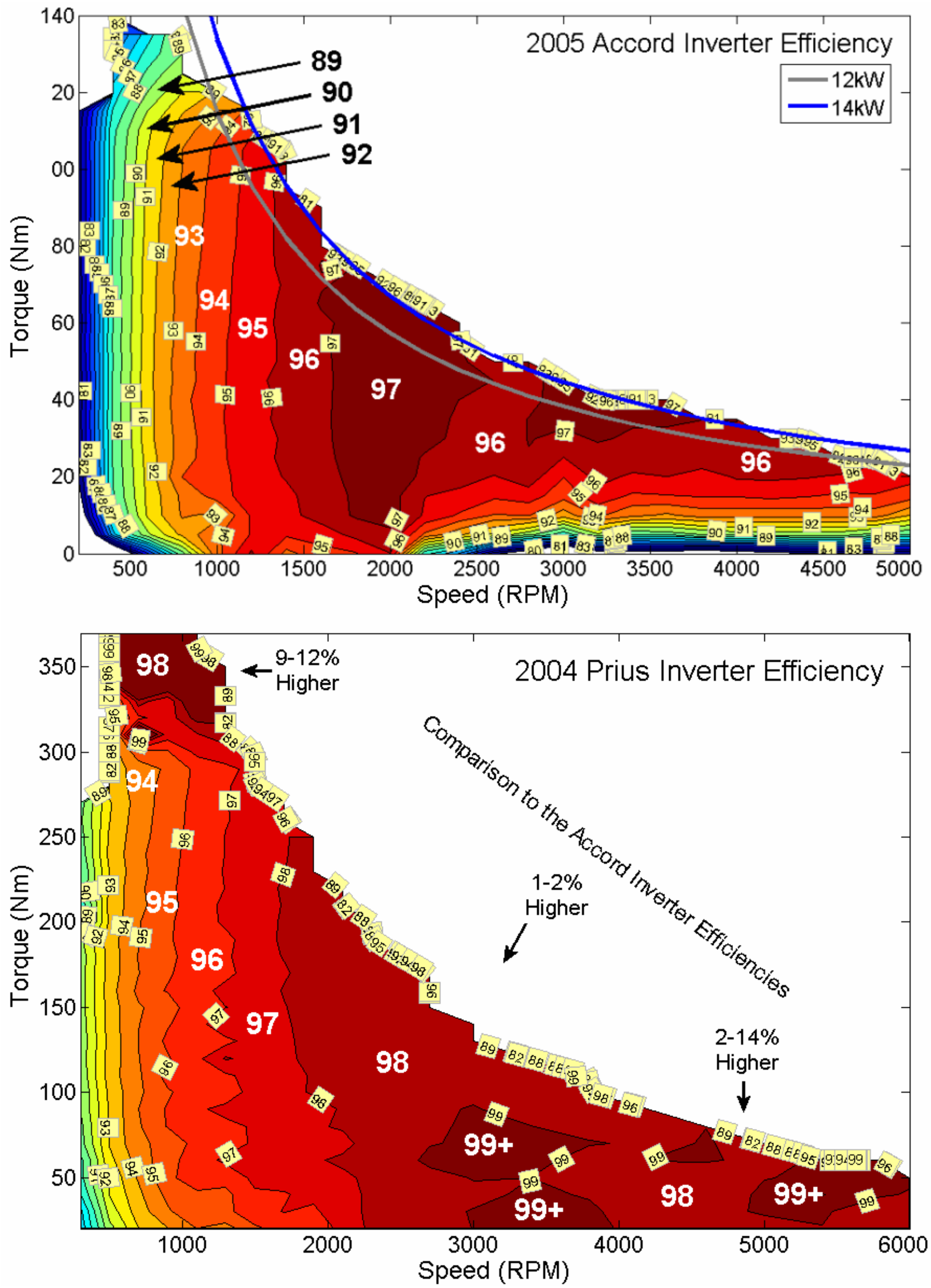

Figure 5. Comparison of Accord and Prius inverter efficiency contour maps.

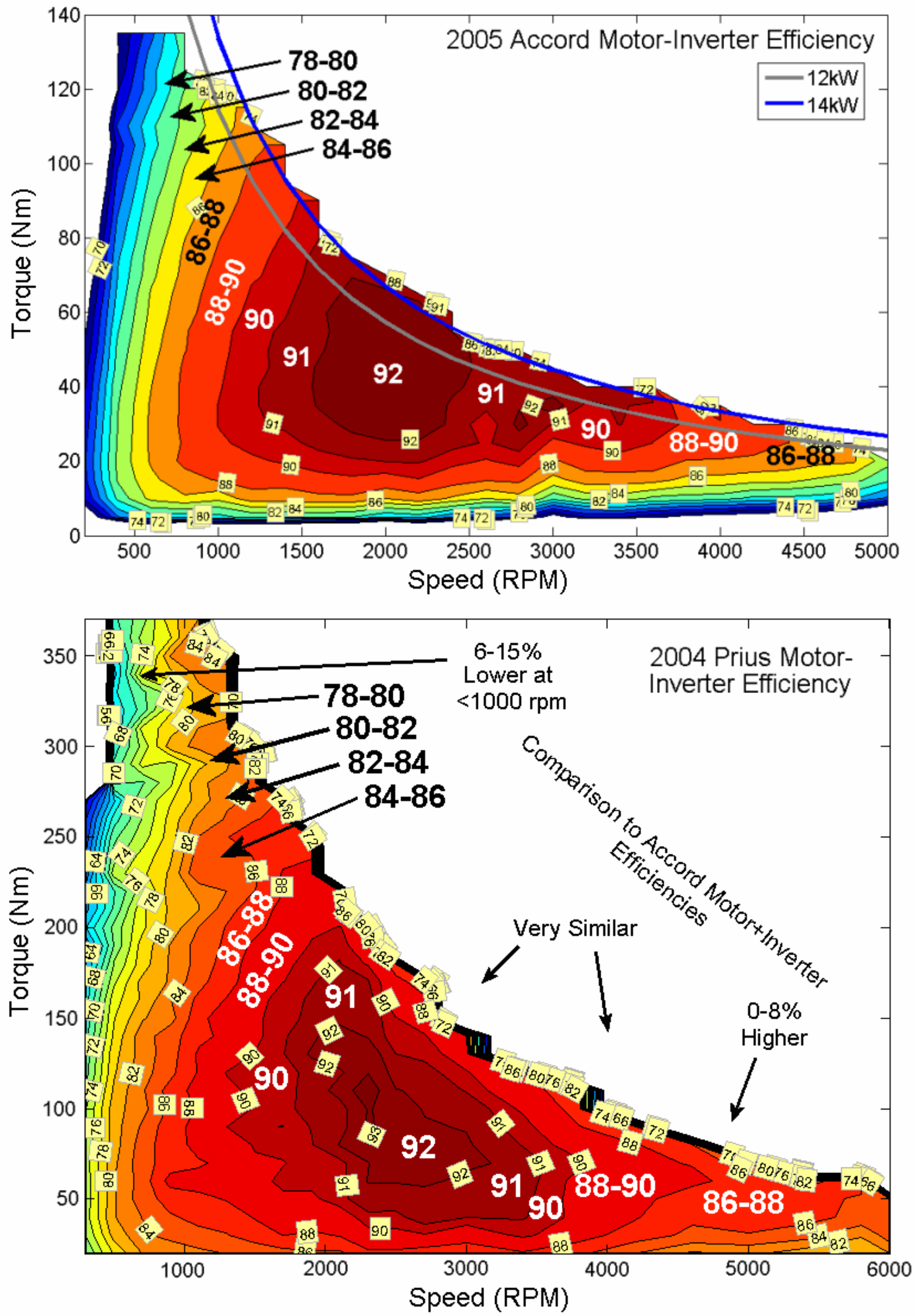

Figure 6. Comparison of Accord and Prius motor plus inverter efficiency contour maps.

Design Parameters for Prius/Accord

Table 2 summarizes the motor design and inverter insulated gate bipolar transistor (IGBT) ratings for the original Prius, the 2004 Prius, and the 2005 hybrid Accord designs. Included in the table are several design parameters describing each PMSM stator and rotor assembly and the PM volume and mass. Figure 7 provides clarification regarding the PM configurations used in each of the vehicle designs.

Table 2. Comparison of design parameters for Prius and Accord

Parameter	Prius I	Prius II	Accord	Comments
Stator OD, mm	269	269	315.5	
Stator ID, mm	162	162	232	
Rotor OD, mm	160	160	230	
Rotor ID, mm	115.6	111	188	
Rotor stack length, mm	90.7	83.6	41.2	Lamination only
Stator stack length, mm	89	84	40.1	Lamination only
Air gap, mm	1	1	1	
Lamination thickness, mm	0.356	0.33	0.343	
End-turn length, mm	83	80	35	Approx middle line
End-turn length (phase lead side), mm	83	80	35	Approx middle line
End turn arc extension, mm	31.8	30.5	~6.5–10	
Stator turns per coil	9	9	52	
Parallel circuit per phase	2	0	8	
Turns in series per phase	4	8	0	
Number of poles	8	8	16	
Number of stator slots	48	48	24	
Number of wires in parallel	13	13	0	
Wire diameter	Awg 19	Awg 19	1.55 mm	
Slot depth, mm	33.5	33.5	30.6	
Slot opening, mm	1.93	1.93	4.75	
Slot area, mm	–	–	307	
Phase resistance at 21°C, ohm	0.017	0.069	0.0097	
Stator winding mass, kg	7.48	6.8	3.01	
Stator core mass, kg	19.7	19.05	7.704	Laminations only
Rotor mass, kg	10.2	10.2	8.02	Prius I/II included bearings; Accord without bearings
Magnet width, mm	34.8	18.9	18.45	Individual magnets or bonded pairs as applicable
Magnet thickness, mm	6.15	6.5	4.46	Individual magnets or bonded pairs as applicable
Magnet length, mm	90.3	83.1	40.4	Individual magnets or bonded pairs as applicable
Magnet volume, mm	19330	10210	3320	For a pole, double Prius II and Accord volumes
Magnet mass, g	144	76	25	For a pole, double Prius II and Accord masses
IGBT current rating, A	Not tested	~195	~175	Max i during tests (per phase or IGBT pair)
IGBT voltage rating, V	600	1200	300 or 600	Assumed rating based on peak V

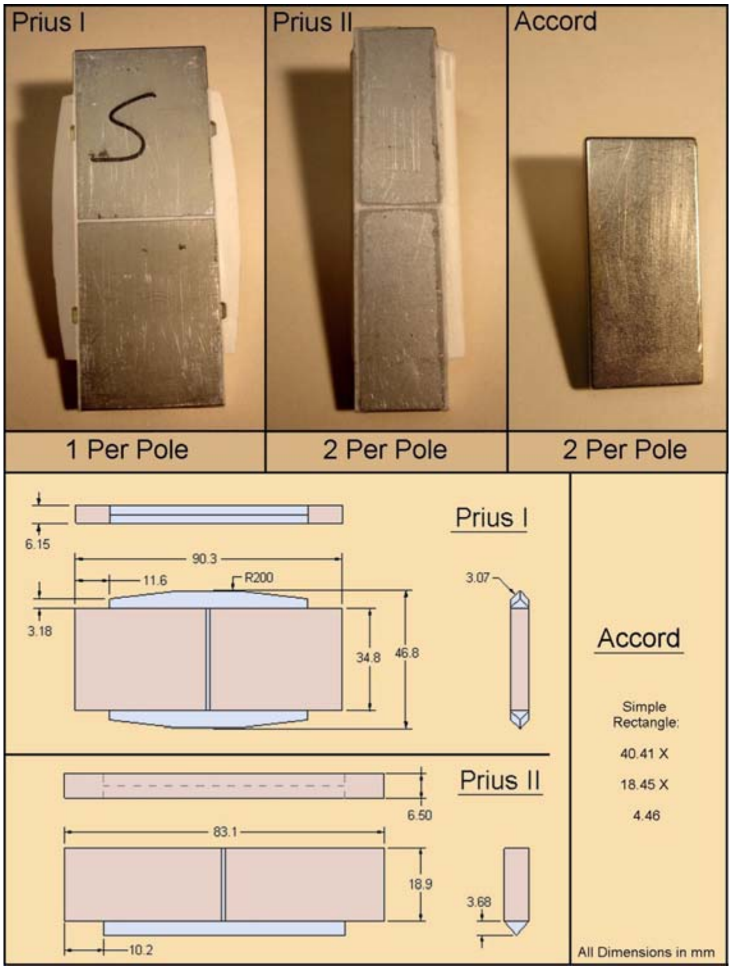

Figure 7. PM configurations and dimensions for three hybrid rotor designs.

Prius Inverter-only Mass and Volume Estimates

This section derives the inverter and casing mass and volume estimates for the Prius as if the buck/boost converter and generator-related circuitry did not exist. This has not been previously documented in any benchmarking report. The total volume of the Prius inverter/converter casing is 17.8 L as depicted in Figure 8.

The total volume of the Prius "inverter *only"* with resized casing is 9.9 L and is derived as follows:

- The midsection volume is reduced by 55% to account for the exclusion of the converter components, the generator portion of the inverter board (a 1/2 reduction), the generator portion of the power module (a 1/3 reduction), and the corresponding portion of the cold plate (a 60% reduction). See the change in the size of the cold plate in Figure 9 as a visualization aid.
- The casing is also reduced by the deletion of the bottom compartment (unrelated circuitry).
- The "cap" volume (or lid and capacitor volume) is retained in full.

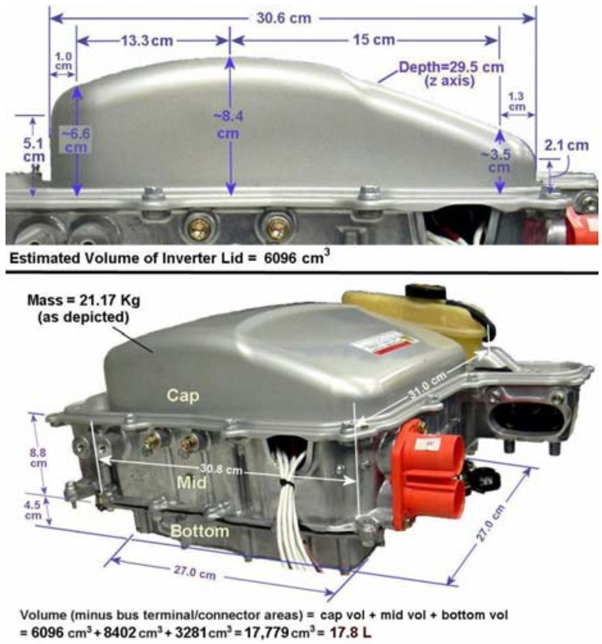

Figure 8. Volume of entire Prius inverter/converter assembly.

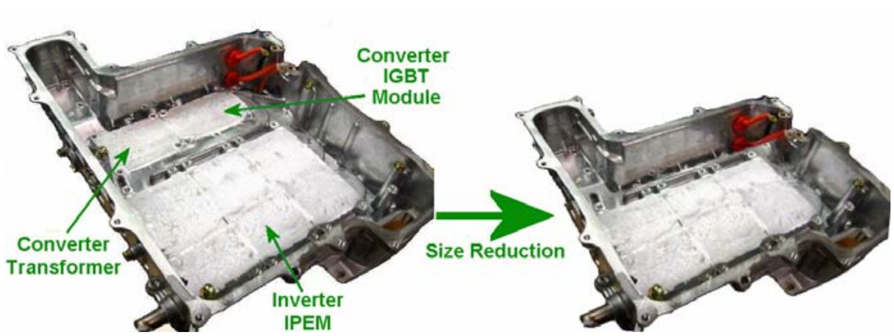

Figure 9. Conceptual change to inverter/converter casing for excluding the buck/boost converter.

The total mass of inverter/converter casing as depicted in Figure 8 is 21.2 kg.

The total mass of the "inverter *only*" is 9.4 kg and is derived in a similar manner to the volume (100% of cap mass, 45% of midsection mass, and 0% of bottom section mass). To be more precise, the mass of the converter transformer and converter power module were first fully excluded before the 45% was applied to the remainder of the midsection. This is quite significant considering that the converter transformer has a mass of 2.57 kg.

Prius Planetary Gear Packaging

The 2004 Prius has a planetary gear assembly that is integral to the motor/generator casing, and it is linked to reduction gears and a differential. Figure 10 shows the gear assembly with number-of-teeth

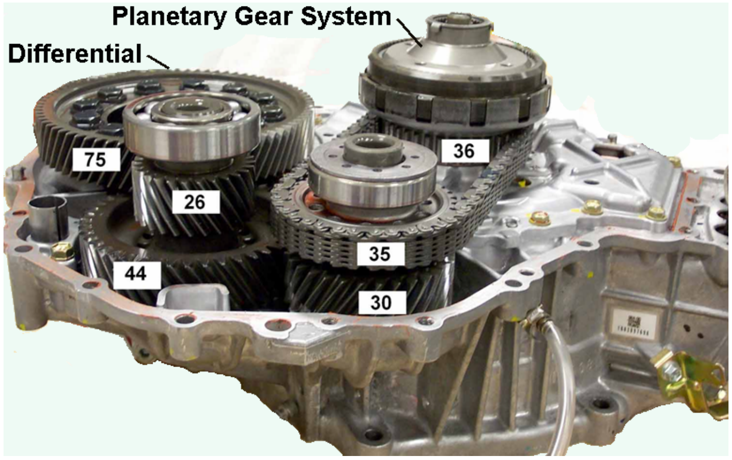

Figure 10. 2004 Prius gear assembly in an open casing.

labels on each gear. The planetary gear system uses the chain depicted in the figure to drive a series of reduction gears that power the differential and the axles. Because of the integral design, certain assumptions and estimates must be made to determine approximate mass and volume of the planetary gear system. The information provided in this section will include certain details on discrete components.

Figure 11 lays out the same gearing components as shown in Figure 10 and supplies masses associated with each. The fasteners represent an approximation because they were not fully inventoried.

Figure 11. Components making up the Prius gear box.

The casing for the assembly is not shown, and because of the two-piece design that is shared with the generator and motor, mass and volume estimates are difficult to produce with precision. Nevertheless, it is estimated from mass measurements of selected and modified Prius gear/motor casing parts that the entire gear assembly could be housed in an ~8-kg casing with a 17-L volume [also see Figure 12(a)].

A close-up of the partially disassembled planetary gear assembly with the top and bottom plates removed is shown in Figure 12(b).

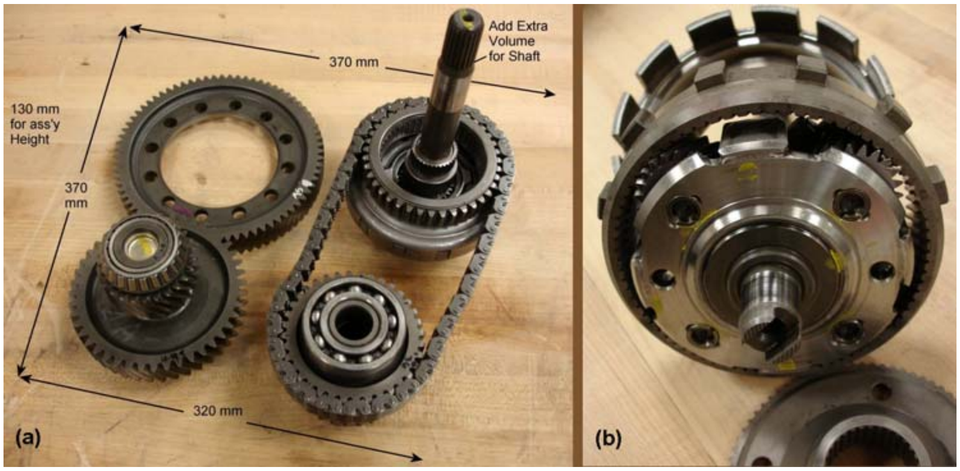

Figure 12. Approximate volume estimation and planetary gear assembly.

Additional information regarding dimensions for both components and the assembly are given in Figure 13.

Core loss tests

The core losses can be determined from energized spin tests where the motor shaft is uncoupled. Figure 14 provides the ac electrical power vs speed plot for the Accord PMSM.

Figure 13. Dimensions for planetary gear, the first reducer gear, and extension.

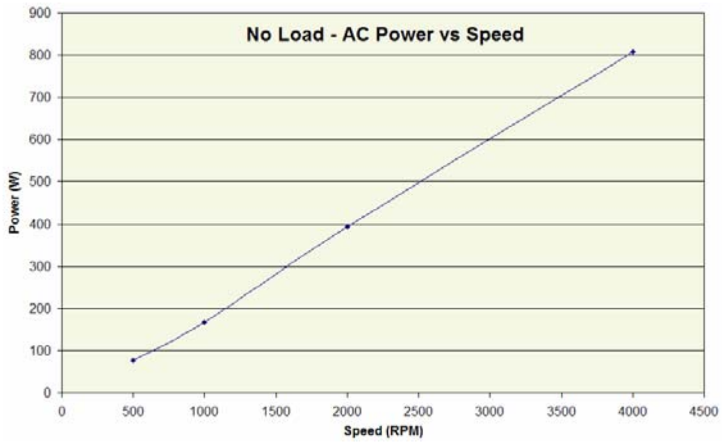

Figure 14. Uncoupled, energized spin test of the Accord motor to assess core losses.

Conclusion

The benchmarking project has been very successful in assessing the Prius and Accord designs and completing a full range of tests, including back-emf, locked-rotor, and efficiency mapping tests. The sets of data obtained from these tests have (1) helped to provide a technical basis for the FCVT management to determine program targets/direction and (2) enabled researchers to improve/refine their analytical models so that greater accuracy is obtained for high-power density PMSMs.

Future Direction

The FY 2007 goal of the benchmarking project is to complete testing of various traction drive subsystems that would be useful to the FCVT program integration/management. The design, packaging, and fabrication assessments will be combined with comprehensive performance mapping test results to enable analysts to determine how each HEV/PHEV traction drive subsystem compares with the other and with program technology targets (thermal efficiency, peak power density, and peak specific power goals). The project will focus on inverters, converters, and PMSMs. Since FY 2006, the impact of the collective data obtained from each vehicle has impacted the broader program, including program planning. This is expected to continue in FY 2007.

One specific test planned for FY 2007 is an assessment and performance evaluation of a high-speed PMSM such as used in the Toyota Highlander and the Lexus GS450 and RX400h. High-speed operation, up to 12,500 rpm, is clearly the most recent hybrid technology that has been successfully introduced into the market.

The Benchmarking project will continue its efforts to improve the accuracy of a PMSM model using data obtained from no-load and back-emf tests. Because the empirical approaches used in the performance tests ensure optimal operation, high-quality data are obtained that are well suited for this purpose. The model will effectively incorporate effects of saturation and the impact of variance in other parameters such as stator resistance and inductance, all of which fluctuate with speed, current, or temperature. The efforts to improve the motor model will aid in understanding the operational behavior of the 2006 Accord motor and other interior PM motors of similar design.

If capital funding is obtained in FY 2007, the project will upgrade the test cell with a larger dynamometer to permit the testing of high-power motors. The need for this can be underscored by considering that if the Prius motor had actually been capable of providing 400 Nm without rapid thermal escalation beyond short-term limits, the ORNL dynamometer would have proved to be inadequate to support thorough testing.

Limited evaluation of state-of-the-art capacitors and magnetic materials will be performed to ascertain their applicability for use in high-power, high-temperature FreedomCAR automotive applications.

Publications

R. H. Staunton, C. W. Ayers, J. Chiasson, T. A. Burress, and L. D. Marlino, *Evaluation of 2004 Toyota Prius Hybrid Electric Drive System*, ORNL/TM-2006-423, Oak Ridge National Laboratory, May 16, 2006.

R. H. Staunton, T. A. Burress, and L. D. Marlino, *Evaluation of 2005 Honda Accord Hybrid Electric Drive System*, ORNL/TM-2006-535, Oak Ridge National Laboratory, UT-Battelle, LLC, September 2006.

5.2.2 Component Characterization

Principal Investigator: Larry Seiber
Oak Ridge National Laboratory
National Transportation Research Center
2360 Cherahala Boulevard
Knoxville, TN 37932
Voice: 865-946-1334; Fax: 865-946-1400; E-mail: seiberle@ornl.gov

DOE Technology Development Manager: Susan A. Rogers
Voice: 202-586-8997; Fax: 202-586-1600; E-mail: Susan.Rogers@ee.doe.gov

ORNL Program Manager: Mitch Olszewski
Voice: 865-946-1350; Fax: 865-946-1262; E-mail: olszewskim@ornl.gov

---

Objective

As capacitor and magnet technologies mature, it is important to ascertain the limitations of these new technologies by subjecting the components to testing that will evaluate their capabilities and limitations. The object of this project is to test and characterize new capacitor and magnet components to determine their ability to provide improvements in power electronics and motor designs to meet the FreedomCAR goals.

Approach

- Capacitor performance data were acquired by testing over temperature in both static and dynamic modes of operation. A data acquisition system (DAQ) was developed and used to log the test results for the capacitor parameter evaluations.
- A full four-quadrant hysteresis graph was used to evaluate the new magnet technologies over an expanded temperature range.

Major Accomplishments

- Commercial film and ceramic capacitor benchmarks were defined and characterized.
  Capacitor test samples were tested in two modes, statically and dynamically. Capacitor testing in the static mode requires a thermal cycling process that must continue uninterrupted for extended periods of time. Capacitor testing in the dynamic mode requires testing at thermal extremes and requires ripple current and bias voltage input from the operator.
- Magnet benchmarks for bonded and sintered magnets were defined and characterized.
- Magnet test samples were tested over a temperature range from 20 to 235ºC.
- The development of a DAQ using LABView was completed to control the environmental chamber and log data from the measuring instruments for capacitor evaluations.

Technical Discussion

Data Acquisition System

The DAQ consists of a Dell Precision 380 Workstation running LABView 7.1. In the static mode the instruments used are an Espec environmental chamber and an Agilent 4284 LCR meter. Figure 1 shows the input screen for the static test.

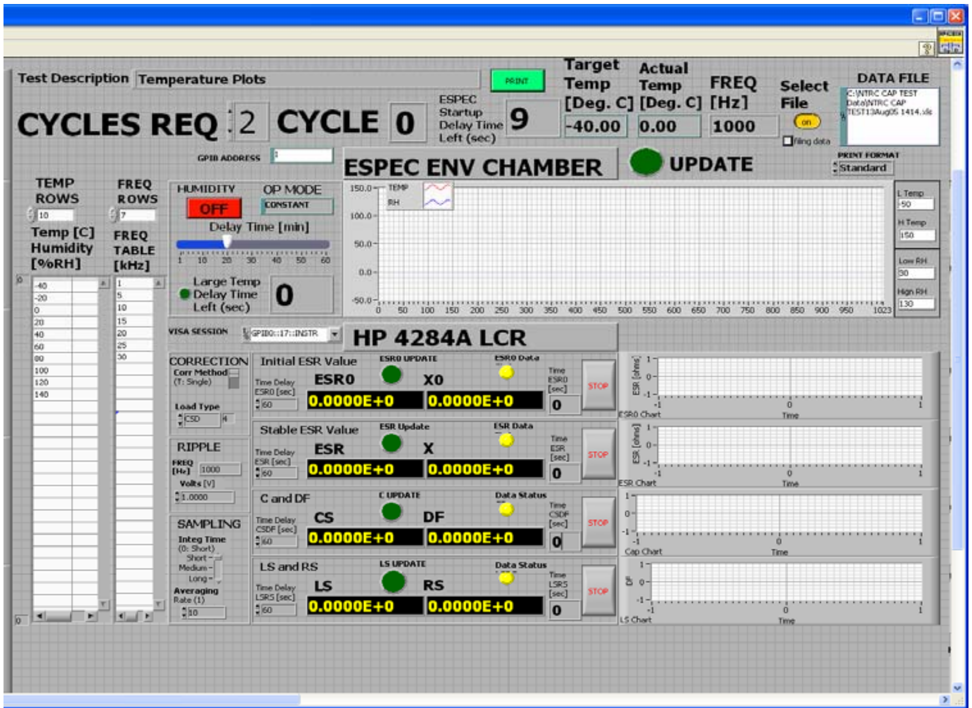

Figure 1. Static test input screen.

At the beginning of the static thermal cycling test, temperature steps and test frequencies are entered in the tables on the left of the screen. A test description is entered at the top of the screen, and the number of cycles requested is also entered. A delay time is set using the slider bar in the large temperature delay time window. This preprogrammed delay is to ensure that the temperature of the dielectric has equalized once the target temperature of the environmental chamber has been reached. When the temperature difference between the ambient temperature of the chamber and the target temperature of the chamber is 40ºC or greater, the preprogrammed delay is invoked after the target temperature is reached. The amount of delay is determined by the operator and is based on the size of the capacitor. A larger capacitor will require a larger delay to ensure that the temperature of the dielectric is uniform.

Once data have been entered, the program turns on the environmental chamber and commands a target temperature to the chamber. After the target temperature is reached and the preprogrammed delay time is met, the program sends a command to the LCR meter to output the first test frequency and then begin to monitor the equivalent series resistance (ESR) from the capacitor under test. When that value is stable, the ESR is recorded, and the next parameter is measured and recorded. After the ESR, the dissipation factor (DF), and capacitance value are recorded at the first test frequency, the command is given to the LCR meter to output the next test frequency and the monitoring and recording process is repeated. After all data are recorded at all test frequencies, the next temperature step is commanded to the environmental chamber, and the process is repeated.

Capacitor testing in the dynamic mode also uses the DAQ. Figure 2 shows the dynamic test input screen.

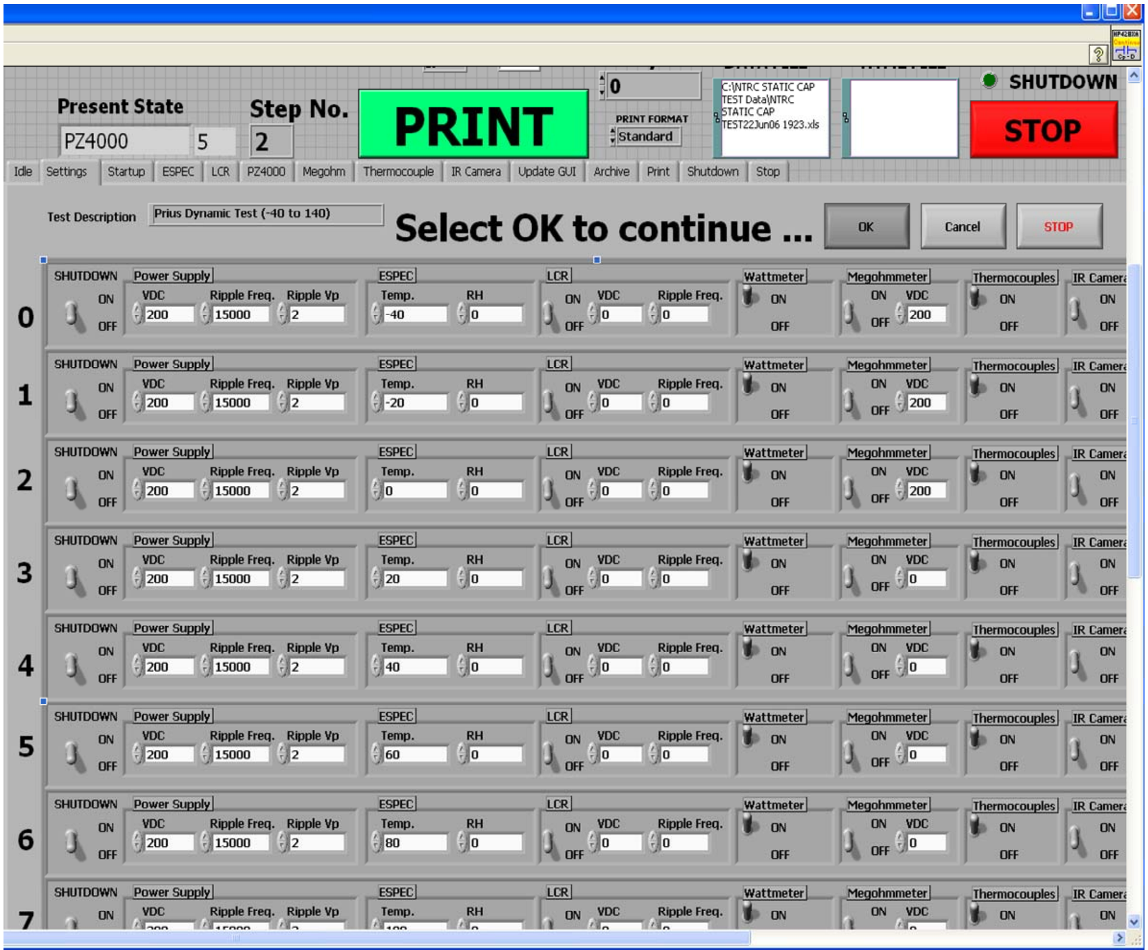

Figure 2. Dynamic test input screen.

Capacitor testing in the dynamic mode requires a dc bias voltage to be applied to the capacitor under test along with a ripple current. The maximum bias voltage value is 75% of the maximum rated dc voltage of the capacitor. The dc bias voltage is applied in series with the secondary of a transformer and across the capacitor under test. The primary of the transformer is connected to the output of an ac amplifier, and a signal generator is connected to the ac amplifier. This configuration will provide a ripple current that is at a dc level similar to what would be seen in an inverter. The signal generator also allows the ripple current frequency to be adjusted. The ripple current value in amps can be adjusted by adjusting the gain of the ac amplifier.

Thermocouples are attached at three different locations on the capacitor, one on each end and one in the middle to monitor temperature rise as ripple current values increase.

After the bias voltage and ripple current have been adjusted, the DAQ dynamic mode is activated, and temperature limits and steps are entered. Ripple current amplitude and frequency can be changed along with the dc bias voltage at each temperature step if needed. Different measuring instruments can also be selected or turned off at each temperature step. Instruments can be selected or deselected by clicking on the toggle switch located on the front panel of the dynamic test input screen in Figure 2.

After all temperature step values, dc voltage values, and test frequencies have been entered, the program turns on the environmental chamber, commands a target temperature, and begins monitoring the chamber temperature. When the target temperature is reached, the program waits for operator input before logging ripple current, chamber temperature, and thermocouple data. The next temperature step will then be commanded.

Static Testing

Single Prius film capacitor

A single 140-μF 600-Vdc film capacitor was extracted from the 2004 Prius capacitor module to use as a benchmark for film capacitor evaluations. The module was taken to a materials lab to be x-rayed to identify the layout of the ten capacitors in the module. The film was brought back to the Power Electronics on Electric Machines Research Center lab, and several single capacitors were extracted for testing. Figure 3 shows the test configuration used to evaluate the single Prius capacitor, in the static and dynamic mode, inside the environmental chamber.

The capacitor was placed in a vise with copper strips on each end bent to allow connection to a cable capable of carrying high ripple currents. Electrically insulating material was added between the vise and the copper strips. This material also provided some thermal insulation in an effort to keep the vise from becoming a heat sink during the ripple current vs temperature evaluation.

Figure 4 shows the results of the static test on the single Prius film capacitor.

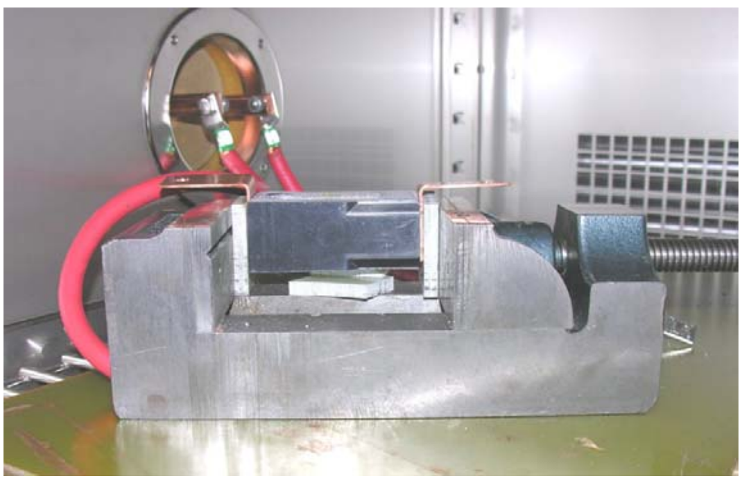

Figure 3. Single Prius film capacitor test set up.

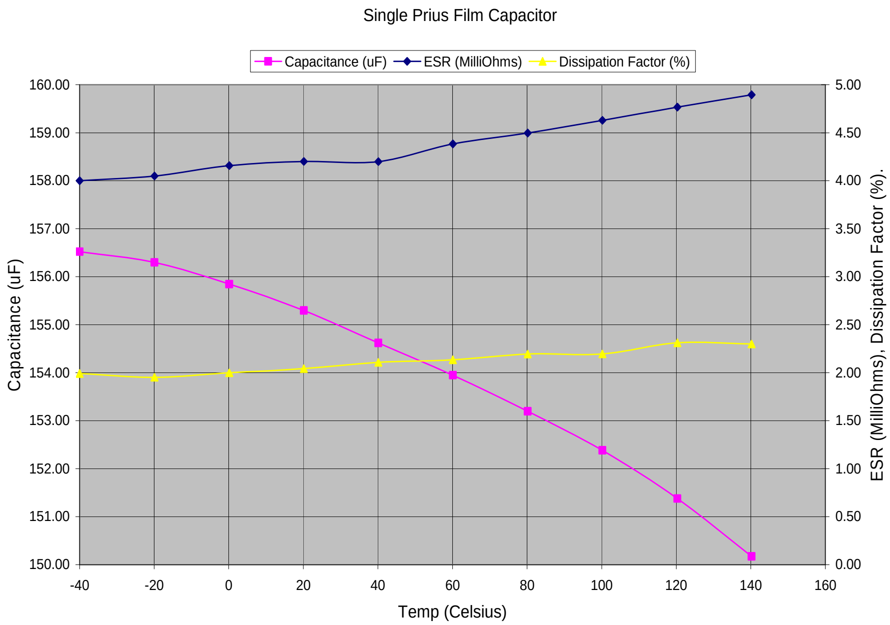

Figure 4. Single Prius film capacitor tested in the static mode at 5 kHz.

When tested at 5 kHz, the DF increased less than 0.5% over the entire temperature test range of –40ºC to 140ºC. The capacitance value decreased less than 5%, and the ESR increased less than 1 mΩ.

The ESR, DF, and capacitance values of the single Prius capacitor were evaluated at frequencies of 1 kHz, 2 kHz, 5 kHz, 10 kHz, and 15 kHz at three different temperatures: –40ºC, 20ºC, and 120ºC. Figures 5–7 show these results.

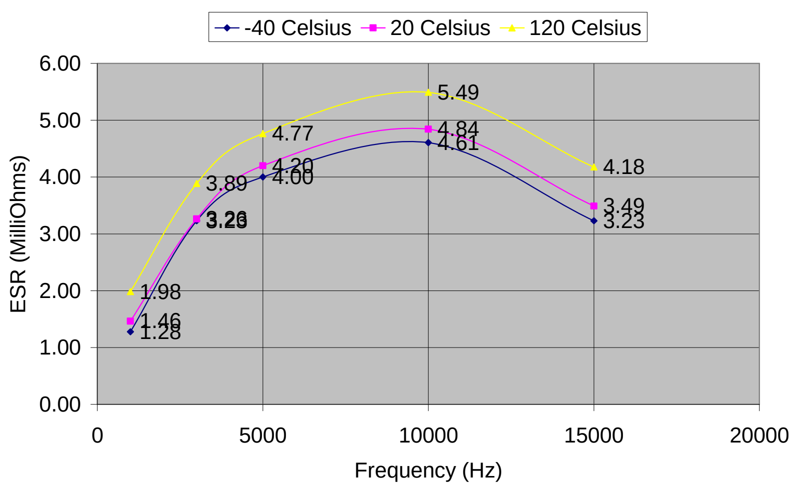

Figure 5. Single Prius film capacitor ESR frequency response.

The ESR peaked at 10 kHz at all temperatures and increased from an average of 1.57 mΩ at 1 kHz to an average of 4.98 mΩ at 10 kHz. The average at 5 kHz was 4.32 mΩ.

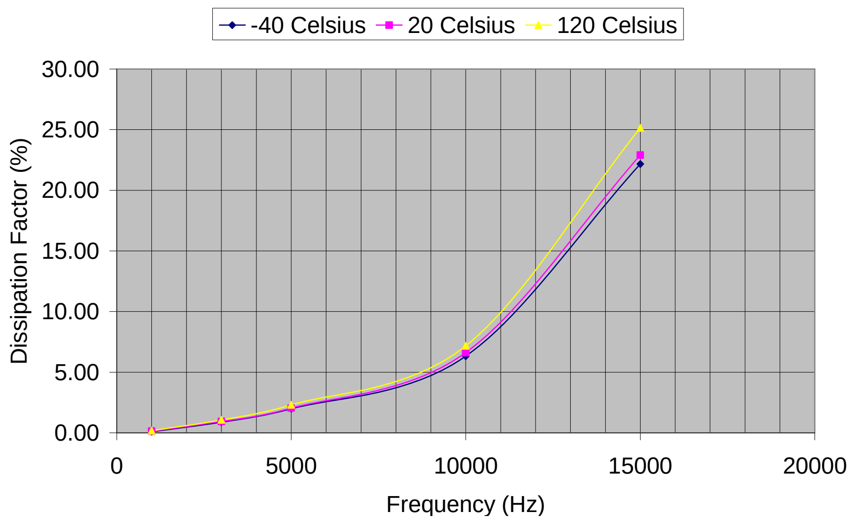

Figure 6. Single Prius film capacitor DF frequency response.

The DF increased from a value of 0.14% at 1 kHz to a value of 2.04% at 5 kHz. At 10 kHz, the average value was 6.7%. The increase was substantial above 10 kHz.

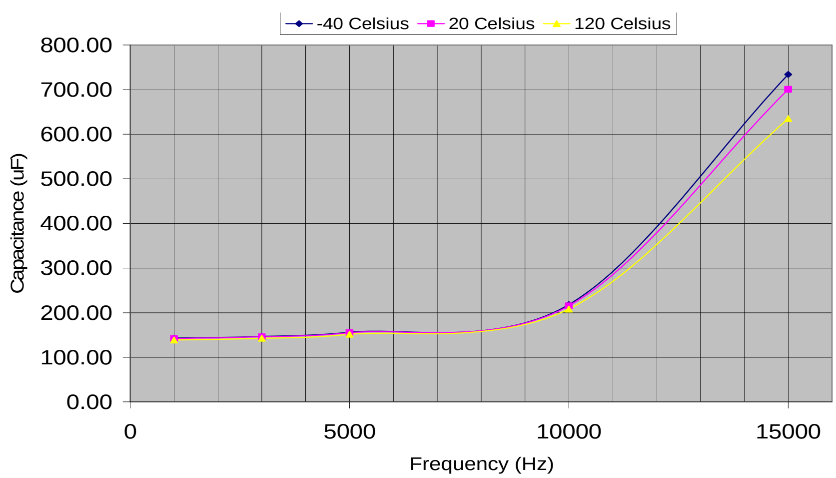

Figure 7. Single Prius film capacitor frequency response.

The capacitance value increased 9% from 1 kHz to 5 kHz at all three temperatures. Above 10 kHz, there was a very substantial increase in capacitance that was evident up to 15 kHz.

Kemet ceramic capacitor

A Kemet 1-μF 500-Vdc ceramic capacitor was tested in the static mode as a ceramic benchmark. The capacitor is rated at 200ºC. Figure 8 shows ESR, DF, and capacitance values over the temperature range of –40ºC to 180ºC.

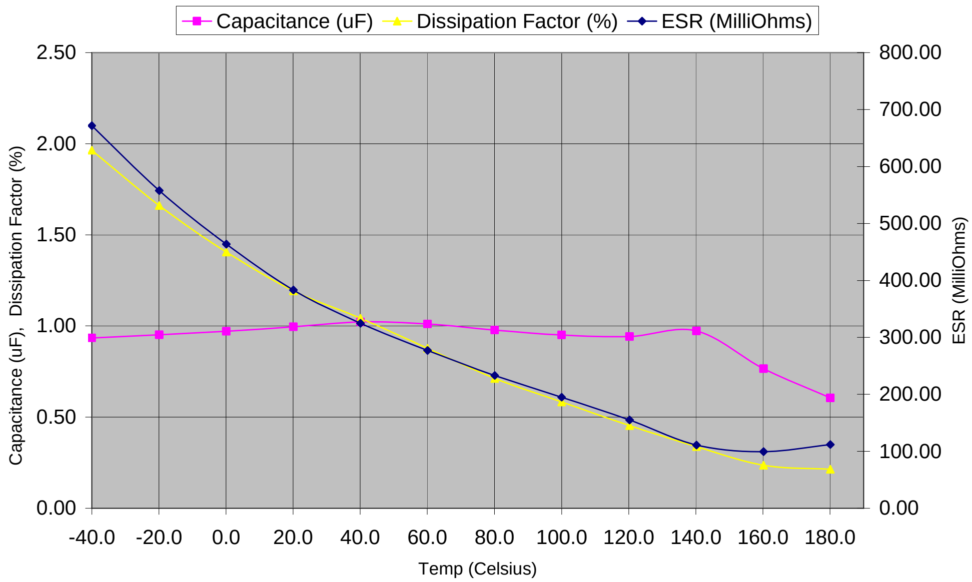

Figure 8. Kemet ceramic capacitor static test at 5 kHz.

The Kemet 1-μF ceramic capacitor was tested over the temperature range of –40ºC to 180ºC. The DF decreased from 1.96% to 0.21%, and the ESR changed from 671 mΩ to 111 mΩ. The capacitance value was basically flat up to 140ºC; at that point it changed from 0.93 μF to 0.61 μF at 180ºC.

Penn State multilayer ceramic capacitor

Pennsylvania State University (Penn State) supplied a 90-nF 500-Vdc high-temperature prototype multilayer ceramic capacitor for evaluation. The capacitor is rated at 300ºC. The static test of this capacitor at 5 kHz is shown in Figure 9.

The Penn State 300ºC prototype multilayer ceramic capacitor was tested in the static mode at 5 kHz over the temperature range of –40ºC to 180ºC. The DF decreased from 6.39% to 1.8%, and the ESR decreased from 144 Ω to 8.68 Ω. The capacitance value increased from 14.1 nF to 66.5 nF.

This capacitor did not function well at lower temperatures, but as the temperature increased it continued to improve. The capacitor was rated at 300ºC, but the evaluation was made to 180ºC because of the limitations of the environmental chamber.

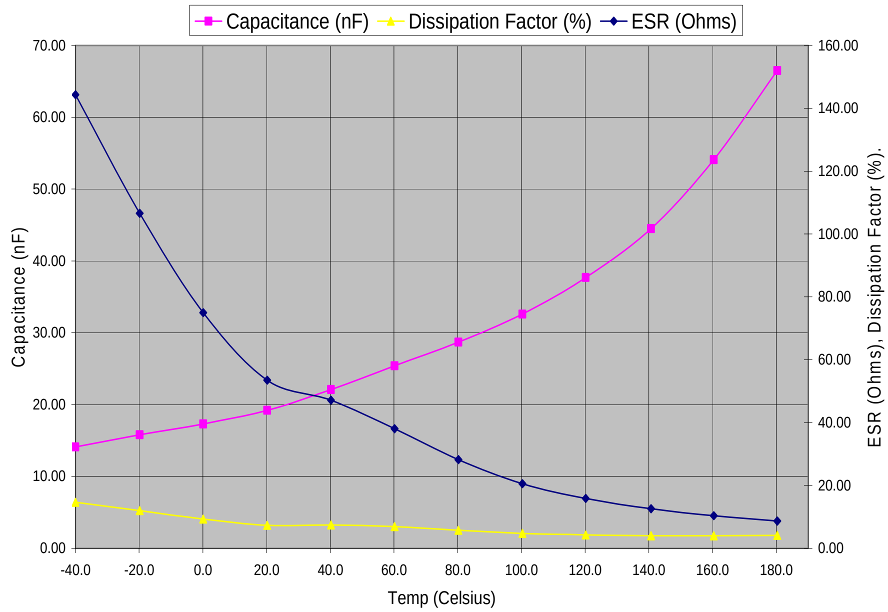

Figure 9. Penn State ceramic high-temperature static test at 5 kHz.

Dynamic Testing

The single film capacitors extracted from the Prius capacitor module were also tested in the dynamic mode. The bias voltage was 250 Vdc. Maximum ripple current was determined at several different ambient temperatures; leakage current and effective series inductance (ESL) were also measured. No prototype film capacitors were supplied to Oak Ridge National Laboratory for dynamic tests during this reporting period.

Because of the size and the fact that they will not be used as a dc bus filtering capacitors, the smaller value ceramic capacitors were not tested in the dynamic mode.

Single Prius film capacitor ripple current

Figure 10 shows the results of a single 140-µF Prius film capacitor's ripple current test. This capacitor was extracted from the Prius capacitor module and was tested by increasing the ripple current and measuring the temperature rise above an ambient temperature of 22ºC. The test was repeated at an ambient temperature of 100ºC.

The maximum ripple current was determined by increasing the current in 5-A steps until the capacitor failed. After each increase, the temperature on the surface of the capacitor was allowed to stabilize before increasing the ripple current to the next value. At 100ºC ambient, the capacitor failed after 20 min at 70 A of ripple current. The ambient temperature was raised to 140ºC, and another single film capacitor was tested from the Prius module. This capacitor failed at 20 A ripple current after 30 min. The ambient temperature was decreased to –40ºC, and another single film capacitor was tested from the Prius module. This capacitor failed at 100 A of ripple current after 35 min. Table 1 lists these ripple current limits. All tests were done at 5 kHz. The capacitors failed when their film melted and thus shorted.

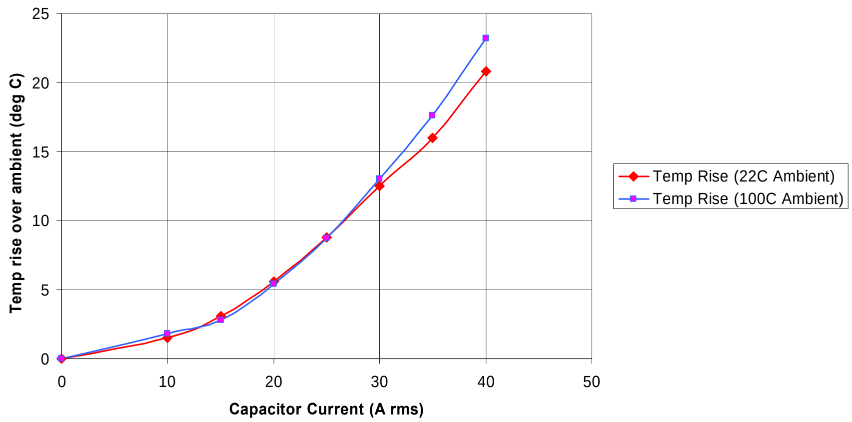

Figure 10. Temperature rise over ambient at 5 kHz.

Table 1. Maximum ripple current for the single Prius film capacitor

Ambient temperature	20 A	70 A	100 A
–40ºC			Failure after 35 min
100ºC		Failure after 20 min	
140ºC	Failure after 30 min		

Single Prius film capacitor leakage current

Leakage current test results measured on a single Prius film capacitor using a Danbridge 621 megohmmeter are listed in Figure 11. The capacitor was placed in the environmental chamber, and leakage current was measured at five different temperatures: 25ºC, 40ºC, 60ºC, 80ºC, and 100ºC.

Leakage current increased through the single Prius film capacitor from 16 nA to 16 µA over the test range of 25ºC to 100ºC.

Single Prius film capacitor ESL

ESL was measured on the single Prius film capacitor using a method and circuit configuration offered by Electronic Concepts, Inc. This circuit is shown in Figure 12.

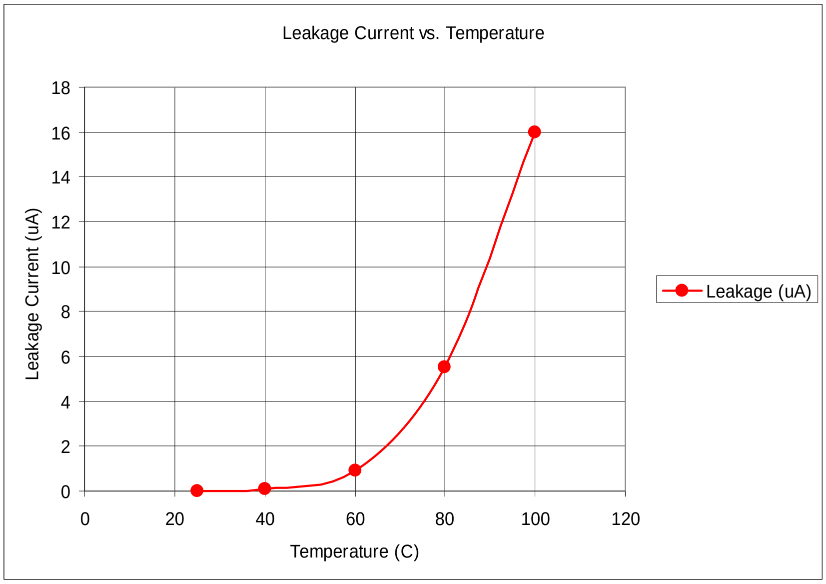

Figure 11. Single Prius film capacitor leakage current vs temperature.

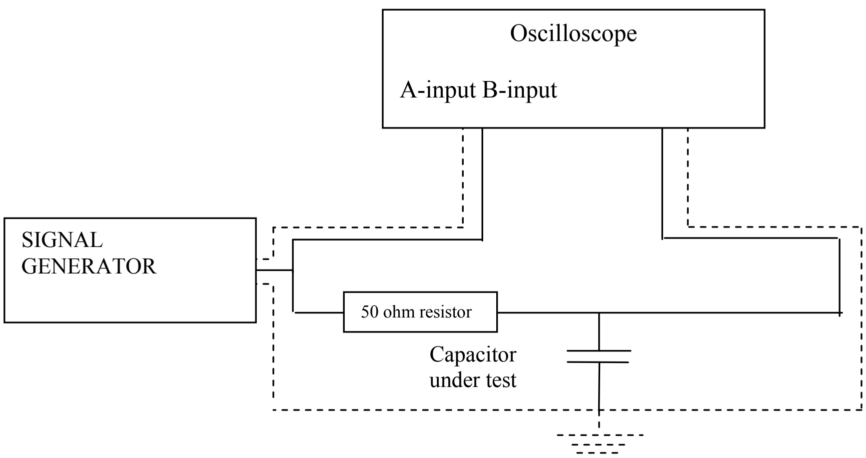

Figure 12. Circuit used to calculate ESL.

After the resonant frequency was found using the circuit in Figure 12, the ESL was derived as a function of the inductive reactance (X_L) and the capacitive reactance (X_C). At resonant frequency, the two are equal so that $X_L = X_C$; therefore, $2\pi fL = 1/(2\pi fC)$, and from this the equation for inductance is ESL = $L = 1/(4\pi^2 f^2 c)$. The ESL of the single Prius film capacitor was found to be 147 nH at an ambient temperature of 22ºC.

Magnet Evaluation

Magnet samples were evaluated using a Walker Scientific AMH-40 automatic hysteresisgraph. This computer-controlled system is used for testing, analyzing, and evaluating the hysteresis properties of magnetic materials. The system consists of a PC-based control console, two computer-interfaced integrating flux meters, a gauss meter, B and B-H coil sets, two 7-in.-diam variable-gap water-cooled electromagnets with cobalt-iron tipped poles, and a 5-kW 50-A programmable power supply. The 1200-lb electromagnets are capable of generating demagnetizing forces up to 30,000 Oersteds. This system allows the operator to perform five different types of tests: (1) manual H-Field sweep, (2) second-quadrant demagnetization curves, (3) complete four-quadrant full hysteresis loops, (4) recoil minor loops after saturation in the first quadrant, and (5) first-quadrant saturation or demagnetization of the samples. Also complementing the system is a pulse charger capable of saturating very hard magnetic materials and a Model TCS2 temperature-controlled, water-cooled fixture for testing materials at temperatures ranging from –100 to +300ºC. This fixture is used with a compatible, high-temperature coil set with integral thermocouples.

The basic magnetic properties measured using the AMH-40 automatic hysteresisgraph are residual induction (Br), coercive force (Hc), intrinsic coercivity (Hci), and energy product (BHmax).

Sintered magnets

A Prius magnet was evaluated as the sintered magnet benchmark using the AMH-40 Hysteresisgraph, four-quadrant full hysteresis loop. Two other sintered magnets were evaluated against the Prius benchmark using the same four-quadrant full hysteresis loop: Shin-Etsu's N43TS and a magnet developed at Argonne National Laboratory (ANL).

Table 2 shows that the Hci value for the Shin-Etsu N43TS sintered magnet is 30% less than the Prius benchmark magnet at 183ºC. The intrinsic coercivity (Hci) parameter, is used as an indication of a magnet's resistance to demagnetization. The hysteresis plot of the N43TS will show the knee of the demagnetization curve in the second quadrant. If the operating point of the magnet falls below the knee of this curve, the magnet will have an irreversible loss of magnetization. The Prius magnet had better resistance to demagnetization at elevated temperatures than other sintered magnets tested. The maximum energy product (BHmax) of the N43TS magnet is 12% better than the Prius at 183ºC, and the residual induction (Br) of the N43TS is 6% better than the Prius.

The magnet developed at ANL was not tested beyond 175ºC because it falls far below the Prius benchmark in all areas except Br. In this area, the ANL magnet is 3% better than the benchmark.

Figures 13–15 show the full four-quadrant hysteresis graph of the Prius sintered magnet, the Shin-Etsu N43TS sintered magnet, and the ANL sintered magnet at elevated temperatures.

Table 2. Sintered magnet test results

Magnet type	Residual induction (Br) (kG)	Coercivity (Hc) (kOe)	Intrinsic coercivity (Hci) (kOe)	Energy product (BHmax) (MGOe)
Prius (sintered) [a]	**12.55 (ambient)** **10.42 (183ºC)** **9.37 (235ºC)**	**12.18 (ambient)** **9.13 (183ºC)** **5.44 (235ºC)**	**>24 (ambient)** **9.87 (183ºC)** **5.63 (235ºC)**	**38.19 (ambient)** **26.17 (183ºC)** **20.83 (235ºC)**
Shin-Etsu N43TS (sintered)	13.33 (ambient) 11.09 (182ºC)	12.92 (ambient) 6.79 (182ºC)	>24 (ambient) 6.87 (182ºC)	42.95 (ambient) 29.43 (182ºC)
ANL (sintered)	12.91 (ambient) 10.75 (175ºC)	11.85 (ambient) 3.05 (175ºC)	15.01 (ambient) 3.07 (175ºC)	38.68 (ambient) 19.6 (175ºC)

[a] Bold indicates benchmark magnet.

Br = 10.42 kG
Hc = 9.13 kOe
Hci = 9.87 kOe
BHmax = 26.17 MGOe

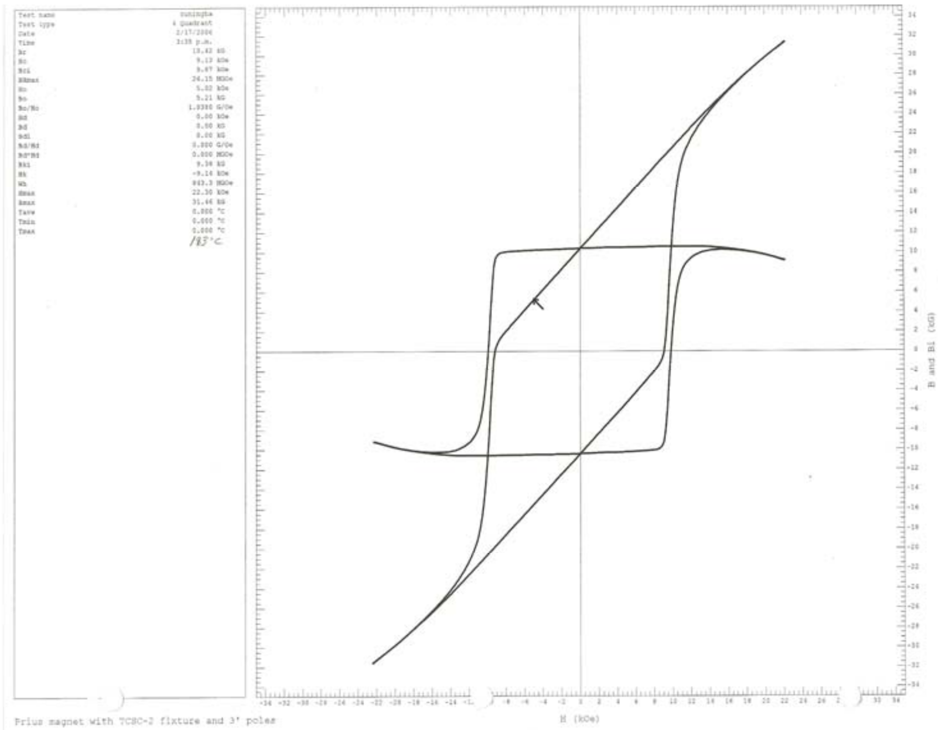

Figure 13. Hysteresis plot of the Prius sintered benchmark magnet at 183ºC.

Br = 11.09 kG
Hc = 6.79 kOe
Hci = 6.87 kOe
BHmax = 29.43 MGOe

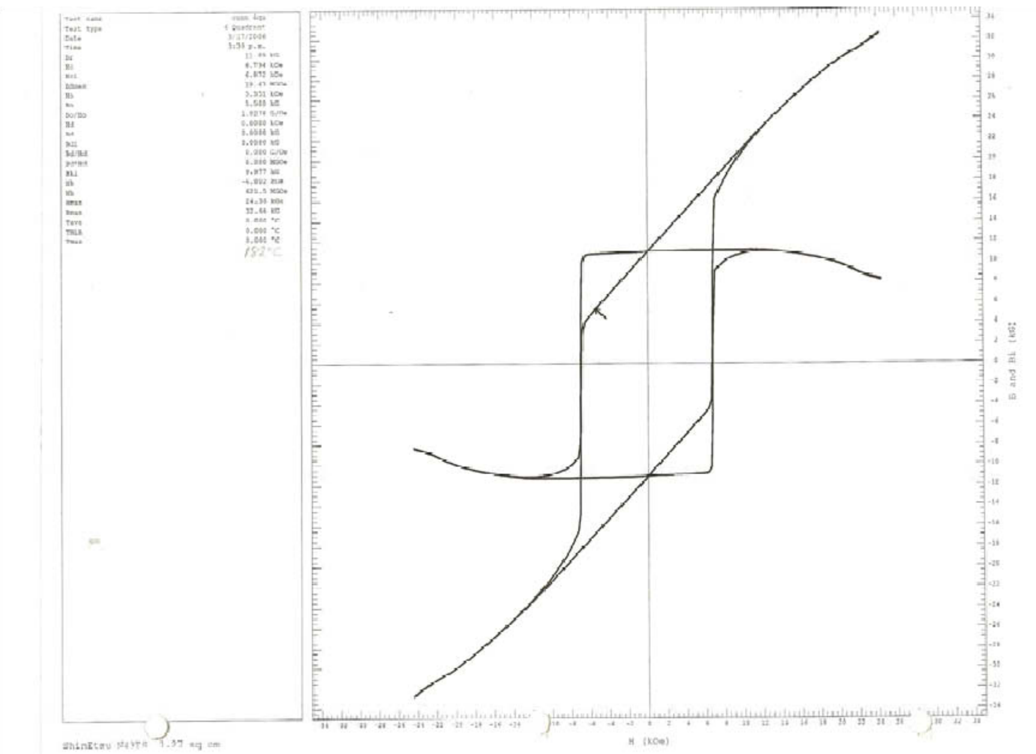

Figure 14. Hysteresis plot of the Shin-Etsu N43TS sintered magnet at 182ºC.

Br = 10.75 kG
Hc = 3.05 kOe
Hci = 3.07 kOe
BHmax = 19.60 MGOe

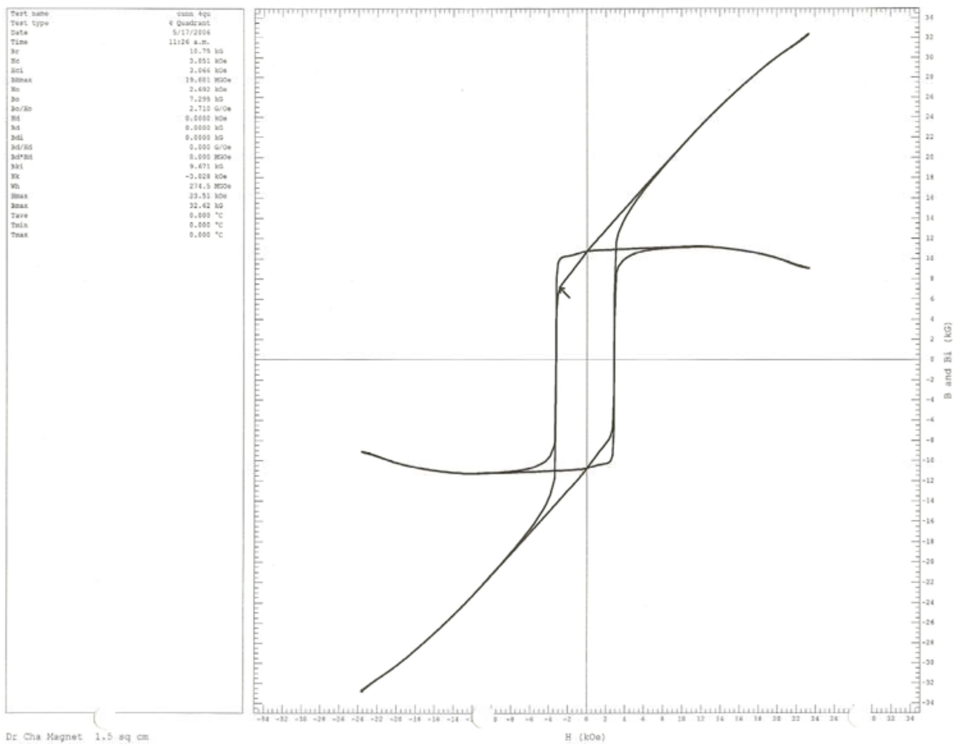

Figure 15. Hysteresis plot of the ANL sintered magnet at 175ºC.

Bonded magnets

Arnold Magnetics Plastiform 2205 was evaluated as the bonded magnet benchmark using the AMH-40 Hysteresisgraph, four-quadrant full hysteresis loop. Two other bonded magnets were evaluated against the Arnold Magnetics benchmark using the same four-quadrant full hysteresis loop: Ames Laboratory (Ames) MQP-11HTP and Ames MQP-O. The Ames MQP-O bonded magnet was made from the same alloy powder used to make the plastiform 2205 benchmark magnet. However, this magnet was fabricated using a hot-pressured process instead of being extruded. The Ames MQP-11 HTP magnet was fabricated with the same process, but it used an alloy powder developed by Iver Anderson at the Ames Lab. Table 3 lists the test results.

Table 3. Bonded magnet test results

Magnet type	Residual induction (Br) (kG)	Coercivity (Hc) (kOe)	Intrinsic coercivity (Hci) (kOe)	Energy product (BHmax) (MGOe)
Arnold Magnetics Plastiform 2205 (bonded) [a]	**5.03 (ambient)** **3.70 (200ºC)**	**4.24 (ambient)** **2.85 (200ºC)**	**11.49 (ambient)** **5.10 (200ºC)**	**5.29 (ambient)** **2.68 (200ºC)**
Ames MQP-11HTP (bonded)	3.93 (ambient) 3.41 (200ºC)	3.56 (ambient) 2.89 (200ºC)	11.87 (ambient) 5.72 (200ºC)	3.49 (ambient) 2.51 (200ºC)
Ames MQP-O (bonded)	4.46 (ambient) 3.15 (200ºC)	4.03 (ambient) 2.55 (200ºC)	12.23 (ambient) 5.25 (200ºC)	4.53 (ambient) 2.03 (200ºC)

[a] Bold indicates benchmark magnet.

At 200ºC, the Ames MQP-11 HTP magnet has a 12% higher Hci than the benchmark, indicating a superior resistance to demagnetization at elevated temperatures. The BHmax of the MQP-11 HTP is 6% less than the benchmark at 200ºC. The Br of the MQP-11 HTP is just under 8% less than the benchmark at 200ºC.

At 200ºC, the Ames MQP-O magnet has a 3% higher Hci than the benchmark, indicating a slightly better ability to resist demagnetization at elevated temperatures. The BHmax of the MQP-O magnet is 24% less than that of the benchmark at 200ºC. The Br of the MQP-O magnet is 15% less than that of the benchmark at 200ºC.

Figures 16–18 show the full four-quadrant hysteresis graph of the Arnold Magnetics Plastiform 2205 bonded benchmark magnet, the Ames MQP-11 HTP bonded magnet, and the Ames MQP-O bonded magnet at 200ºC.

Br = 3.70 kG
Hc = 2.85 kOe
Hci = 5.10 kOe
BHmax = 2.68 MGOe

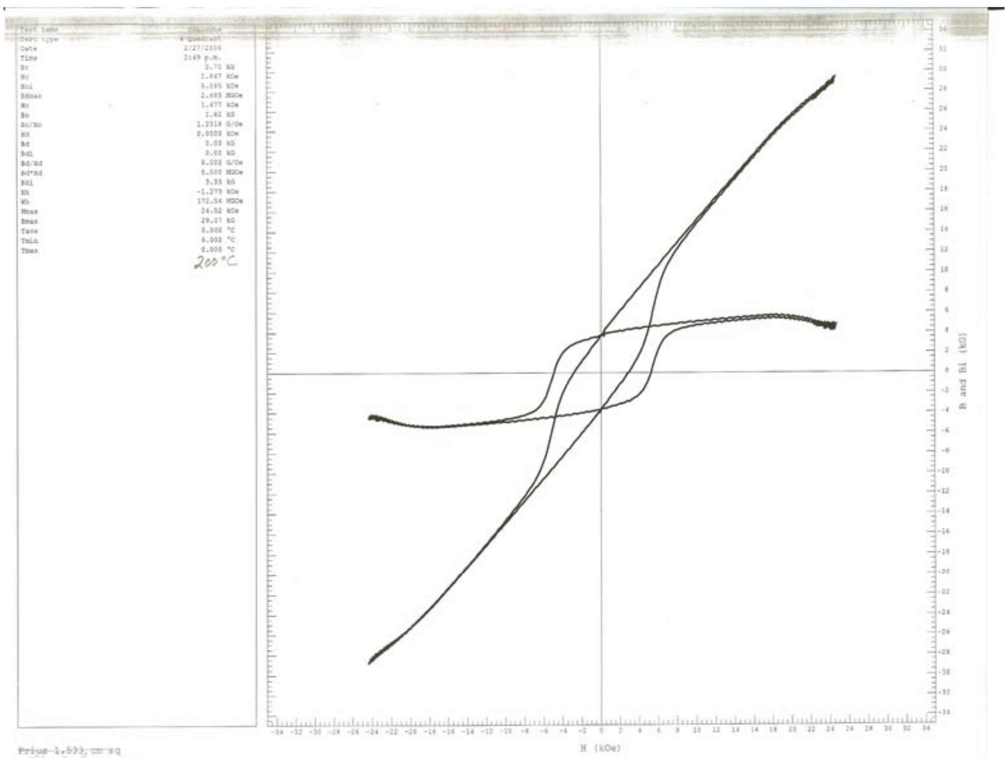

Figure 16. Hysteresis plot of Arnold Magnetics Plastiform 2205 bonded benchmark magnet at 200ºC.

Br = 3.41 kG
Hc = 2.89 kOe
Hci = 5.72 kOe
BHmax = 2.51 MGOe

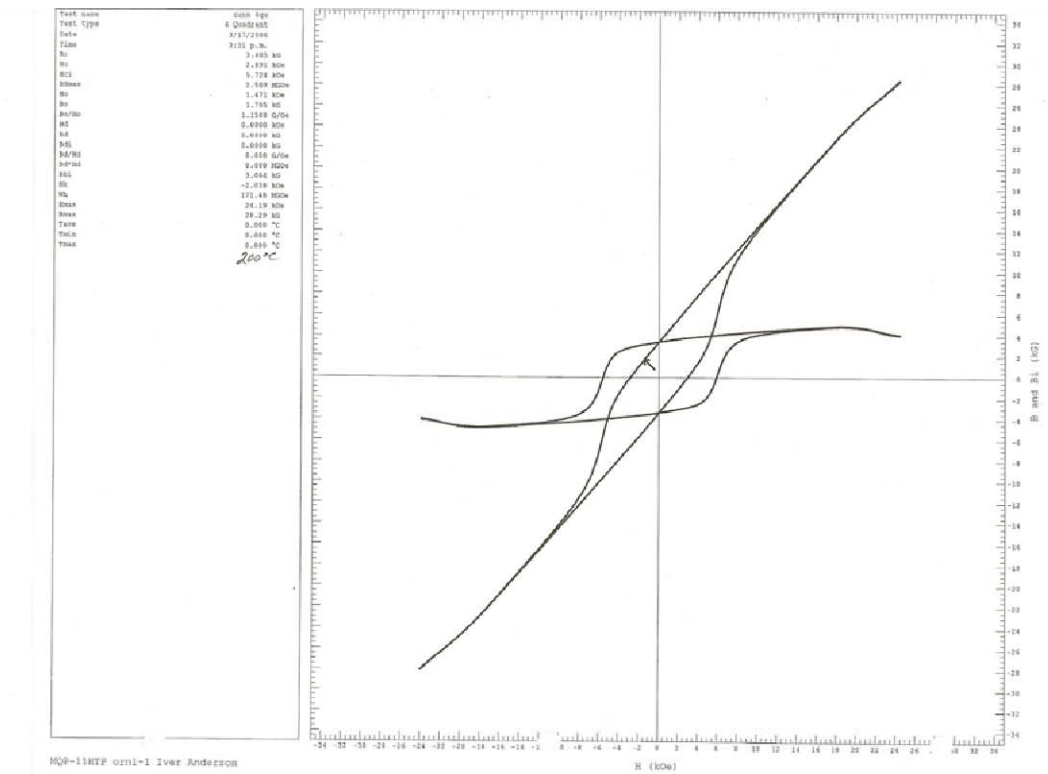

Figure 17. Hysteresis plot of the Ames MQP-11 HTP magnet at 200ºC.

Br = 3.15 kG
Hc = 2.55 kOe
Hci = 5.25 kOe
BHmax = 2.03 MGOe

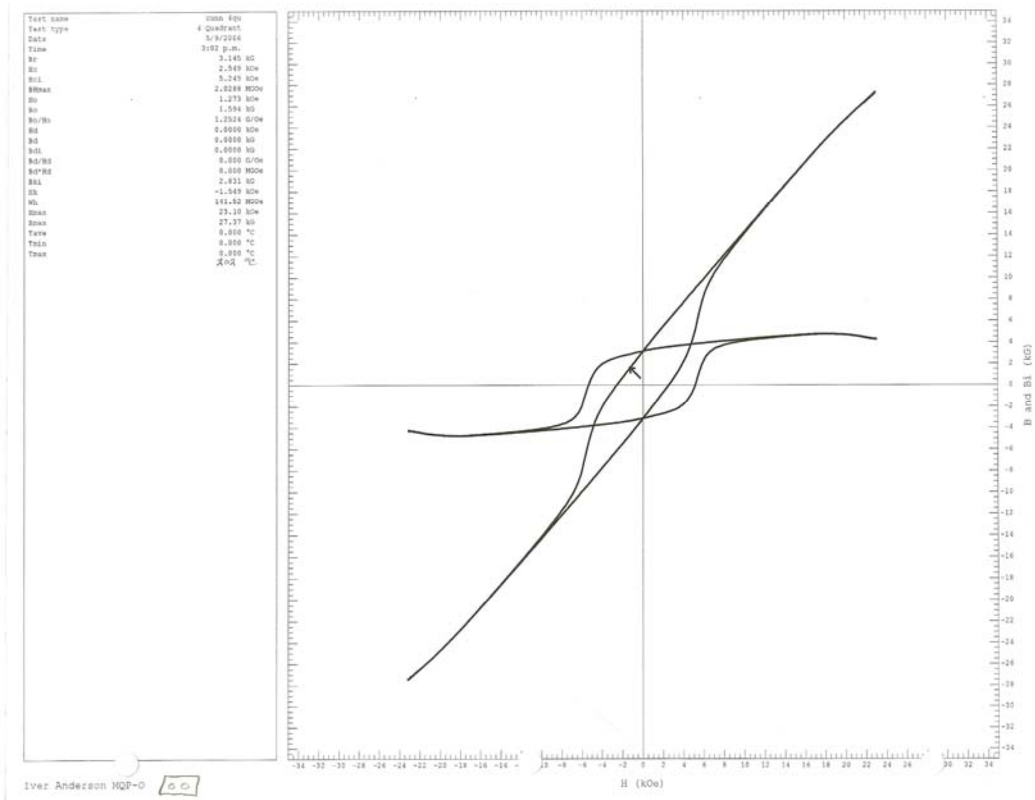

Figure 18. Hysteresis plot of the Ames MQP-O bonded magnet at 202°C.

Conclusion

The evaluation and characterization of capacitor and magnet technologies was accomplished through the testing of these components at elevated temperatures and in simulated operating conditions. All components that were received were evaluated. No prototype film capacitors were received for evaluation during this reporting period.

The film capacitor evaluated as the benchmark was taken from the Prius HEV capacitor module. The Prius capacitor module contains ten film capacitors in parallel. Several of these were extracted and used in the evaluation process.

A Kemet 1-μF 500-Vdc ceramic capacitor was evaluated as the ceramic benchmark. Penn State supplied a prototype 90-nF 500-Vdc ceramic capacitor for evaluation. No other prototype ceramic capacitors were received from developers for evaluation during this reporting period.

The Kemet capacitor performed worse in the area of capacitance value and ESR as the temperature approached its rated value. The Penn State capacitor started out poorly in both of those areas at lower temperatures, but as the temperature increased the ESR improved by over 70%, and the capacitance value improved by over 370%.

Benchmark characterizations of anisotropic sintered and isotropic bonded rare earth magnets were performed to determine the basic properties of these very hard magnetic materials. Magnets taken from the Prius motor were used as the sintered benchmark, and commercial Arnold Plastiform bonded magnets were used as the bonded magnet benchmark.

Tests included pulse charging the magnetic samples to saturation and performing second quadrant demagnetization curves. Sintered magnets from Shin-Etsu as well as bonded magnets from Ames Laboratory were tested. Several samples of both types of magnets were evaluated and compared with the benchmarks. The performance of all the magnets varied with temperature and was unique for each sample. The actual performance of any magnet in a magnetic circuit depends on the geometric design and operating conditions such as temperature and demagnetizing fields. The basic properties of the Shin-Etsu magnet indicate it could possibly be used with good results if the temperature can be kept low.

Future Direction

Evaluation of prototype components will be done on a case-by-case basis as the need arises.

This document highlights work sponsored by agencies of the U.S. Government. Neither the U.S. Government nor any agency thereof, nor any of their employees, makes any warranty, express or implied, or assumes any legal liability or responsibility for the accuracy, completeness, or usefulness of any information, apparatus, product, or process disclosed, or represents that its use would not infringe privately owned rights. Reference herein to any specific commercial product, process, or service by trade name, trademark, manufacturer, or otherwise does not necessarily constitute or imply its endorsement, recommendation, or favoring by the U.S. Government or any agency thereof. The views and opinions of authors expressed herein do not necessarily state or reflect those of the U.S. Government or any agency thereof.

Printed on
recycled
paper

A Strong Energy Portfolio for a Strong America
Energy efficiency and clean, renewable energy will mean a stronger economy, a cleaner environment, and greater energy independence for America. Working with a wide array of state, community, industry, and university partners, the U.S. Department of Energy's Office of Energy Efficiency and Renewable Energy invests in a diverse portfolio of energy technologies.

For more information contact:
EERE Information Center
1-877-EERE-INF (1-877-337-3463)
www.eere.energy.gov